AD-A055 176   CALSPAN CORP BUFFALO N Y   F/G 8/2
ARRAY SCANNING TECHNIQUES.(U)
APR 78   H F RYAN, R C WAAS, P G PFLUEGER   F30602-76-C-0294
UNCLASSIFIED   CALSPAN-ME-5955-X-1   RADC-TR-78-71   NL
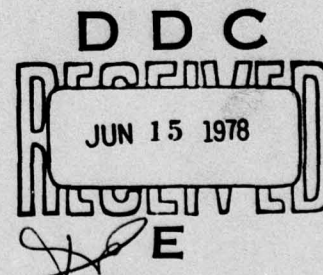
1 OF 3
AD
A055176

RADC-TR-78-71
Final Technical Report
April 1978

ARRAY SCANNING TECHNIQUES

Hollis F. Ryan
Roy C. Waas
Phillip G. Pflueger
Leland D. Hamilton

Calspan Corporation

D D C
RECEIVED
JUN 15 1978
E

AD A055176

AD No.
DDC FILE COPY

78 06 14 016

This report has been reviewed by the RADC Information Office (OI) and is releasable to the National Technical Information Service (NTIS). At NTIS it will be releasable to the general public, including foreign nations.

RADC-TR-78-71 has been reviewed and is approved for publication.

APPROVED: *Stanley P. Damon Jr.*

STANLEY P. DAMON, JR.
Project Engineer

APPROVED: *Howard Davis*

HOWARD DAVIS
Technical Director
Intelligence and Reconnaissance Division

FOR THE COMMANDER: *John P. Huss*

JOHN P. HUSS
Acting Chief, Plans Office

REPORT DOCUMENTATION PAGE	READ INSTRUCTIONS BEFORE COMPLETING FORM

1. REPORT NUMBER	2. GOVT ACCESSION NO.	3. RECIPIENT'S CATALOG NUMBER
RADC-TR-78-71		

4. TITLE (and Subtitle)

ARRAY SCANNING TECHNIQUES

5. TYPE OF REPORT & PERIOD COVERED

Final Technical Report
10 Jun 76 - 9 Dec 77

6. PERFORMING ORG. REPORT NUMBER

ME-5955-X-1

7. AUTHOR(s)

Hollis F. Ryan   Leland D. Hamilton
Roy C. Waas
Phillip G. Pflueger

8. CONTRACT OR GRANT NUMBER(s)

F30602-76-C-0294

9. PERFORMING ORGANIZATION NAME AND ADDRESS

Calspan Corporation
P.O. Box 235
Buffalo NY 14221

10. PROGRAM ELEMENT, PROJECT, TASK AREA & WORK UNIT NUMBERS

62702F
55690339 03

11. CONTROLLING OFFICE NAME AND ADDRESS

Rome Air Development Center (IRRP)
Griffiss AFB NY 13441

12. REPORT DATE

April 1978

13. NUMBER OF PAGES

196

14. MONITORING AGENCY NAME & ADDRESS(if different from Controlling Office)

Same

196 p.

15. SECURITY CLASS. (of this report)

UNCLASSIFIED

15a. DECLASSIFICATION/DOWNGRADING SCHEDULE

N/A

16. DISTRIBUTION STATEMENT (of this Report)

Approved for public release; distribution unlimited.

CALSPAN-ME-5955-X-1

17. DISTRIBUTION STATEMENT (of the abstract entered in Block 20, if different from Report)

Same

18. SUPPLEMENTARY NOTES

RADC Project Engineer:
Stanley P. Damon, Jr. (IRRP)

19. KEY WORDS (Continue on reverse side if necessary and identify by block number)

cartography   line following
map   interactive graphics
electrooptics   photodiode arrays
scanning
image processing

20. ABSTRACT (Continue on reverse side if necessary and identify by block number)

The objective of this study was to determine the feasibility of scanning cartographic documents by large, semiconductor linear arrays and by specially shaped geometric arrays. The Calspan flatbed image scanner with its linear array sensor was used with supporting computer software to scan and process small sections of the USAF's Cartographic Test Standard (mylar version).

The basic properties of the monolithic linear array of silicon photodiodes for the generation of imagery were studied by directly examining the imagery →

DD FORM 1473   EDITION OF 1 NOV 65 IS OBSOLETE
1 JAN 73

78 06 14 016
407 727

Item 20 (Cont'd)

output of the scanner. Two geometric arrays were studied by simulating their aperture geometries with software in a PDP-9 computer.

Analysis of the imagery output of the flatbed scanner showed that the linear array produced excellent imagery. Examination of the behavior of the two simulated geometric arrays showed that the line directions found were the ones desired in most cases. Solid state photosensor technology was evaluated. Methods were presented for hardware implementation of geometric array processing algorithms. It was concluded that current array sensing technology is suitable for digitally encoding cartographic documents.

ACCESSION for

NTIS   White Section ⊠
DOC   Buff Section   ☐
UNANNOUNCED   ☐
JUSTIFICATION.........................

....

BY...
DISTRIBUTION/AVAILABILITY CODES

Dist.	AVAIL. and/or SPECIAL	
A		

TABLE OF CONTENTS

TABLE OF CONTENTS
(CONTD)

EVALUATION

The purpose of this effort was to determine the feasibility of scanning cartographic documents using a large linear array and specially shaped array configurations. The investigation of scanning technology is based upon the need to evolve and implement techniques which will enhance the conversion of analog graphics to digital records. A detailed study was made of existing capabilities of solid state photosensor technology and supporting computational algorithms. The effort directly addresses the needs of TPO Thrust R03 which has the major goal of providing new techniques to improve the accuracy and efficiency of the cartographic processes.

Stanley Damon

STANLEY DAMON
Project Engineer

v

Section 1
INTRODUCTION

The objective of this study was to determine the feasibility of
(a) the scanning of cartographic documents by large linear arrays and
(b) the scanning of cartographic documents by specially shaped array con-
figurations. This investigation into scanning technology is based upon
the need to evolve and implement techniques which will enhance the con-
version of analog graphics to digital records. This project supports an
integrated program at the U. S. Air Force's Rome Air Development Center
which is designed to introduce automation into the cartographic field.

A test bed facility was used to determine the feasibility. The
major components of this facility are a flatbed image scanner, a PDP-9
digital computer, and a software system for automatically digitizing
cartographic data. The two pieces of equipment are major elements of
Calspan Corporation's Image Processing Laboratory. The map digitizing
software system, called DIGIMAP, is a prototype system for encoding
cartographic line data. The computer software was modified to create an
experimental test bed for evaluating the array scanning techniques.

The Calspan developed flatbed image scanner uses a linear diode
array as the sensing element. It is moved in a raster mode over the image
field by X and Y rack and pinion drives. The scanner is interfaced to
the PDP-9 computer which controls the scanner and processes the image data
generated by it.

The basic properties of the linear array for the generation of
imagery were studied by directly examining the imagery output of the
scanner. The geometric arrays were studied by simulating their aperture
geometries with software in the PDP-9 computer. The Cartographic Test
Standard developed by RADC was used as input data for the investigations.

1-1

In the experimental work the emphasis was placed on the sensing operation and the initial processing of the cartographic imagery. The basic tools used for investigating performance were a graphic imagery display and a line printer. The line printer was used to print both imagery and computational data. Imagery was selected from the Cartographic Test Standard to provide suitable material to evaluate the performance of the arrays. The resolution bar charts were used to evaluate the basic sensing performance of the linear array flatbed scanner. Two samples from the composite map and four samples from the circular arcs were used as test data for the simulated geometric arrays. One of the composite samples contained curved lines close together, the other intersecting straight lines.

Analysis of the imagery output of the flatbed scanner showed that the linear array produced excellent imagery. Examination of the behavior of the two simulated geometric arrays showed that the line directions found were the ones desired in most cases. It has thus been concluded that the current array sensing technology is suitable for digitally encoding cartographic documents.

Five technical investigations were pursued on this program, two experimental and three theoretical. The studies conducted were:

    (1) Linear array scanning (experimental)
    (2) Geometric array simulation (experimental)
    (3) Array technology state of the art
    (4) Geometric array implementation
    (5) System throughput analysis

In Section 2 the basic problem is defined and the investigative approach chosen is described. The test bed facility used to collect the experimental data and the geometric array simulation algorithms are described in Sections 3 and 4 respectively. The experimental work is reported in Sections 5 and 6. A state-of-the-art evaluation of solid

1-2

state photosensor technology is presented in Section 7. A specific CCD array, light source and filter type are recommended. Section 8 gives three alternative methods for implementing the geometric array processing algorithms in hardware. Section 9 contains conclusions and recommendations. Section 10 documents the new and modified computer software programs which were developed for and used by the test bed facility. The specifications for the large linear array which was used to scan the test data are given in Appendix A. The system throughput study is reported in Appendix B.

Section 2
PROBLEM DEFINITION AND APPROACH

The technical objective being addressed by this project is to be able to automatically find cartographic features on a cartographic manuscript using a scanning and processing operation. For purposes of this program a cartographic feature is assumed to be a line. This is the simplest type of feature.

There are three steps in digitizing a line:

    (1) Detecting a line

    (2) Determining the direction of the line

    (3) Following the line

The third operation, line following, does not involve the array directly. It is a computer processing step which uses the data generated by the array. This project addresses the first two steps in the line digitizing operation.

There are two basic types of arrays which can be used to digitize maps - a linear array and a geometric array. A linear array is an integrated semiconductor device which has a line array of photodiode elements. The photodiode can be interrogated in succession very rapidly and the light intensity that each one sees read out into a data buffer. A raster scan pattern is generated by mechanically moving the linear array after each scan, sweeping out an area or band whose width is equal to the length of the array, adjusted by the optical magnification factor.

A geometric array is a semiconductor device which has a number of photosensitive areas or apertures of specific sizes and shapes combined in a specific pattern. The output of each aperture for a given array

position on a cartographic manuscript is a measure of the density of that part of the document covered ("seen") by the aperture. The set of outputs can be processed to yield information regarding cartographic features seen by the geometric array. In particular, the direction of a line passing through the area seen by the array can be determined.

Details of the state of the technology for fabricating linear and geometric arrays are given in another section of this report.

The objective of this effort is to determine the feasibility of scanning graphics by large linear arrays and by specially shaped array configurations. The scanning operation includes the generation of a digital image of the document, the detection of a line in the image field, and the determination of the direction of the line.

The feasibility has been determined by performing these three operations and examining how well each function was accomplished. Selected cartographic imagery has been used to evaluate each function.

Line detection and line direction determination are processing operations whose details depend directly on the specific geometry of the array being used.

The scanning performance depends directly on the nature of the cartographic material being scanned. Cartographic manuscripts, black ink on film transparencies, have uniformly high contrast lines with smooth, sharp edges. The pertinent variables are the line width, line separation, and the radius of curvature.

A linear array's function is to generate a digital image of the cartographic document. Its performance is evaluated in terms of the quality of the image produced. Image quality is described in terms of the contrast, edge sharpness, minimum line width, and minimum line separation.

The function of a geometric array is to detect a line and determine its direction. The geometric array produces digitial image information which is then processed to yield the detection and direction data. It is necessary to evaluate these two operations as a pair operating together. It is more meaningful to look at both operations functioning together than each separately.

The geometric array is then considered to be a combination of a sensor having a certain configuration of light sensitive apertures and a data processing algorithm which performs mathematical computations on the image intensities or densities measured by the apertures. An examination of how the aperture intensities vary as the geometric array crosses a line or set of lines will indicate if the array is providing the necessary information to determine line direction.

The feasibility of array technology was established empirically by experimentation. A linear array mounted on a flatbed scanner was used to scan selected cartographic test data. Geometric arrays were simulated on the computer using image data generated by the linear array.

The experimental work was done on a testbed facility which was assembled from the Calspan Image Processing Laboratory equipment and from the DIGIMAP digitizing computer software system.

Section 3
TESTBED FACILITY

The testbed used for experimentation consists of a computer
software system which runs on a Digital Equipment Corporation PDP-9
digital computer and uses an interactive display built around a Tektronix
611 storage tube, and a Calspan developed flatbed scanner.

3.1   FLATBED IMAGE SCANNER

The key element in the experimental testbed facility used for
this project is the flatbed image scanner. It is operated as an on-line
peripheral to the PDP-9 computer. The sensing element in the scanner is
a 1024 monolithic photodiode array. The photodiode array is based on MOS
silicon technology and is manufactured by Reticon Company. The active
elements are approximately 1 mil square in size and have 1 mil centers.
The specifications of the linear array are given in Appendix A. The
linear array is mounted in a Reticon camera assembly which in turn is
affixed to the moving head of a Mutoh X-Y flatbed plotter. Illumination
of the area being scanned is provided by a line filament tungsten lamp
and a reflector assembly. Light intensity falling on the photodiodes
is controlled by the variable aperture of the camera lens assembly. The
camera aperture is adjustable from f4 to f16. An opening of f4 is
normally used. The focus is adjusted by inserting shims in the lens
assembly. Magnification is determined by moving the whole camera assembly
up or down on a vertical track. The X and Y rack and pinion drives have
a minimum increment (using stepper motors) of 1 mil. Larger increments
are multiples of 1 mil. Thus, by adjusting the magnification resolutions
of 1, 2, ... 8 mils can be obtained.

The normal mode of operation of the scanner is to position the
array sensor, scan that part of the image seen by the sensor (a line of

1024 points), move the sensor via the X motor drive one resolution unit, scan the next line, and by repeating this operation, scan a band across the width of the document. The height of the band which is scanned is determined by the array size and magnification. In the work described in this report half of the array was used (512 points) due to limitations of the software. Thus the scanning is a combination of electronic and mechanical scanning. The nominal average scan rate is 50 microseconds per image point or 20,000 Hz. At a resolution of 2 mils, this is a scan rate of 1 square inch every 12.5 seconds or 288 square inches per hour. The density or intensity resolution is 16 levels.

3.2   MODE OF OPERATION

Sample cartographic imagery is scanned in separate frames and stored on magnetic tape. A frame is 1024 x 512 pixels in size. At the resolution of 2 mils used for the experimentation, the frame size is 2" x 1". When a frame is scanned, it is displayed on the storage oscilloscope. By iteratively repositioning the scanner, the operator selects exactly the part of a map he wishes to record for experimentation.

The image data is printed out on the line printer for detailed examination. Each pixel is printed out as a single alphanumeric character.

Section 4
ALGORITHM DESCRIPTIONS

The digital cartographic imagery produced by the linear array flatbed scanner is processed by a set of digital image processing algorithms implemented in computer software on the PDP-9 computer. The processing has two main parts: (1) simulation of the geometric pattern of the array, and (2) calculations using the intensities of the simulated geometric elements of the array. Each separate, active, sensing aperture of the geometric array records the intensity of the light falling on it. The response of an aperture is simulated by adding up the individual responses of the picture elements representing that aperture. The first part of the processing is then an indexing operation followed by simple summing calculations. The second part of the processing, that of using the intensity information to compute line directions, is more complex.

The two parts together form a simulated geometric array. Two different arrays were investigated in this study. For convenience, they are called the DIGIMAP donut and the TOPS donut. The first array was developed on a Calspan IR&D program called DIGIMAP, the second on the Air Force RADC matrix scanning program (F30602-74-C-0324) called TOPS at Calspan. The details of these two algorithms are described in this section.

The input to the second part of a geometric array algorithm is the set of intensities from the elements of the array. The output of the second part is a set of line directions (or no directions). Implicit in the processing is the detection of a line or lines.

The donut algorithm is a local rather than a global processing technique. Only a small section of the image field, that area seen by the array, is processed at one time.

A geometric array algorithm determines the direction of a line.

4-1

Implicit in this operation is the detection of the line prior to determining its directions. A small circular section of the image field, called a window, is processed at one time. If a line passes through this local area, the algorithm will find its entry and exit points. Figure 4-1 illustrates this operation.

The processing technique is based on the concept of a geometric array. The circular section is divided up into a number of apertures. The aperture configurations of the two geometric arrays simulated in this study are shown in Figures 4-2 and 4-3. The cartographic image being processed is a black line on a white background. A line passing through the window will cover up, partially or completely, one or more of the apertures. The algorithm examines the apertures to see if this has occurred. The more an aperture is covered up by a line, the less light it will receive. That is, the perceived image density will increase as more of the aperture is covered up by the line. An evaluation of the perceived aperture densities establishes the directions of the line or lines passing through the window.

The input to the algorithm is a set of densities, one for each aperture in the window. A zero value means that the aperture is looking at the white background of the cartographic document. If, for a given window position, all the densities are zero, there are no lines present. In general an aperture density will range from zero (white) to a maximum value (black). The in-between values represent shades of gray. Usually a line, depending on the gain characteristic of the scanner video signal, will appear black in its central portions and gray along its edges. Cartographic documents have sharp, high contrast lines and consequently the gray transition zone between the black line and the white background is quite narrow.

The aperture pattern forming the window or local image area is chosen to be close circularly symmetric. Thus the algorithm will process a line equally well no matter what its orientation. The algorithm uses the gray level density information from each picture element (pixel) rather

4-2

PART OF IMAGE FIELD

ENTRY/EXIT POINTS

**LOCAL AREA
OR WINDOW**
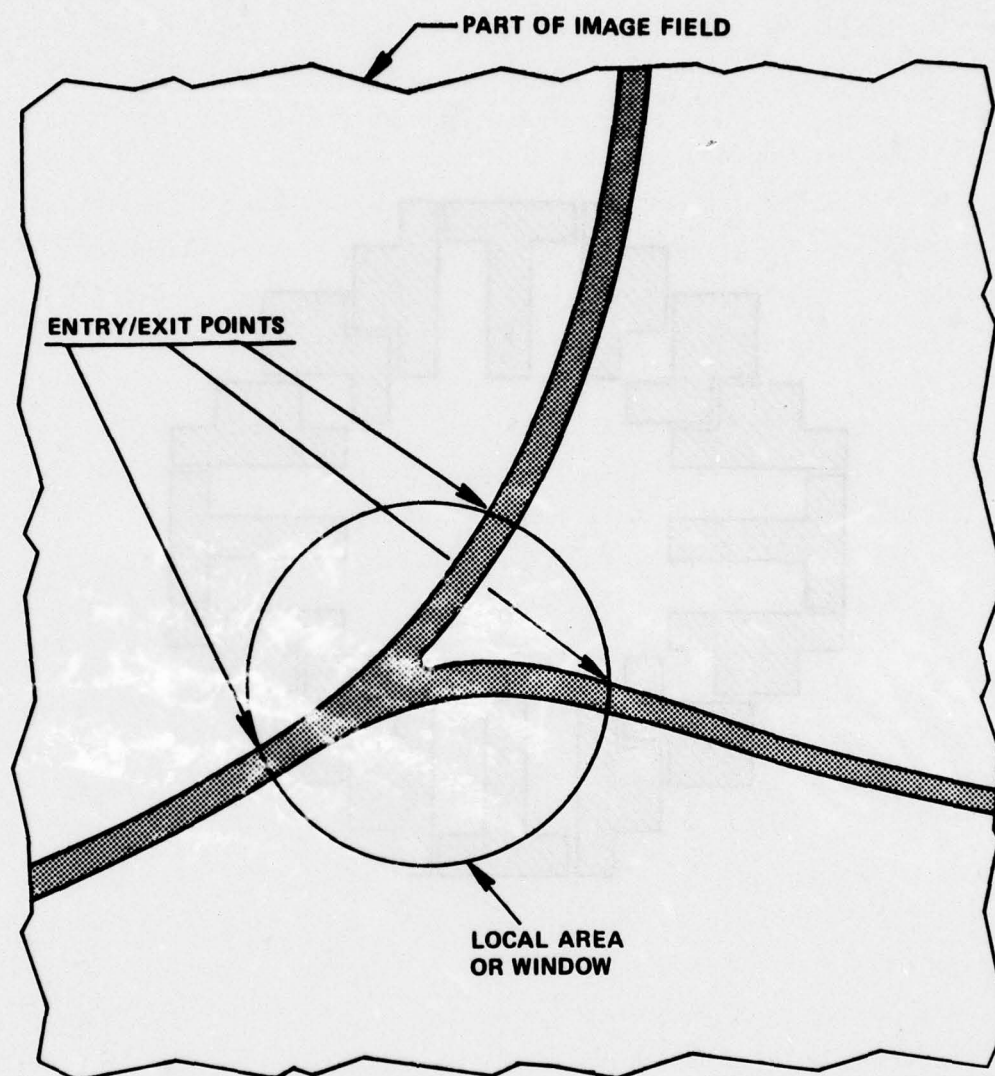
Figure 4-1   WINDOW LINE ENTRY/EXIT POINTS
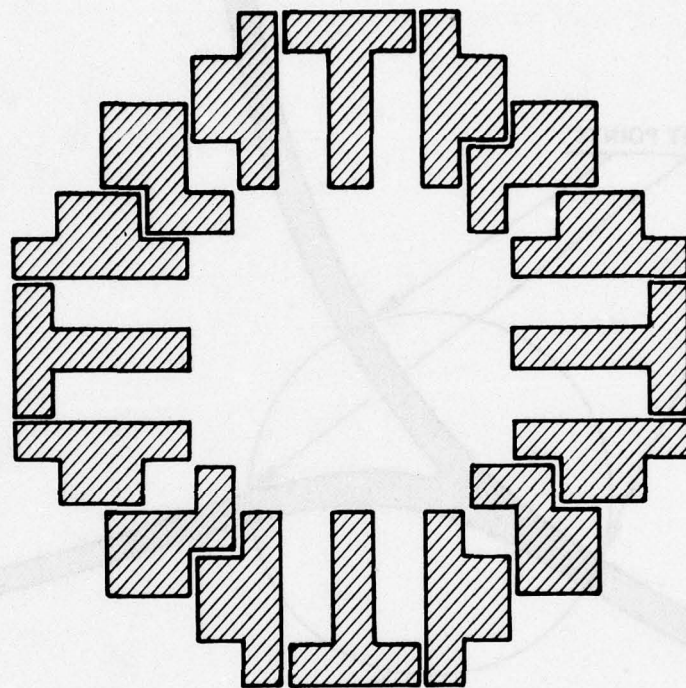
Figure 4-2   DIGIMAP GEOMETRIC ARRAY CONFIGURATION
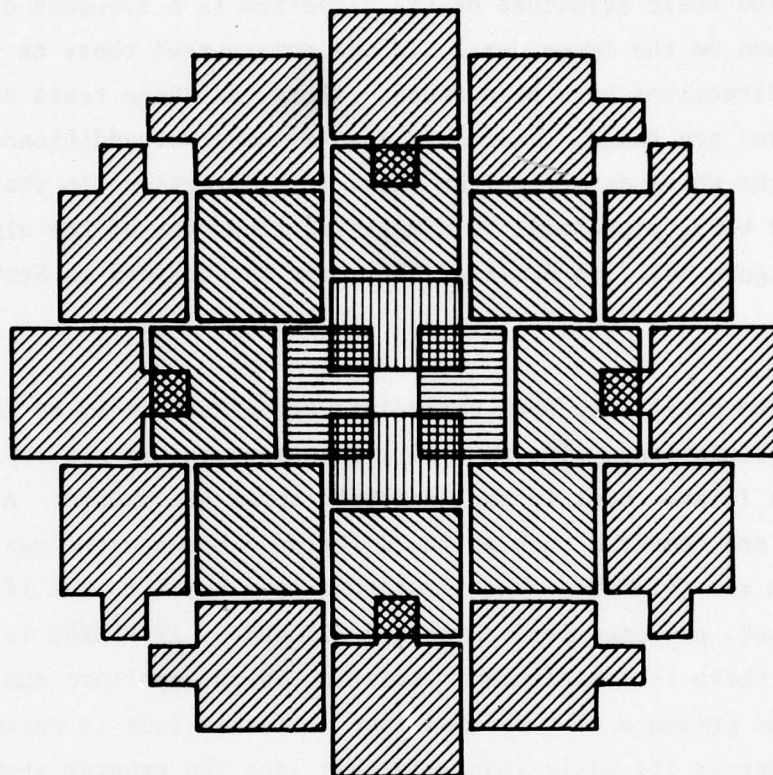
Figure 4-3   TOPS GEOMETRIC ARRAY CONFIGURATION

than considering each pixel to be either black or white. This approach makes it possible to find line directions on medium or low contrast as well as high contrast documents.

4.1   DIGIMAP GEOMETRIC ARRAY

The basic structure of the algorithm is a sequence of tests which are performed on the image data. If the data passes these tests, one or more line directions have been found. If any of these tests are not passed, no directions are found. There are also a number of additional tests in the algorithm which determine the valid line directions in that part of the image field being processed. A simplified flowchart of the algorithm is given in Figure 4-4. (A detailed flowchart is provided in Section 10.)

The first step upon entry into the algorithm is to do some preliminary calculations. The intensity values of the pixels representing each of the 16 apertures in the geometric array are summed. A number of thresholds are computed such as the difference between the maximum sum and the minimum sum (PTHRES). The first test is a check to see if PTHRES is above a fixed, predetermined threshold (CTHRES). If PTHRES is below this threshold, there is insufficient variation in the aperture sum values to indicate the presence of a defined line. If this test is passed, the algorithm enters its basic loop. In this loop the program steps in sequence around the circumference of the donut shaped array, processing each aperture value in turn. The procedure looks for peak values (black) or maxima of the aperture sums. The presence of a maximum indicates a line cutting the donut pattern.

In the basic loop a background threshold is used to separate neighboring maxima. The background threshold is calculated from the aperture values. The first differences between neighboring aperture sums are computed. A change in the sign of the difference indicates a maximum or a minimum. If there are too many extrema (more than 7), it is

4-6

DONUT

CALCULATE SUMS AND THRESHOLDS

ABOVE MAX/MIN THRESHOLD ? — NO → RETURN

YES

SELECT APERTURE SUM

ALL SUMS PROCESSED ? — YES → RETURN

NO

CURRENT AND PREVIOUS APERTURE SUMS BELOW BACKGROUND THRESHOLD ? — YES

NO

CALCULATE FIRST DIFFERENCE

SIGN CHANGE ? — NO

YES

MORE THAN 7 MAX, MIN ? — YES → RETURN

NO

SUM BELOW BACKGROUND THRESHOLD ? — NO

YES

MULTIPLE MAX/MIN ? — YES → SELECT MAX/MIN PAIR → FIRST DIFFERENCE ABOVE THRESHOLD ? — NO → DELETE A MAX/MIN PAIR

NO

YES

SUM OF SUMS ABOVE THRESHOLD ? — NO

ALL PAIRS PROCESSED ? — NO / YES

YES

CALCULATE WEIGHTED LINE DIRECTION — NO ← MORE THAN ONE MAX/MIN ?

YES

SAVE DIRECTIONS

Figure 4-4 LOGIC OF DIGIMAP GEOMETRIC ARRAY ALGORITHM

assumed there are no clearly defined lines or line directions.

If there is a single maximum, another threshold check is made, and then a weighted line direction is computed. The direction found is weighted by the intensity values of the aperture sums on either side of the maximum.

If multiple maxima are found, a deletion loop is entered to remove pairs of maxima and minima which are too close together in value. If the first difference is below a computed threshold, a maximum and a minimum are deleted from the list of maxima and minima which has been found in the basic loop. A pair is chosen for deletion to maximize the differences among the remaining extrema.

The algorithm enters the deletion loop having a candidate list of 2, 3, or 4 maxima with an interspersed set of 1, 2, or 3 minima respectively. If only one maximum remains after completing the deletion loop, a weighted line direction is computed. If several maxima have been found, the directions are not weighted.

4.2   TOPS GEOMETRIC ARRAY

The TOPS geometric array has 24 apertures as shown in Figure 4-3. The apertures are arranged in three rings of 4, 8, and 12 apertures each. These rings are called the inner, middle, and outer rings respectively. In this array, as is evident in Figure 4-5, some of the apertures overlap. That is, in the simulation of the array some picture elements fall into two different apertures.

The logic of the TOPS algorithm is given in simplified form in Figure 4-5. A detailed flowchart of the program is contained in Section 10. The first step is to compute the intensities of the apertures. This is done by adding up the intensities of the pixels making up each aperture. As the apertures do not all have the same number of pixels, it is necessary

4-8

```
                          ┌─────────┐
                          │  HEART  │
                          └────┬────┘
                               │                                  ┌──────────────┐
        ┌──────────────┐       │                         ┌───────▶│  SELECT AN   │
        │   COMPUTE    │       │                         │        │ UNPROCESSED  │
        │  NORMALIZED  │◀──────┤                         │        │ MIDDLE RING  │
        │   APERTURE   │                                 │        │  ADJACENCY   │
        │    SUMS      │                                 │        └──────┬───────┘
        └──────┬───────┘                                 │               │
               │                                         │               ▼
               ▼                                         │        ┌──────────────┐
        ┌──────────────┐                                 │        │    SELECT    │
        │   COMPUTE    │                                 │        │   HIGHEST    │
        │  THRESHOLD   │                                 │        │   VALUED     │
        │              │                                 │        │  APERTURE IN │
        └──────┬───────┘                                 │        │  ADJACENCY   │
               │                                         │        └──────┬───────┘
               ▼                                         │               │
                                                         │               ▼
         ╱────────────╲                                  │        ┌──────────────┐
        ╱    INNER     ╲         ┌────────┐              │        │ SELECT HIGH- │
       ╱ RING AVERAGE   ╲   NO   │ RETURN │              │        │ EST VALUED,  │
       ╲ ABOVE THRSH    ╱───────▶└────────┘              │        │ NEIGHBORING, │
        ╲      ?       ╱                                 │        │  OUTER RING  │
         ╲────────────╱                                  │        │  APERTURE    │
               │                                         │        └──────┬───────┘
               │ YES                                     │               │
               ▼                                         │               ▼
        ┌──────────────┐                                 │         ╱────────────╲
        │  THRESHOLD   │                                 │        ╱     IS       ╲
  ┌────▶│ MIDDLE RING  │                                 │       ╱  OUTER RING    ╲  NO
  │     │  APERTURE    │                                 │       ╲ APERTURE SUM   ╱────────┐
  │     │    SUMS      │                                 │        ╲ ABOVE THRSH  ╱         │
  │     └──────┬───────┘                                 │         ╲     ?      ╱          │
  │            │                                         │          ╲────────╱            │
  │            ▼                                         │               │ YES            │
  │      ╱────────────╲                                  │               ▼                ▼
  │     ╱     ANY      ╲        ┌────────┐               │        ┌──────────────┐  ┌──────────────┐
  │    ╱    MIDDLE      ╲  NO   │ RETURN │               │        │ SAVE DIREC-  │  │ SAVE DIREC-  │
  │    ╲  RING SUMS     ╱──────▶└────────┘               │        │  TION OF     │  │  TION OF     │
  │     ╲ ABOVE THRSH  ╱                                 │        │ OUTER RING   │  │ MIDDLE RING  │
  │      ╲     ?      ╱                                  │        │  APERTURE    │  │  APERTURE    │
  │       ╲────────╱                                     │        └──────┬───────┘  └──────┬───────┘
  │            │ YES                                     │               │                 │
  │            ▼                                         │               ▼                 │
  │     ┌──────────────┐                                 │         ╱────────────╲          │
  │     │  FIND ALL    │                                 │        ╱    ALL       ╲  NO      │
  │     │SINGLE, DOUBLE│                                 └───────╱  ADJACENCIES   ╲◀────────┘
  │     │  AND TRIPLE  │                                         ╲  PROCESSED     ╱
  │     │  ADJACENCIES │                                          ╲     ?        ╱
  │     └──────┬───────┘                                           ╲────────────╱
  │            │                                                        │ YES
  │            └────────────────────────────────────┐                  ▼
  │                                                  │            ╱────────────╲
  │                                                  │           ╱    ANY       ╲
  │                                                  │          ╱  QUADRUPLE     ╲  NO   ┌────────┐
  │                                                  │          ╲  OR GREATER    ╱──────▶│ RETURN │
  │                                                  │           ╲ ADJACENCIES  ╱        └────────┘
  │                                                  │            ╲     ?      ╱
  │                                                  │             ╲────────╱
  │                                                  │                  │ YES
  │                                                  │                  ▼
  │                                                  │           ┌──────────────┐
  │                                                  │           │   INCREASE   │
  └──────────────────────────────────────────────── ┴──────────│   THRESHOLD  │
                                                                 └──────────────┘
```
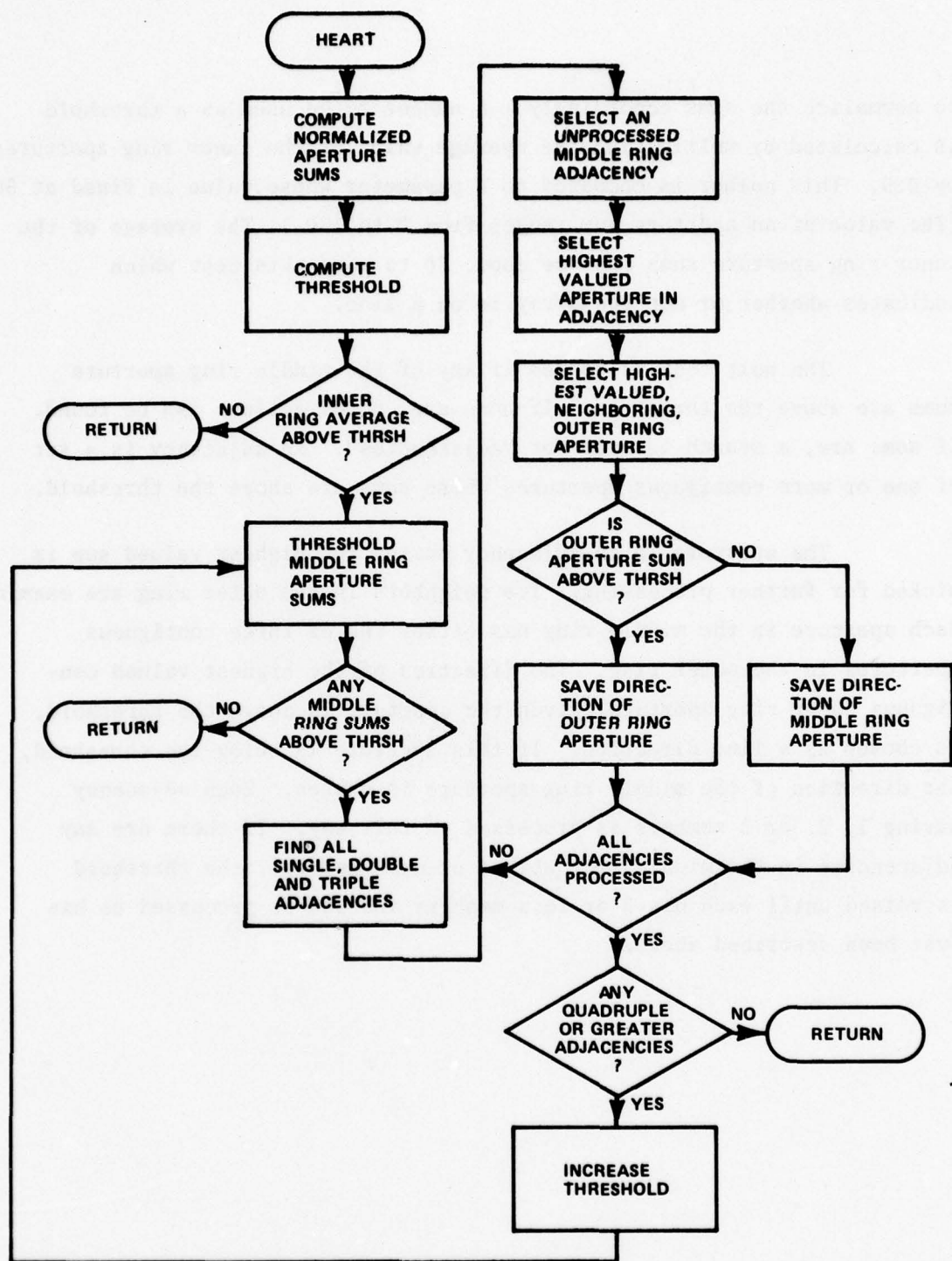
Figure 4-5   LOGIC OF TOPS GEOMETRIC ARRAY ALGORITHM

4-9

to normalize the sums accordingly. A number to be used as a threshold is calculated by multiplying the average value of the inner ring apertures by 0.9. This number is compared to a parameter whose value is fixed at 50. (The value of an aperture sum ranges from 0 to 150.) The average of the inner ring aperture sums must be above 50 to pass this test which indicates whether or not the array is on a line.

The next test is to see if any of the middle ring aperture sums are above the threshold. If none are, no directions can be found. If some are, a search is made for "adjacencies". An adjacency is a set of one or more contiguous apertures whose sums are above the threshold.

The aperture in an adjacency having the highest valued sum is picked for further processing. Its neighbors in the outer ring are examined. Each aperture in the middle ring has either two or three contiguous apertures in the outer ring. The direction of the highest valued contiguous outer ring aperture, given the aperture is above the threshold, is chosen as a line direction. If this aperture is below the threshold, the direction of the middle ring aperture is chosen. Each adjacency having 1, 2, or 3 members is processed in this way. If there are any adjacencies in the middle ring with 4 or more members, the threshold is raised until each has 3 or less members and can be processed as has just been described above.

Section 5
EXPERIMENT DESIGN

The testbed facility was used to conduct experiments to evaluate the feasibility of large linear arrays and geometric arrays for cartographic input processing. Input test data was provided by the graphical (film) form of the Cartographic Test Standard (CTS).

Two sets of experiments were conducted. The first set evaluated the performance of the large linear array; the second set evaluated the performance of two geometric arrays. The geometric arrays were simulated using the image data generated by the linear array.

5.1   LINEAR ARRAY EXPERIMENTS

The performance of the linear array was evaluated in terms of its ability to generate digitized imagery from the three resolution patterns on the CTS. Each resolution pattern consists of a series of straight, parallel lines. The lines are arranged in 8 groups of 6 lines each. All the lines in a group are the same width and have the same interline spacing. The line width increases from group to group from a minimum of 2 mils to a maximum of 20 mils. The three patterns are oriented vertically, horizontally, and diagonally. (The linear array is mounted vertically in the scanner.) These three patterns show the scanner performance at different line separations, line widths, and orientations.

These three test patterns were scanned and digitized. A scanner resolution of 2 mils was used. The scanner gain characteristic was set to give the sharpest line definition. The shape of the gain characteristic of the sensor output amplifier can be changed within limits by adjusting the amplifier's gain and offset potentiometers. The gain and offset were set so that the signal went very quickly from the zero level to saturation when the scanner went from a black line to white background. Giving the sensor amplifier this hard saturation characteristic provides sharp edges

5-1

to the lines.

The scanning head is driven in X and Y by stepper motors which impart some vibration to the sensor as they move it from scan to scan. This effect can be minimized by putting a time delay in the scan control program after the sensor is moved but before it is interrogated. This was done to obtain both normal or "fast" scanned images and "slow" scanned images. A comparison of a "fast" image with a "slow" image of the same data establishes whether or not any distortion is introduced by this mechanical vibration. The three resolution patterns were scanned at the slow speed and one was scanned at the fast speed also.

The performance of the linear array sensor was evaluated by examining printouts of the imagery. In an imagery printout each picture element is encoded into one of sixteen symbols (0, 1,...9, A, B,...F) according to the intensity or density of the gray level which has been sensed. Examination of this printout shows

(1) The sharpness of line edges.
(2) The diffraction induced resolution loss caused by lines being close together.
(3) Preferential orientation effects.

5.2   GEOMETRIC ARRAYS

The geometric array experiments were designed to evaluate the performance of two simulated geometric arrays on sample data obtained from the Cartographic Test Standard.

5.2.1   Sample Data

Six frames were selected. Each section or test frame is an

imagery sample of 1024 x 512 points. Four sections covering the semi-circles were used. The arcs increase in width from 1 mil to 20 mils. Two sections from the composite version were chosen. The first of these map samples has many closely spaced, rapidly curving non-intersecting lines. The second map sample contains intersecting straight lines. These sample imagery frames were scanned and digitized and stored on magnetic tape using the large linear array sensor.

5.2.2 Simulation

The simulation approach was chosen to investigate the feasibility of geometric arrays. The special geometries of the two arrays studied were simulated in computer software on the PDP-9. In the simulation each active or sensing area in a geometric array is represented by a set of image points which closely approximate its size, shape, and location. The intensities of the points are summed giving a single intensity for that particular area. This is the way a geometric array was simulated. Various computations are performed on the intensity sums to generate candidate line directions. A geometric array consists then of a particular geometric configuration of sensing areas, plus a computational algorithm to process the intensities.

Two geometric arrays were selected for study - the DIGIMAP donut and the TOPS donut. Both of these arrays had previously been implemented in computer software at Calspan. The DIGIMAP donut was designed to process low to high contrast line features at high speed and consequently is computationally complex and tightly coded. As it was developed on the PDP-9 computer it was available for experimentation with minimum modifications. The TOPS donut was designed to process high contrast cartographic imagery. It is computationally less complex. It also was designed to follow lines which are close to other lines. This donut was originally developed on the HP-2100A computer. It was recoded in PDP-9 assembler to run on the testbed facility. Details of these two donuts have been given in Section 4.

5.2.3   Interactive Operation

        The testbed facility which has been described in Section 3 was
used to conduct the experiments described above. The sample cartographic
imagery was scanned and stored on magnetic tape. With the imagery data
stored on magnetic tape the experimenter can easily call up whichever
frame is required for experimentation.

        An experiment consists of the following steps:

        (1) Select an imagery frame.
        (2) Select the geometric array to be simulated.
        (3) Display imagery on storage tube.
        (4) Select, using the track ball, two points in the image
             field. Specify the spacing between neighboring array
             positions.
        (5) Let the simulation run, printing out the array cal-
             culations.
        (6) Print out the sample imagery.
        (7) Analyze the data.

        The key data collection step is the selection of the two points
defining a "donut track". A donut track is a straight line along which
the center of the donut or geometric array is stepped. The tracks are
chosen to provide the desired information regarding the behavior of the
arrays in different situations. For example, tracks were chosen to cross
(1) an isolated straight line, (2) a sharply curving line, and (3) a line
intersection.

5.2.4   Data Collection

        There are two main types of data which are collected, both from
the line printer. Firstly, the original image data which has been stored
on magnetic tape was printed out for examination. Secondly, the results

of the intermediate computations of the donut simulation and processing algorithms were captured and printed out for each location of a donut. In addition, pictures of sample imagery frames were taken from the storage tube display.

Section 6
EXPERIMENTATION

This section of the report gives the details of the data collection experiments which have been described in the previous section and presents an analysis and interpretation of the results.

Ten imagery frames were scanned, digitized, and stored on magnetic tape. Four frames were for the large linear array analyses; six were for the geometric array simulation studies. Table 6-1 lists the ten sample images, giving their sources. All test frames were recorded at a pixel resolution of 2 mils with the video amplifier gain and offset adjusted to give maximum discrimination between the black lines and the white background.

Extensive computer printouts were generated of both the imagery and the geometric array simulation computations. Excerpts from the printouts have been included in this section of the report.

6.1   LINEAR ARRAY EXPERIMENTS

The three resolution patterns on the Cartographic Test Standard (CTS) were scanned and digitized. Each one fits into one imagery frame of 1024 x 512 picture elements at the resolution of 2 mils used for all of the digitizing. The resolution pattern with horizontal lines was scanned at both the normal (fast) scan rate and the slow scan rate. The vertical and diagonal line patterns were scanned at the slow rate. The normal scan takes approximately one minute, the slow scan about 25 minutes.

The imagery printouts were examined to determine the quality of the digitized imagery. A comparison of frames 1 and 4, the slow and fast scans of the horizontal lines, reveals no differences in the sharpness of the line edges, the apparent line width, or the line resolution. Thus the

Table 6-1 CARTOGRAPHIC TEST IMAGERY SELECTED FOR ANALYSIS

Frame Number	Imagery Source Description	Scan Speed
1	Resolution Pattern - Horizontal Lines	Slow
2	Resolution Pattern - Vertical Lines	Slow
3	Resolution Pattern - Diagonal Lines	Slow
4	Resolution Pattern - Horizontal	Fast
5	Semicircles 1-5	Fast
6	Semicircles 5-10	Fast
7	Semicircles 9-14	Fast
8	Semicircles 11-15	Fast
9	Composite Version	Slow
10	Composite Version	Fast

mechanical scanner drive is adequately damped. Figures 6-1 and 6-2 are
portions of the imagery printout for the two frames 1 and 4. The electronic
scan is in the Y direction, perpendicular to the lines, the mechanical scan
is in the X direction, parallel to the lines.

Examination of the line edge imagery reveals that the lines have
intensity shoulders about two pixels wide. That is, to transition from a
maximum black of a line (the letter F, gray level 15) to a maximum white
(the number 0, gray level 0) of the background, takes 2 to 3 pixels. The
exact number of pixels between F and 0 on an edge depends on the spatial
quantization of the image which in turn is a function of the relative
(random) positions of the sensor and the cartographic documents. The gray
level shoulders are equal in width independent of line width or line
orientation. In general, no preferential orientation effects were observed.
A portion of the diagonal resolution line imagery is given in Figure 6-3.
This figure shows the 4th set of parallel lines and parts of the 3rd and
5th sets (the widest set being numbered as the 1st). Imagery containing
vertical lines, from set number 1 is given in Figure 6-4. This imagery
is from Frame No. 3 which has the diagonal lines. However, the frame also
does cover a small part (for $X > 982$) of the vertical line resolution pattern.

The resolution pattern consists of 8 sets of 6 parallel lines of
decreasing line width and spacing. Figure 6-5 shows part of the 5th and
all of the 6th, 7th, and 8th sets of parallel lines in the horizontal
resolution pattern. The lines are adequately defined up to and including
the 6th set which has lines approximately 5 mils in width. It is concluded
from this that a good rule of thumb is that the minimum perceivable line
is 2½ resolution points wide. The lines in the 7th set could be defined
by a filtering step, if required. The lines in the 8th set (2 mil width)
are not discernable.

Although a pixel resolution of 2 mils is good only down to line
widths of about 5 mils when the lines are close together, isolated lines

6-3
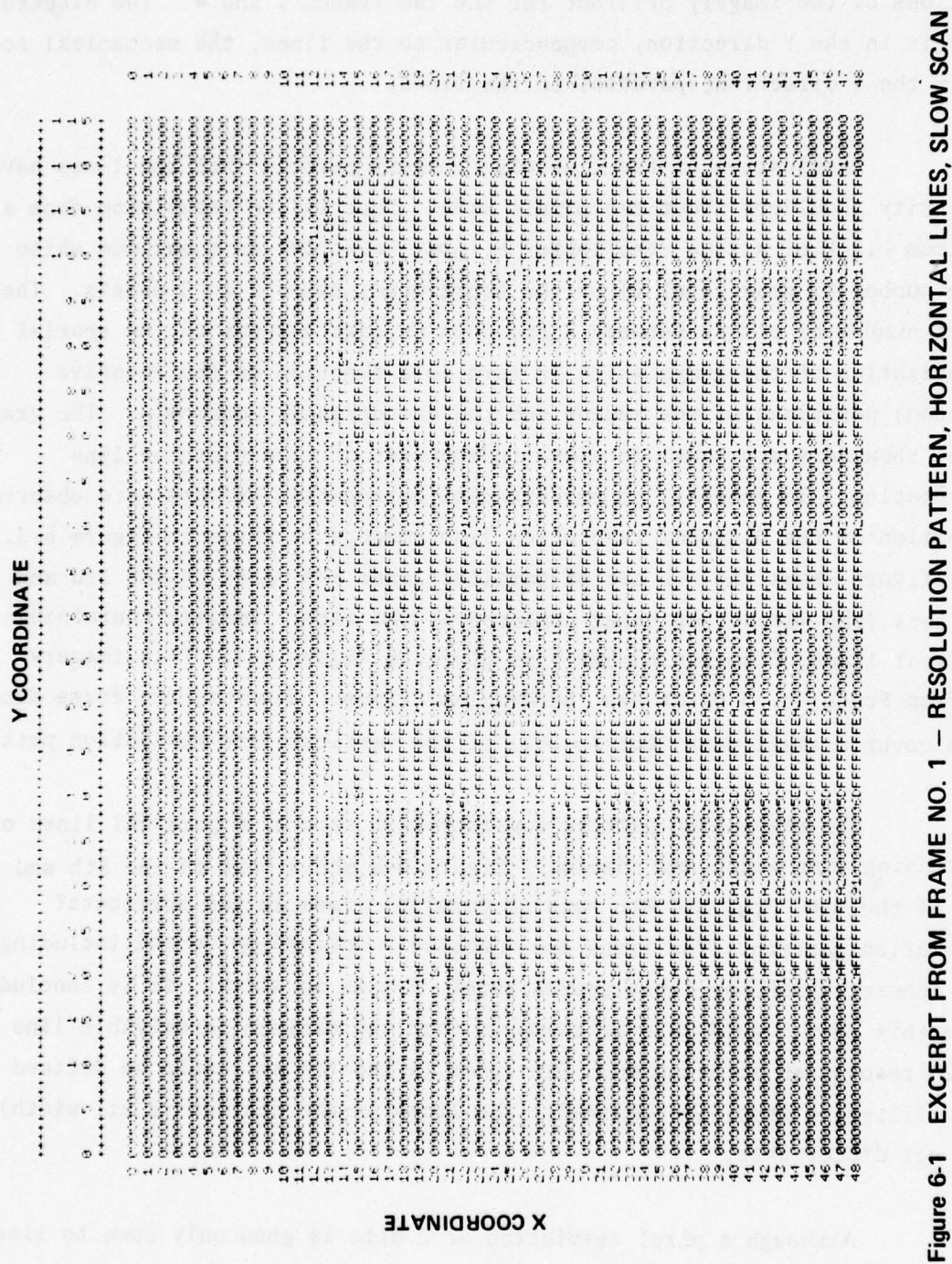
Figure 6-1   EXCERPT FROM FRAME NO. 1 — RESOLUTION PATTERN, HORIZONTAL LINES, SLOW SCAN
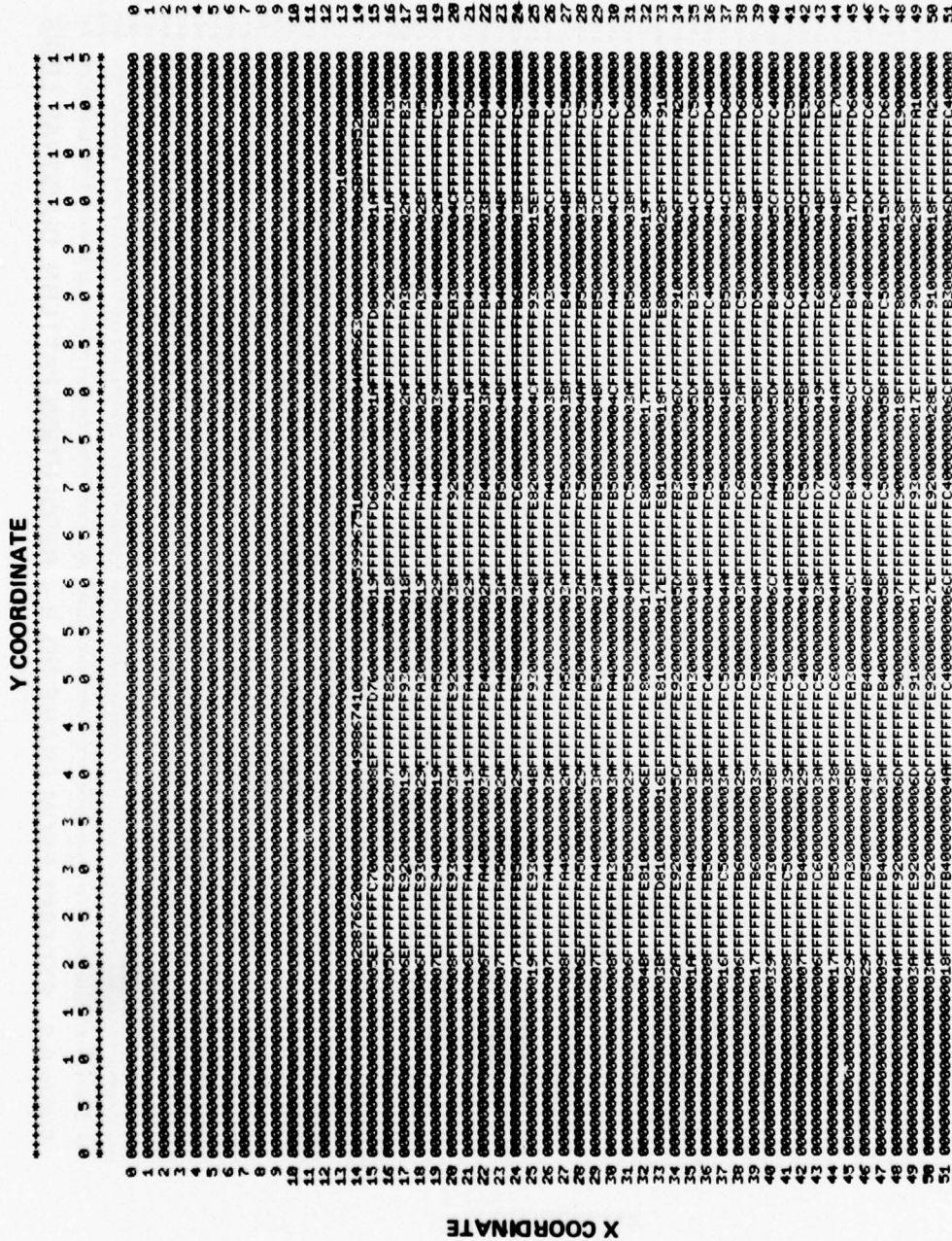
Figure 6-2 EXCERPT FROM FRAME NO. 4 — RESOLUTION PATTERN, HORIZONTAL LINES, FAST SCAN

Y COORDINATE

X COORDINATE
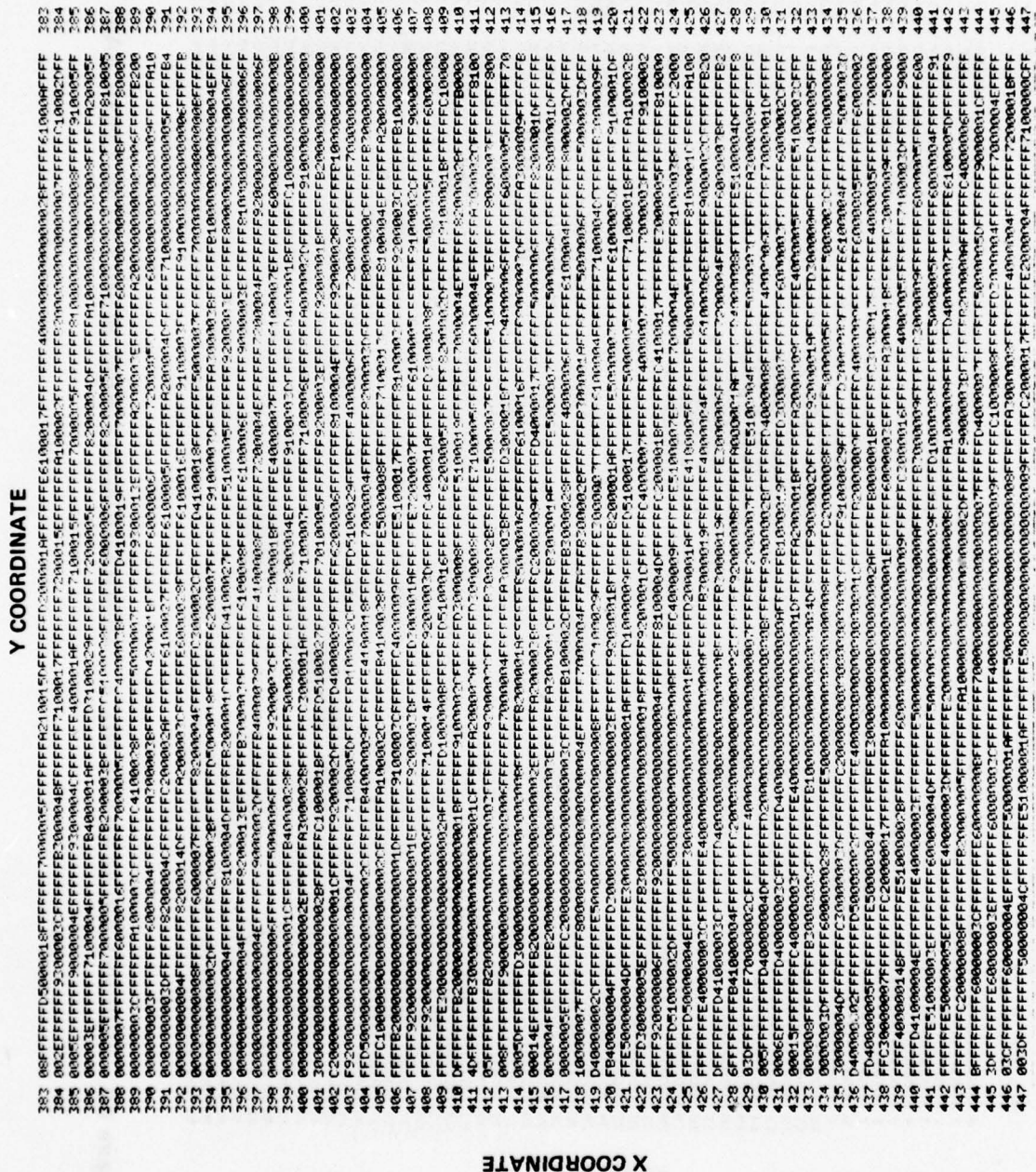
Figure 6-3 EXCERPT FROM FRAME NO. 3 – RESOLUTION PATTERN, DIAGONAL LINES

Figure 6-4   EXCERPT FROM FRAME NO. 3 – RESOLUTION PATTERN SHOWING VERTICAL LINES
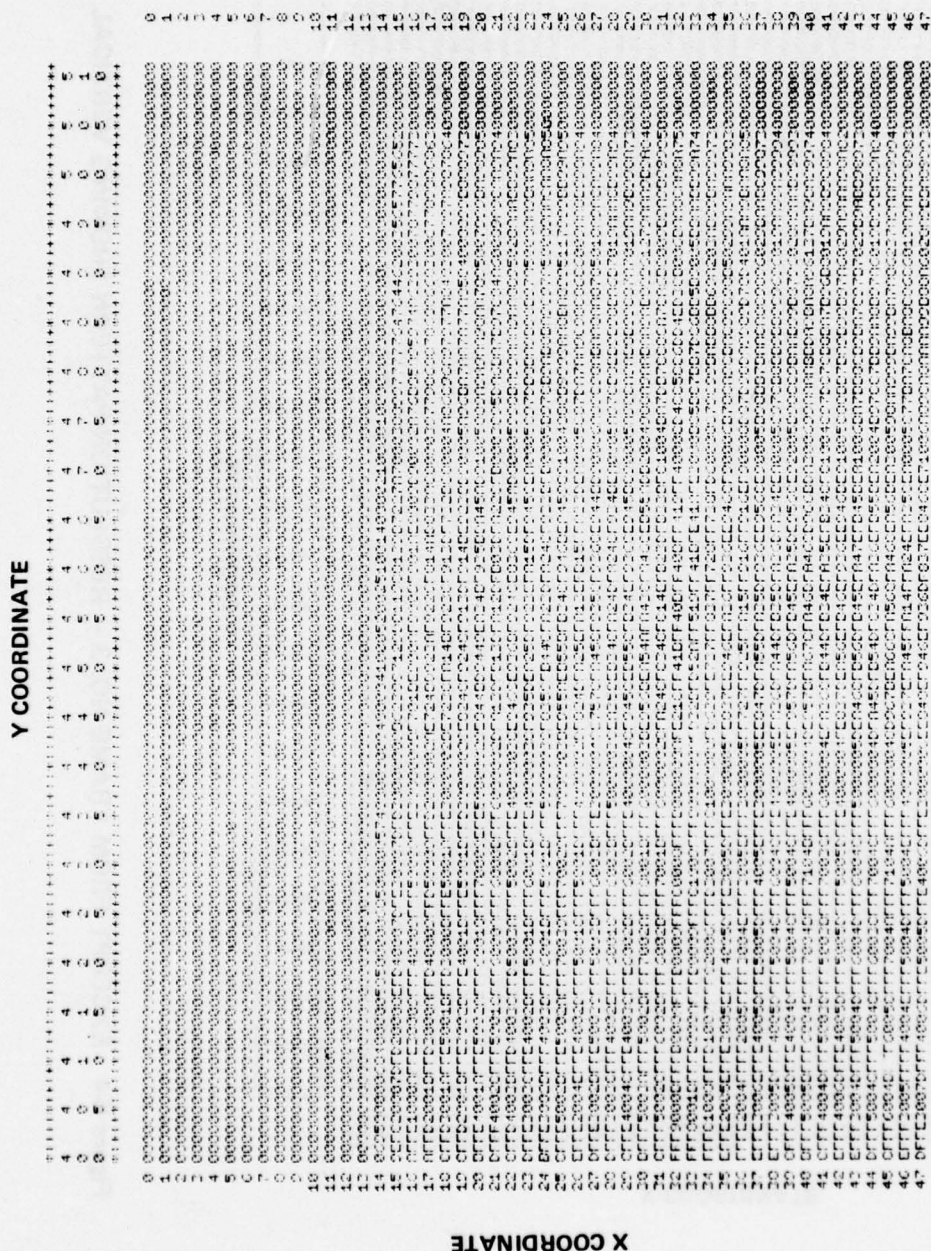
Figure 6-5   EXCERPT FROM FRAME NO. 4 — RESOLUTION PATTERN, HORIZONTAL LINES, SHOWING RESOLUTION LIMIT

6-8

of narrower width will be perceived. The 1 mil wide semicircle was
clearly picked up at the 2 mil resolution (Frame No. 5). The maximum
pixel value obtained at the middle of the line was 4 out of a possible
(maximum black) value of 15. (The background pixels have value 0.) That
is, the 1 mil line is detected as a faint gray line against a white back-
ground. Four pixels are above the background; the apparent line width is
8 mils.

The edges of the lines are blurred somewhat in the sensing
operation. There are two causes for this effect. One is the spatial
quantization of the array. On an edge the photosensitive elements will be
partly on the black line and partly on the white background. The second
cause is the optical diffraction of the light at the line edge. This
effect starts to become noticeable as 1 mil resolution is approached.

6.2   GEOMETRIC ARRAY EXPERIMENTS

The geometric array experiments used the imagery data in frames
5 through 10, listed in Table 6-1. The first four frames are of the 15
semicircles on the CTS. These frames overlap each other slightly. The
semicircles, whose line widths range in increasing steps from 1 mil to
20 mils, were used to test the geometric arrays against isolated lines of
varying widths. Figure 6-6 shows Frame No. 6. This frame contains portions
of the 5th through the 10th semicircles. The line widths are 5 mils through
10 mils in steps of 1 mil.

Two frames, 9 and 10, are portions of the composite version of
the CTS. Frame No. 9 contains lines that are close together and lines that
have small radii of curvature. Frame No. 10 contains (for the most part)
intersecting straight lines. These two frames are shown in Figures 6-7
and 6-8. These figures and Figure 6-6 are photographs taken from the face
of a Tektronix 611 storage oscilloscope which was used to display the map
images.
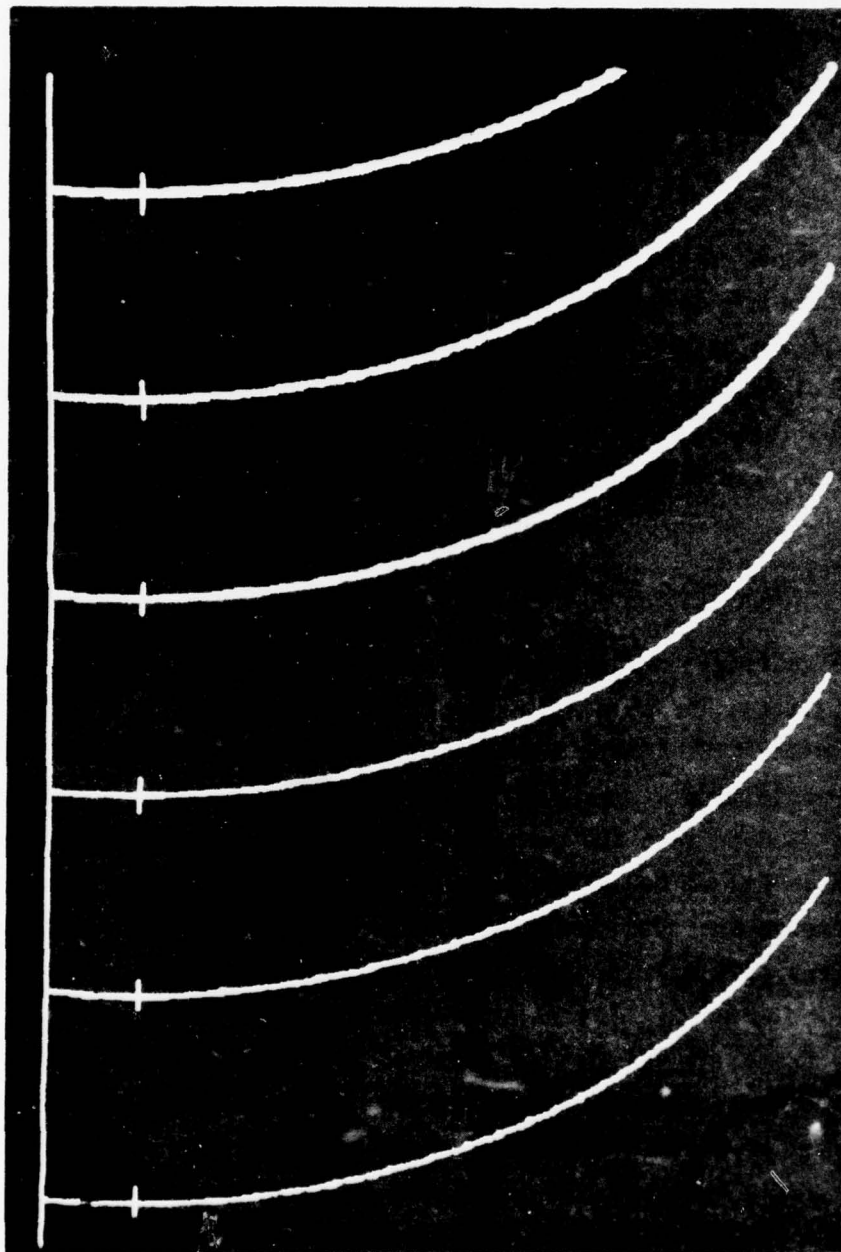
Figure 6-6 FRAME NO. 6 – SEMICIRCLES 1 THROUGH 5

Figure 6-7 FRAME NO. 9 – COMPOSITE VERSION, CURVED LINES

6-11
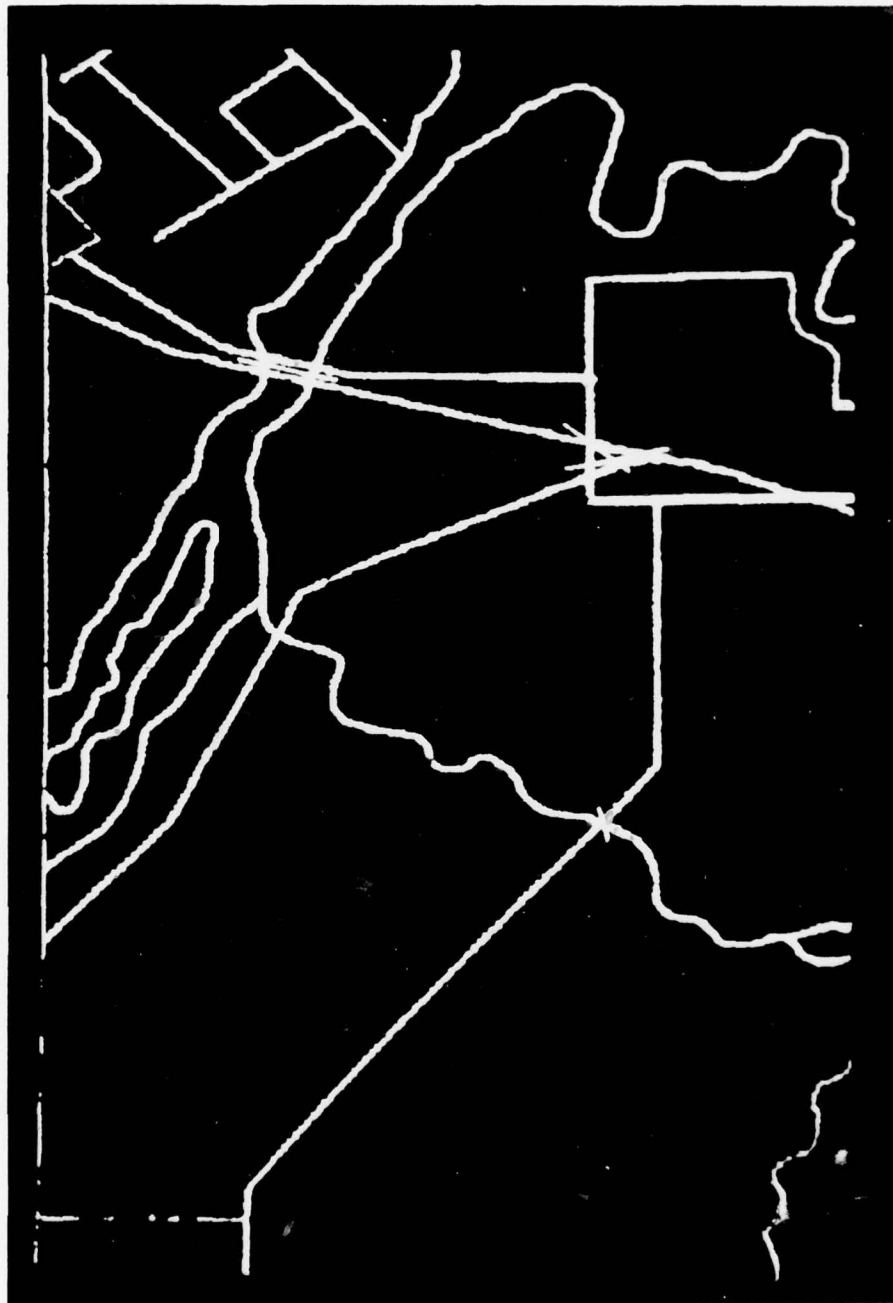
Figure 6-8 FRAME NO. 10 – COMPOSITE VERSION, INTERSECTING STRAIGHT LINES

6.2.1   Donut Tracks

A donut track is a straight line along which the center of the donut or geometric array is stepped. In Section 5.2.3, it was described how the donut tracks were interactively selected and how the simulation was run. A step size of one pixel between donuts was used for all tracks.

The donut tracks chosen are depicted by short straight lines in Figures 6-6, 6-7, and 6-8. The donut tracks in Figure 6-6 can be seen to cross the semicircles at approximately right angles near their center. The donut tracks in Frames 5, 7, and 8 (not shown) are similarly positioned.

Six donut tracks were chosen in Frame No. 9. These are shown in Figure 6-7. Tracks 1 and 2 were chosen to cut a thick line having a short radius of curvature. Tracks 3, 4, and 5 intersect a thin line which has a very short radius of curvature. Track No. 6 cuts across two lines which are very close together.

Frame No. 10 contains four donut tracks. The first two tracks pass through line intersections. The other two tracks are placed to pass near line intersections.

A donut track is specified by the X and Y coordinates of the ends of the track line. The coordinate system of the scanner was used in this study. For each frame of data recorded, an arbitrary X-Y coordinate system was established by the scanner. X runs from 0 to 1023, Y from 0 to 511. The coordinates of the ends of the track lines are listed in Table 6-2 for the DIGIMAP donut. The coordinates are slightly different for the TOPS donut track lines because the TOPS donut differs in size and shape slightly from the DIGIMAP donut. The coordinate differences, where they occur, are usually only 1 or 2 pixels and in no case are more than 4 pixels. The coordinates are used to reference the imagery printouts (excerpts have been given in Figures 6-1 through 6-5) and the donut data printouts (to be described next).

6-13

Table 6-2 TRACK LINE COORDINATES

Frame Number	Donut Track Number	Starting Point Coordinates		Ending Point Coordinates	
		X	Y	X	Y
5	1	228	435	252	435
	2	403	435	425	435
	3	570	435	600	435
	4	752	435	776	435
	5	925	435	953	435
6	1	29	450	55	450
	2	203	450	228	450
	3	376	450	406	450
	4	552	450	580	450
	5	728	450	756	450
	6	900	450	934	450
7	1	22	440	57	440
	2	196	440	236	440
	3	371	440	413	440
	4	547	440	587	440
	5	726	440	766	440
	6	903	440	943	440
8	1	29	430	64	430
	2	204	430	239	430
	3	379	430	415	430
	4	554	430	590	430
	5	729	430	769	430
9	1	292	78	292	116
	2	302	75	302	122
	3	313	430	366	430
	4	313	441	362	441
	5	325	413	353	459
	6	606	419	606	473
10	1	359	154	389	160
	2	669	138	713	182
	3	676	181	693	108
	4	751	324	768	387

6-14

6.2.2   Simulation Data

The behavior of the two simulated geometric arrays was studied by examining the donut data printouts and the imagery printouts. The data from the donut computations was captured on the fly as it was calculated and printed out. The formats used for the donut data are given in Tables 6-3 and 6-4. This data made it possible to observe the inner workings of each donut as it approached, crossed, and receded from line data.

A set of data was printed out for each position of the geometric array. An example of the printout for the DIGIMAP donut is given in Figure 6-9. This example is from the 4th track line in the 6th frame. The coordinates of the center of the geometric array are (569, 450). In this example the donut is approximately centered on a line whose width is 9 pixels. (The actual line is the 8th semicircle which is 8 mils wide.) As the maximum array dimension is 15 pixels, the donut extends past or covers the line. Two directions have been computed: PDX 2 18 30. The directions are encoded according to which of the 16 apertures (see Figure 4-2) is closest to the line directions. The apertures are numbered from 0 to 15 starting at the -Y axis and proceeding counterclockwise. The direction is encoded as twice the aperture number. In the DIGIMAP array an additional 16 directions are computed by interpolation.

The two directions computed, 18 and 30, correspond to the 9th $(18 \div 2)$ aperture and the 15th $(30 \div 2)$. The direction angles are $+112.5^{\circ}$ and $+247.5^{\circ}$ using the customary angle convention of the positive X axis being the reference direction of 0°. The second column of numbers from the right in Figure 6-9 gives the aperture sums or intensities. It is seen that peak intensities of 68 and 63 occur at the 9th and 15th apertures respectively. It should be noted that in the data printout for the DIGIMAP donut the lines starting with PD4 and PD5 occur only when multiple maxima have been detected and the program has entered the extrema pair deletion loop. (See Figure 4-4.)

Table 6-3 DIGIMAP DONUT PRINTOUT FORMAT

$\underline{@}$ $\underline{X}$ $\underline{Y}$

@:	identifies donut position printout
X:	X coordinate of donut position center of donut
Y:	Y coordinate of center of donut position

PD2 v_i a_{i1} a_{i2} a_{i3} a_{i4} a_{i5} a_{i6} $a_{i\Sigma}$ $a_{i\Delta}$ $(a_{i\Delta_1})$

PD2:	identifies DIGIMAP donut aperture element, sum, and difference printout
v_i:	aperture number
a_{i_1} thru a_{i_6}:	elements of aperture
$a_{i\Sigma}$:	aperture sum
$a_{i\Delta}$:	Delta of current aperture minus previous aperture
$a_{i\Delta_1}$:	Delta of first aperture minus last aperture, appears only on last line of PD2 printout

PD3 a b c d e f g h i j k

PD3:	identifies DIGIMAP donut
a:	total sum of the 16 aperture sums
b:	average of total sum (a), rounded
c:	aperture number of first minimum aperture
d:	(negative of) minimum aperture sum $\rightarrow$ DMIN
e:	(negative of) maximum aperture sum $\rightarrow$ DMAX
f:	Delta maximum aperture sum minus minimum aperture sum $\rightarrow$ PTHRES
g:	(negative of) background threshold = minimum aperture sum plus g = DMIN + $\dfrac{(DMAX-DMIN)}{4}$ $\rightarrow$ DMIN

Table 6-3 DIGIMAP DONUT PRINTOUT FORMAT
(CONTD)

	i:		(negative of) minimum allowed Delta between minimum and maximum aperture sums CTHRES.
	j:		PTHRES - CTHRES: amount background threshold is above or below minimum background threshold.
	k:		1/8 f, rounded down—→PTHRES.

$$\frac{\text{maximum aperture sum - minimum aperture sum}}{8}$$

k appears only if j is positive.

PD4	n	a_1 through a_n	d_1 through d_n where n = 3, 5, or 7
PD5	n	a_1 through a_n	d_1 through d_n

	PD4:	identifies local maximum and minimum printout before testing for deletion of pairs
	PD5:	identifies printout after deletion of maximum and minimum points of a pair, before the count n of points is decremented.
	n:	number of local maximum and minimums
	a_1 thru a_n:	local maximums and local minimums. Odd entries are maximums, even entries are maximums
	d_1 thru d_n:	donut directions for corresponding aperture sums

PDX	n	d_1 through d_n

	PDX:	identifies donut directions found
	n:	number of donut directions found
	d_1 thru d_n:	donut directions found, if any

Table 6-4 TOPS DONUT PRINTOUT FORMAT

<u>@</u> <u>X</u> <u>Y</u>

@:	identifies X and Y coordinates of donut center point
X:	X coordinate of donut center point
Y:	Y coordinate of donut center point

Pn a b c d

r00	r01	r02	r03	r10	r11	r12	r13	r14	r15	r16	r17
r20	r21	r22	r23	r24	r25	r26	r27	r28	r29	r2A	r2B

Pn	identifier
	$n = 1$ raw aperture sum
	$n = 2$ first iteration results
	$n = 3$ final iteration results
a	sum of inner ring zero aperture sums
b	percent of a to be used for background threshold
c	b percentage of a
c	fixed threshold
r00-r03	inner ring zero aperture sums
r10-r17	middle ringe one aperture sums
r20-r2B	outer ring three aperture sums

P4	a
a	an internal vector table information index

P5	a b
a	direction, modulus 32
b	encoded direction and offset information

Table 6-4 TOPS DONUT PRINTOUT FORMAT
(CONTD)

P6   n b_1 through b_n

   n   total number of directions found
   b_i list of directions found

```
@  569  450
PD2    0       1       0       7      13      14      14      49
PD2    1       0       0       0       0       7      13      20  -  29
PD2    2       0       0       0       0       0       1       1  -  19
PD2    3       0       0       0       0       0       0       0  -   1
PD2    4       0       0       0       0       0       0       0       0
PD2    5       0       0       0       0       0       0       0       0
PD2    6       0       0       0       0       1       7       8       8
PD2    7       0       0       0       1       7      14      22      14
PD2    8       1       1       7      14      15      14      52      30
PD2    9      14      14      15      14       8       3      68      16
PD2   10      14      14       8       2       0       0      38  -  30
PD2   11      14       8       2       0       0       0      24  -  14
PD2   12      14       8       2       0       0       0      24       0
PD2   13      14       7       1       0       0       0      22  -   2
PD2   14      15      15      14       8       2       0      54      32
PD2   15      13      13      14      14       8       1      63       9  -  14
PD3  445      28       3       0  -  68      68  -  17  -  17  -  24      44       8
PD4    5      68      24      24      22      63      18      22      24      26      30
PD5    5      68      22      63       0      63      18      26      30       0      30
PD4    3      68      22      63      18      26      30
PDX    2      18      30
```

Figure 6-9   SAMPLE DIGIMAP GEOMETRIC ARRAY SIMULATION DATA PRINTOUT

6-20

A sample set of data from the TOPS donut computations is given in Figure 6-10. This example is also from the 4th track line in the 6th frame, that is the 8th semicircle. The coordinates of the center of the array are (566, 450). This point is where the TOPS donut finds the center of the line. It is close to, but is not exactly the same as the center of the sample DIGIMAP donut which is the center of the line according to the DIGIMAP array.

Two directions have been computed by the TOPS array: P6 2 16 0. The directions are those of the 0th and 8th apertures of the DIGIMAP array. For compatibility with the DIGIMAP array simulation, the TOPS aperture numbers and directions have been converted into the equivalent numbered DIGIMAP aperture numbers and directions. The two angles are 270° and 90°. From Figure 6-10 it can be seen that the directions found correspond to the 0th and 6th apertures of the outer ring.

Note that a P3 data line appears in the TOPS array printout only when more than one iteration of increasing the threshold has been used. (See Figure 4-5.)

6.2.3   Isolated Lines

The donut tracks in Frames 5 through 8 showed the geometric array behavior in crossing a single isolated line at various line widths. The arrays have fixed sizes at fixed resolutions and by their natures are sensitive to line width. For a line which falls within the width ranges of the geometric arrays the behaviors are as follows:

When an array is in the background, no line directions are found. When the DIGIMAP array first encounters a line edge it finds a single direction pointing into the line and perpendicular to it. As the array moves into the line, the single direction splits into two directions which, as the array crosses the line, swing apart until they are pointing in opposite directions, and then swing together again in the opposite sense so that

6-21

```
@    566  450
P1   122    90 -109 - 50
     136  105  140  110   140   25    2   24  140   33    5   31
     141   22    0    0     0   22  139   31    1    2    2   28
P2   122    90 -109 - 50
     136  105  140  110    31    0    0    0   31    0    0    0
      32    0    0    0     0    0   30    0    0    0    0    0
P4     4
P5    16 100007
P4     0
P5     0  71
P6     2   16    0
```

Figure 6-10   SAMPLE TOPS GEOMETRIC ARRAY SIMULATION DATA PRINTOUT

when the array exits the line a single direction is found pointing back at the line.

This phenomenon is illustrated in Table 6-5. It lists the directions found by the DIGIMAP geometric array as it follows the 4th donut track in the 6th frame. The sample array shown in Figure 6-9 is included in this sequence. The way in which the DIGIMAP geometric array directions change as the array crosses a line is illustrated graphically in Figure 6-11.

The TOPS array behaves similarly but is does not point to the line when the array center is outside of the line. The TOPS processing algorithm (see Figure 4-5) will not find any line directions unless the center apertures show the presence of a line. (The DIGIMAP array has no center apertures.) The directions found by the array when it crosses the 8th semicircle, Track No. 4 in Frame No. 6, are given in Table 6-6. This table shows that it picks up the two line directions. When it is on the line edge at X=568, it misses one of the two directions.

If a line is too wide, the array will be totally within its boundaries and no directions will be found. If a line is too narrow no directions will be found also. In both cases there are insufficient differences between the blackest aperture sums and the whitest aperture sums.

6.2.4 Curved Lines

A section of the composite version on the CTS was selected to test the geometric arrays against sharply curving lines and closely spaced lines. Figure 6-7 shows the Frame 9 imagery and the positions of the donut tracks. Tracks 4 and 6 have been selected to show the behavior of the DIGIMAP array.

The imagery from Frame 9 containing Track No. 4 is given in Figure 6-12. The line indicates that portions of the track bounded at

**Table 6-5 DIRECTION DATA FOR THE DIGIMAP GEOMETRIC ARRAY,
TRACK NO. 4, FRAME NO. 6**

Coordinates of Center of Array		Encoded Directions Found	
X	Y		
559	450	–	
560	450	8	
561	450	8	
562	450	8	
563	450	8	
564	450	4	12
565	450	2	14
566	450	2	14
567	450	0	15
568	450	31	16
569	450	30	18
570	450	28	18
571	450	28	18
571	450	28	18
572	450	24	
573	450	24	
574	450	24	
575	450	23	
576	450	–	
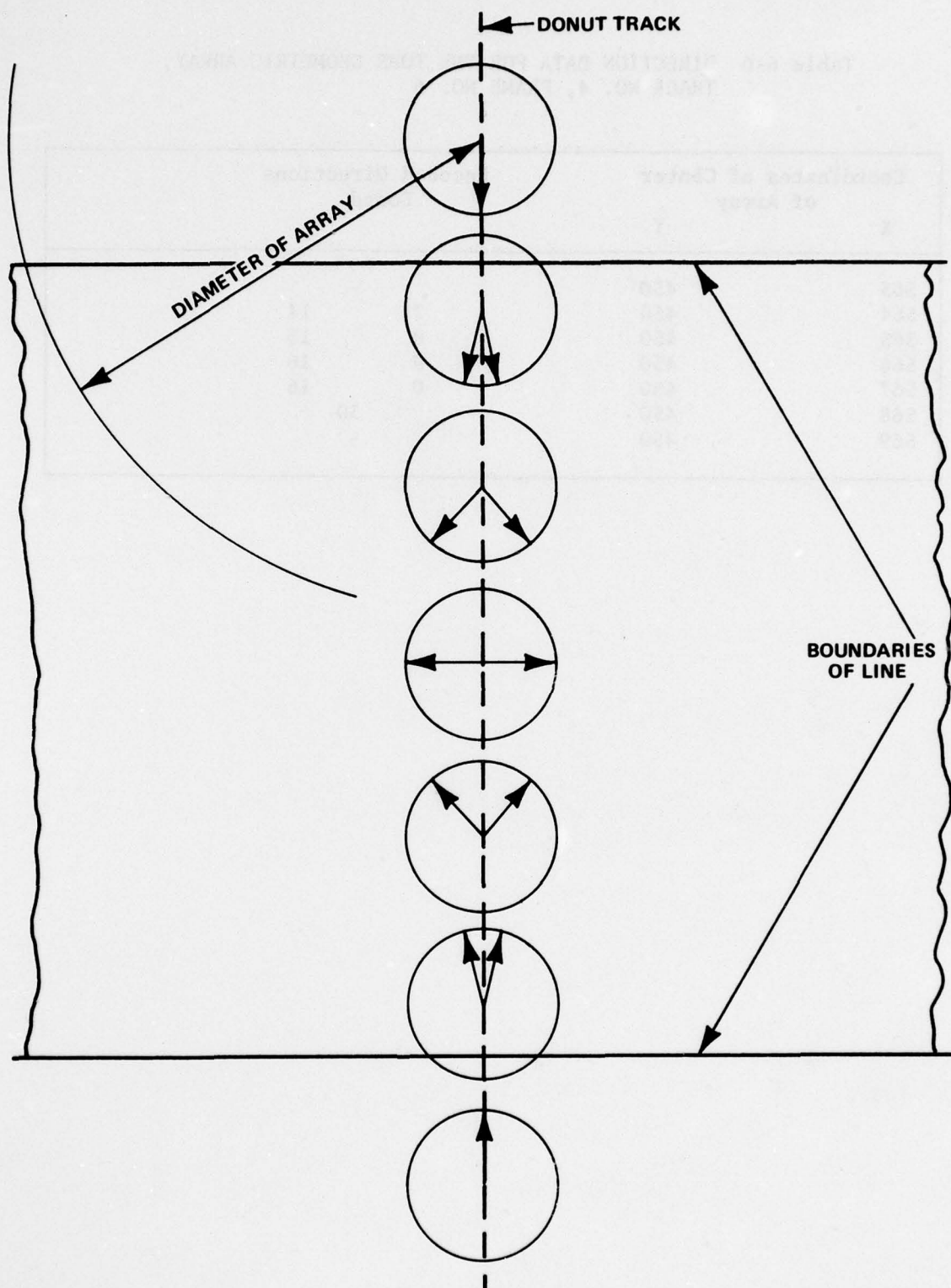
Figure 6-11 SEQUENCE OF DIGIMAP GEOMETRIC ARRAY DIRECTIONS FOR ARRAY CROSSING A LINE PERPENDICULARLY

6-25

Table 6-6 DIRECTION DATA FOR THE TOPS GEOMETRIC ARRAY,
TRACK NO. 4, FRAME NO. 6

Coordinates of Center of Array		Encoded Directions Found	
X	Y		
563	450		-
564	450	2	14
565	450	0	16
566	450	0	16
567	450	0	16
568	450		30
569	450		-

Figure 6-12   FRAME 9 IMAGERY DATA SHOWING TRACK NO. 4

either end (X=319 and X=362) by (DIGIMAP) array positions which find no
line directions. The behavior of the array is examined by seeing how the
line directions computed vary as the donut moves along the track with
increasing values of the X coordinates.

The encoded directions formed by the DIGIMAP array are listed
in Table 6-7 in order of increasing values of the X coordinate. A diagram
is given in Figure 6-13 to aid the reader in relating the directions shown
in Table 6-7 to the imagery data. The points asterisked in Table 6-7 are
circled in Figure 6-12.

The array first points toward the line (direction 9) until it
gets close enough (X=325) to find two directions (6 and 14). It then
continues to find two directions until it reaches a point (X=333) between
two lines when it points backwards to the line it has just left. This
behavior was described in Section 6.2.2. Continuing along the track the
array picks up two directions for the next line which gradually bend
around, folding into a single direction pointing back at the line at
X=345. Then, at X=346, the array points to both the line it has left
(direction 23) and the line it is approaching (direction 8). At X=350 it
stops pointing at the line it has left and starts giving two directions
(4 and 14) for the new (third) line. As the array passes through this
line the directions fold over until a single direction (24) pointing back
at the line is obtained.

The track line does not pass close enough to the end of the
loop, at X=345, to pick up a direction (16) pointing at the end of the
loop.

This DIGIMAP track line data shows the basic behavior of the
DIGIMAP donut as it crosses a short radius, curved line. It illustrates
that no anomalous direction computations occur.

Table 6-7 DIRECTION DATA FOR THE DIGIMAP GEOMETRIC ARRAY,
TRACK NO. 4, FRAME NO. 9

Coordinates of Center of Array		Encoded Directions Found	
X	Y		
*319	441		–
320	441		9
321	441		9
322	441		10
323	441		9
324	441		9
*325	441	6	14
326	441	4	16
327	441	3	15
328	441	18	1
329	441	19	31
330	441	20	31
331	441	20	31
332	441	22	28
333	441		25
334	441	8	25
335	441	8	24
336	441	7	24
337	441	8	25
338	441	4	12
339	441	2	12
340	441	1	14
341	441	15	31
342	441	16	31
343	441	16	30
344	441	18	28
345	441		23
346	441	8	23
347	441	8	23
348	441	8	22
349	441	8	24
350	441	4	14
351	441	2	14
352	441	1	15
353	441	16	31
354	441	17	31
355	441	18	30
356	441	20	28
357	441		24
358	441		24
359	441		24
360	441		24
361	441		24
*362	441		–

*These points are circled in Figure 6-12.
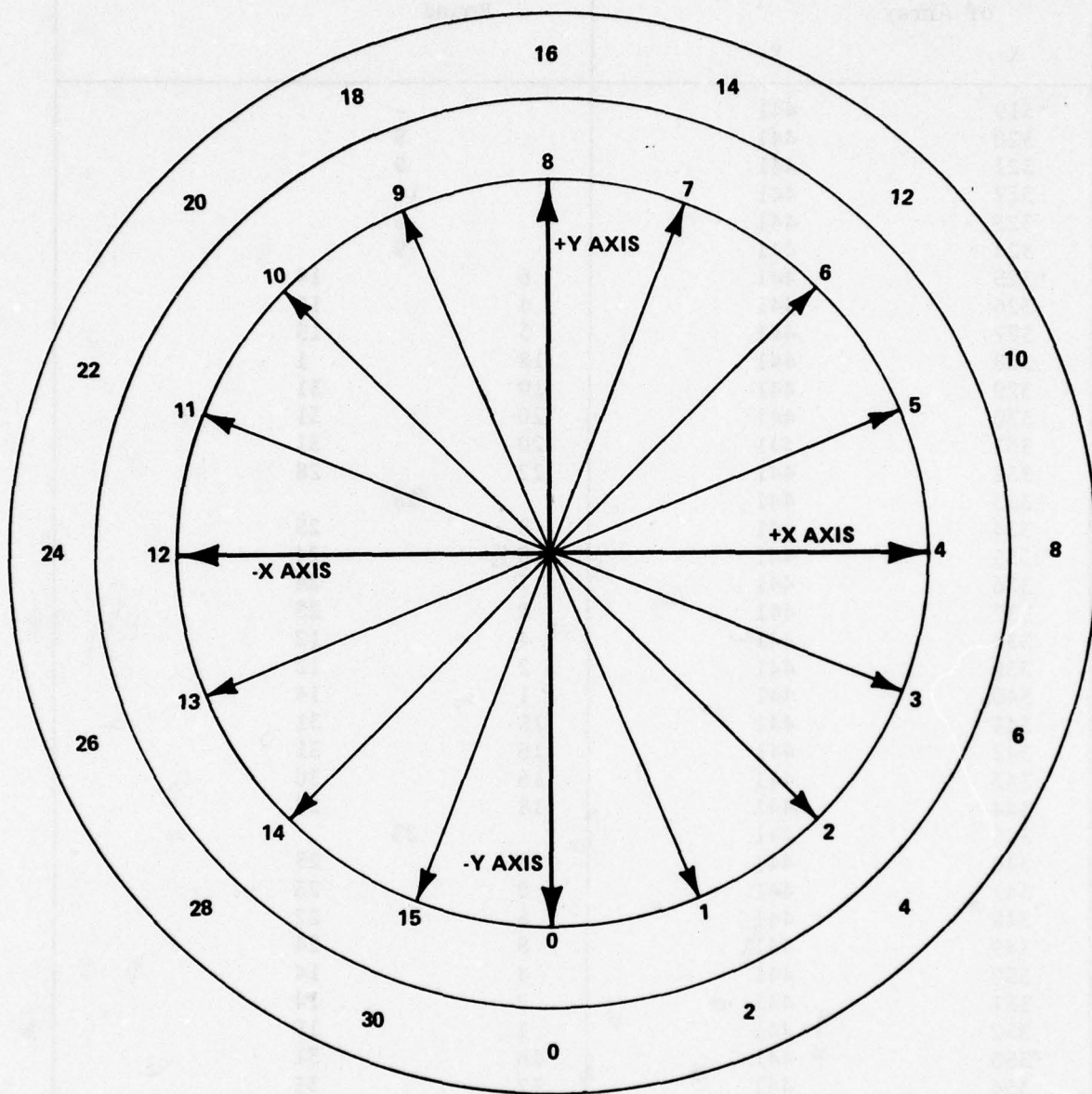
Figure 6-13 GEOMETRIC ARRAY APERTURE NUMBERS (INNER RING) AND DIRECTION ENCODING NUMBERS (OUTER RING)

6-30

The behavior of the DIGIMAP donut crossing two lines close together is determined by examining the data from the 6th track line of Frame No. 9. The imagery containing the track line is given in Figure 6-14. The sequence of directions found by the array as it progresses along the track line in increasing Y is given in Table 6-8 The array first points towards the first line, the single direction splitting into two at Y=426. At Y=432 a new direction, pointing to the second line is added to the two directions pointing along the first line. This behavior continues until at Y=436 the two line directions for the first line merge (0 and 8 into 3) and the direction pointing at the second line splits (19 into 16 and 22). At Y=440 the direction pointing back at the first line (4) is dropped. The two directions of the second line are carried and then merge at Y=446, leaving a direction (3) pointing back at the second line. At Y=448 the array starts pointing forward (17) at the third line as well as continuing to point backward at the second line (4). The backward pointer is dropped at Y=450. The forward pointer is carried until it splits at Y=452. The behavior for the rest of the track is the same as for an isolated line. Two directions are carried, folding back on themselves, merging and pointing back at Y=463, and finally the backwards pointer is dropped at Y=469.

This analysis shows that the behavior of the DIGIMAP geometric array is regular and predictable when lines are close together. The direction effects of each line are essentially superimposed on each other.

The behavior of the TOPS geometric array on a rapidly curving line was observed by examining the 1st and 2nd track lines in the 9th frame. The imagery data is given in Figure 6-15. The TOPS donut direction data is given in Table 6-9 and 6-10 for the two tracks.

The first track line just touches the end of the loop. The donut just points at the line as it passes by.

As the second track line cuts the two sides of the loop in turn
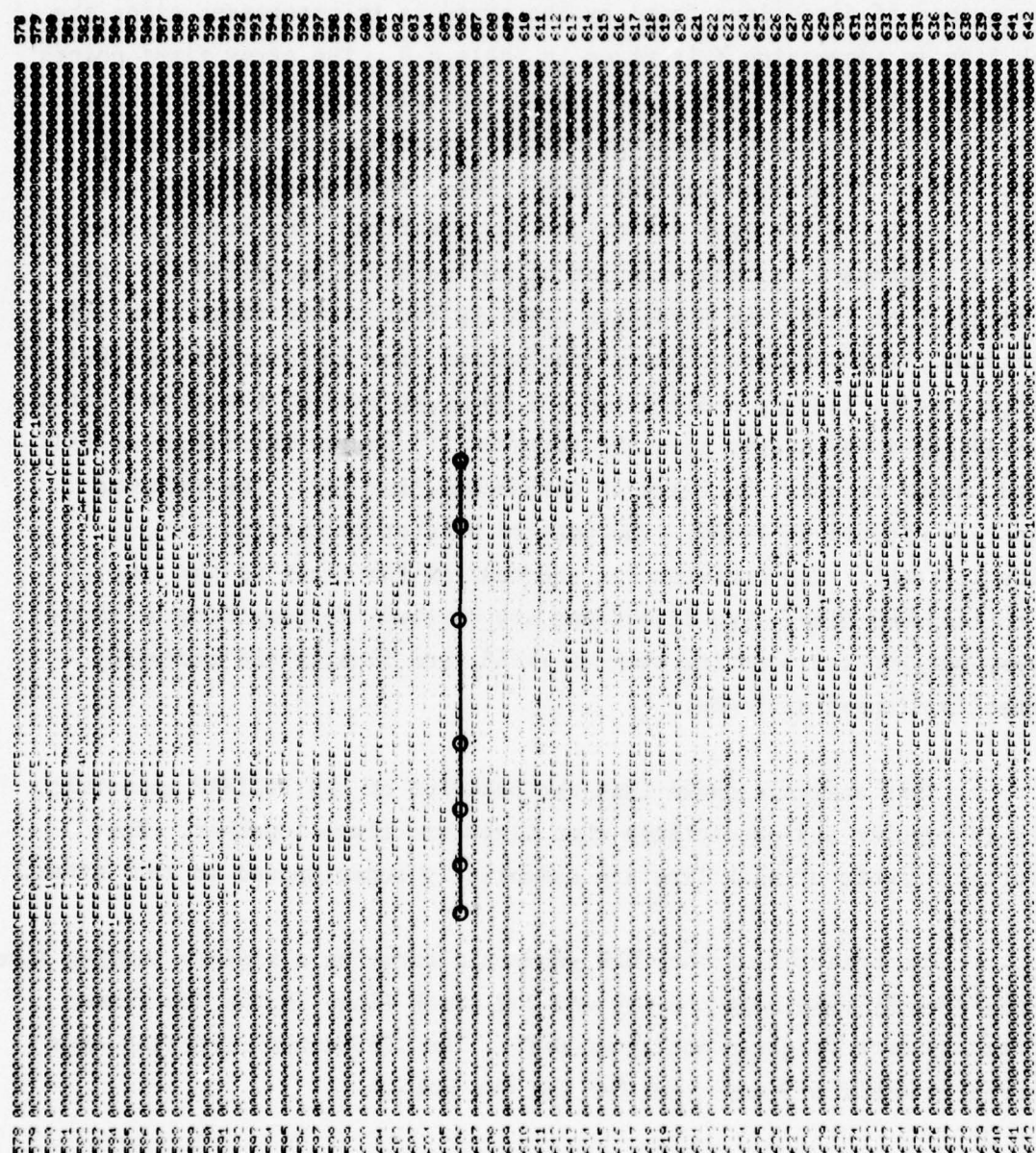
Figure 6-14 FRAME 9 IMAGERY DATA SHOWING TRACK NO. 6

Table 6-8   DIRECTION DATA FOR THE DIGIMAP GEOMETRIC ARRAY,
TRACK NO. 6, FRAME NO. 9

Coordinates of Center of Array		Encoded Directions Found		
X	Y			
*606	421		-	
606	422		18	
606	423		18	
606	424		18	
606	425		18	
*606	426		16	22
606	427		14	22
606	428		14	23
606	429		13	25
606	430		12	25
606	431		11	26
606	432	10	18	28
606	433	8	19	29
606	434	8	18	30
606	435	8	19	0
606	436	16	22	3
606	437	14	24	3
606	438	14	24	3
*606	439	13	25	4
606	440		12	26
606	441		10	27
606	442		10	28
606	443		9	30
606	444		8	30
606	445		6	0
606	446		3	
606	447		3	
606	448		3	17
606	449		4	17
606	450		18	
606	451		19	
*606	452		16	22
606	453		14	24
606	454		14	24
606	455		14	25
606	456		13	26
606	457		12	27
606	458		11	29
606	459		11	30
606	460		10	30
606	461		10	0
*606	462		8	0

Table 6-8 DIRECTION DATA FOR THE DIGIMAP GEOMETRIC ARRAY,
TRACK NO. 6, FRAME NO. 9 (CONTD)

Coordinates of Center of Array		Encoded Directions Found
X	Y	
606	463	4
606	464	4
606	465	4
606	466	4
606	467	4
606	468	3
*606	469	-

*These points are circled in Figure 6-14.

Figure 6-15 FRAME 9 IMAGERY SHOWING TRACKS NO. 1 (X=292) AND NO. 2 (X=302)

Table 6-9 DIRECTION DATA FOR THE TOPS GEOMETRIC ARRAY, TRACK NO. 1, FRAME NO. 9

Coordinates of Center of Array		Encoded Directions Found
X	Y	
*292	91	−
293	92	14
294	93	14
295	94	14
296	95	14
297	96	14
298	97	14
299	98	14
300	99	10
301	100	10
302	101	10
303	102	10
304	103	8
*305	104	−

*These points are circled in Figure 6-15.

Table 6-10 DIRECTION DATA FOR THE TOPS GEOMETRIC ARRAY, TRACK NO. 2, FRAME NO. 9

Coordinates of Center of Array		Encoded Directions Found	
X	Y		
*302	83		-
302	84		18
302	85		18
302	86	8	22
302	87	8	22
302	88	8	22
302	89	6	22
302	90		-
302	91		-
302	92		2
302	93		-
302	94		-
302	95		-
302	96		-
302	97		-
302	98		-
302	99		-
302	100		-
302	101		-
302	102		-
302	103		26
302	104		26
302	105	10	26
302	106	10	26
302	107	10	26
302	108	8	26
302	109	8	26
302	110	8	30
302	111	6	
302	112	6	
*302	113		-

*These points are circled in Figure 6-15.

the donut finds the two directions for each branch of the loop, 8 and 22 for the left branch, 10 and 26 for the right branch. The donut finds no directions when it is inside the loop. The array points towards the lines for only two positions as it approaches the left branch of the loop (at Y=84, 85) and for only two positions (Y=111, 112) as it leaves the right branch. It points back briefly at the first branch at Y=92. No directions are found when it is on the right edge of the left branch at Y=90, 91.

The behavior of the TOPS geometric array for lines close together is demonstrated by the 6th track line of Frame No. 9. (See Table 6-11, the imagery data has been given in Figure 6-14.) The behavior is similar to the DIGIMAP donut behavior on the same track line. It picks up two directions as it crosses the three lines at Y=432, 3, 4, 5. Y=440, 1, 2, 3, 4, and Y=456, 7, 8, 9, 10, 11 respectively. Anomalous directions, both 1, are found at Y=439 points back at the first line. At the points Y=445 and Y=462 only one of the two line directions is found.

When the array is between the first two lines which are very close together it finds no directions for Y=436, 7, and 8. It picks up both lines at only one point, Y=439.

A comparison of the two arrays simulated on the basis of this track line data shows that

(1) the arrays have similar behavior,
(2) the DIGIMAP array behaves regularly and predictably,
(3) the TOPS array behavior is somewhat erratic,
(4) the DIGIMAP array sees both lines when they are close together, and
(5) the TOPS array does not see a line until the center of the array is almost tracking it.

6-38

Table 6-11 DIRECTION DATA FOR THE TOPS GEOMETRIC ARRAY, TRACK NO. 6, FRAME NO. 9

Coordinates of Center of Array		Encoded Directions Found		
X	Y			
606	428	-		
606	429	14	24	
606	430	14	26	
606	431	12	1	
606	432	10	26	
606	433	10	26	
606	434	10	30	
606	435	22	8	
606	436	-		
606	437	-		
606	438	-		
606	439	6	14	24
606	440	14	26	
606	441	12	26	
606	442	10	26	
606	443	10	28	
606	444	10	30	
606	445	10		
606	446	-		
606	447	-		
606	448	-		
606	449	-		
606	450	-		
606	451	-		
606	452	-		
606	453	-		
606	454	-		
606	455	14	1	
606	456	14	26	
606	457	14	26	
606	458	12	26	
606	459	12	28	
606	460	10	30	
606	461	10	30	
606	462	30		
606	463			

6.2.5   Intersecting Lines

The composite version imagery of Frame No. 10 provided the opportunity to examine the behavior of the geometric arrays at and near line intersections. Figure 6-16 shows two lines crossing with a track line passing through the intersection. The sequence of DIGIMAP geometric array directions for this track line are given in Table 6-12.

The array first picks up the upper left arm of the X (5) and then both of the upper arms (6, 14). As the array moves through the center of the intersection it picks up the directions of the four arms most of the time that it is centered within the line intersection (at X=374, 375, 377, and 378). When the array is entering or leaving the intersection the array points to the nearby lines but does so in a somewhat irregular manner.

The DIGIMAP array picks up the four directions as desired when passing through the line intersection except when it is at the very center of the intersection (X=376). The array is size matched to the single lines but is slightly too small to handle the intersection itself. As has been noted before, it points towards the nearby lines when it is not actually on a line.

The behavior of the TOPS geometric array on this same track line is examined next. The sequence of computed directions through the line intersection is given in Table 6-13. No directions are picked up except when the center of the array is on the intersection or very close to it. At one point (X=377) three directions are picked up; otherwise only one or two are found.

This array has little flexibility in accommodating a range of line widths. The line width at the intersection is too great for it to handle.

The second track line in Frame No. 10 passes through another

6-40

Figure 6-16 FRAME 10 IMAGERY DATA SHOWING TRACK NO. 1

Table 6-12   DIRECTION DATA FOR THE DIGIMAP GEOMETRIC ARRAY,
TRACK NO. 1, FRAME NO. 10

Coordinate of Center of Array		Encoded Directions Found					
X	Y						
364	155			-			
365	155			5			
366	155			5			
367	155			6			
368	156		6		14		
369	156		6		14		
370	156			8			
371	156			8			
372	157		12		16		
373	157	0	8			18	
374	157	30	8		12		18
375	157	30	6		12		18
376	157		6		17	29	
377	158	14	20		28		4
378	158	16	20		28		4
379	158	16	20			4	
380	158		22		2		
381	159		26		0		
382	159			25			
383	159			26			
384	159			26			
385	160		22		30		
386	160		22		30		
387	160			-			

6-42

Table 6-13 DIRECTION DATA FOR THE TOPS GEOMETRIC ARRAY, TRACK NO. 1, FRAME NO. 10

Coordinates of Center of Array		Encoded Directions Found			
X	Y				
370	156		-		
371	156		10	30	
372	157		10	30	
373	157			12	
374	157			14	
375	157		20	28	
376	157		20	28	
377	158	4		16	22
378	158			26	
379	158		26	2	
380	158			-	

line intersection. The sample imagery is given in Figure 6-17. The direction data is presented in Table 6-14 for the DIGIMAP array. As the array crosses the first line it is not affected by the other lines. When it approaches the intersection it picks up first the left branch at X=688 and then adds the right branch at X=690. Then the array points at the intersection. Once the array center is in the intersection directions are given for the lines but not for all four directions consistently. After exiting the intersection the array points back at the lines.

The TOPS geometric array behaves similarly but picks up fewer directions. The directions found are given in Table 6-15. It picks up three of the four directions at most when in the intersection area.
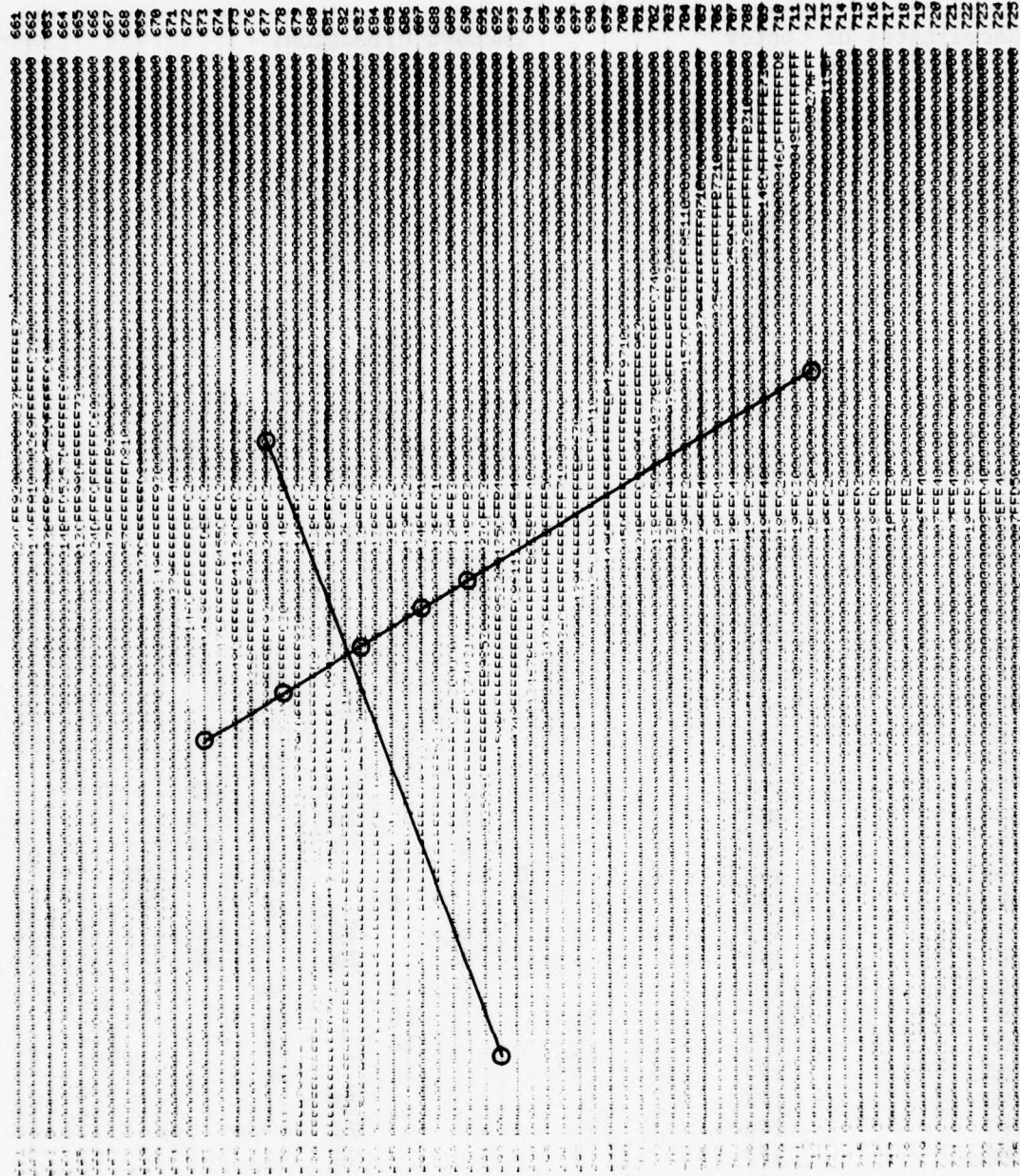
Figure 6-17 FRAME 10 IMAGERY DATA SHOWING TRACK NO. 2 (STARTING AT X=673) AND TRACK NO. 3 (STARTING AT X=677)

Table 6-14 DIRECTION DATA FOR THE DIGIMAP GEOMETRIC ARRAY
TRACK NO. 2, FRAME NO. 10

Coordinates of Center of Array		Encoded Directions Found				
X	Y					
*673	142			-		
674	143			9		
675	144			10		
676	145			9		
677	146			10		
*678	147			4	16	
679	148			4	16	
680	149			2	18	
681	150			0	21	
682	151			30	20	
*683	152			30	24	
684	153			27		
685	154			26		
686	155			27		
*687	156			-		
688	157			6		
689	158			6		
*690	159			6	16	
691	160			6	16	
692	161			11		
693	162			11		
694	163			12	20	
695	164		2	12	22	
696	165		2	10	22	
697	166		0	8	23	
698	167	0		8	12	24
699	168	0		6	14	26
700	169		6	15	26	
701	170		4	16	30	
702	171		2	16		
703	172			18	30	
704	173			18	28	
705	174			18	26	
706	175			23		
707	176			22		
708	177			22		
709	178			22		
710	179			23		
711	180			23		
*712	181			-		

*These points are circled in Figure 6-17.

6-46

Table 6-15 DIRECTION DATA FOR THE TOPS GEOMETRIC ARRAY, TRACK NO. 2, FRAME NO. 10

Coordinates of Center of Array		Encoded Directions Found				
X	Y					
676	145				-	
677	146		2	12		
678	147		2		18	
679	148				-	
680	149		0		18	
681	150		1		22	
682	151				-	
683	152				-	
684	153				-	
685	154				-	
686	155				-	
687	156				-	
688	157				-	
689	158				-	
690	159				-	
691	160				-	
692	161				-	
693	162			10		
694	163			10		
695	164		0		14	
696	165		0		14	
697	166	0		12		24
698	167	8		16		24
699	168		16		30	
700	169		16		30	
701	170		20		26	
702	171				-	

6-47

Section 7
ARRAY TECHNOLOGY

In order to effectively utilize solid state photosensors for cartographic scanning, it is necessary to thoroughly understand device parameters as they relate to scanner performance. The following sections discuss the most critical sensor parameters which must be considered in scanner design and the illumination required for proper sensor utilization.

7.1   DISCRETE PHOTOSENSORS

There are two basic types of discrete solid state photosensors in use today:

    (1) Photoconductive bulk effect cells
    (2) Photodiodes

The photoconductive bulk effect cells are normally made of CdS (Cadmium Sulfide) or CdSe (Cadmium Selenide) and behave like resistors whose resistance decreases nonlinearly as the incident light intensity increases. These devices have response times ranging between 1 millisecond and 1 second, and they exhibit hysteresis or light memory. Therefore, they are suitable for rough sensing applications such as detecting the presence of an object on an assembly line but they are not suitable for high resolution scanning.

Photodiodes can be operated as photovoltaic devices without bias or with a forward bias, or as photoconductive devices with a back bias. In the photovoltaic mode of operation, the cell response ranges from a linear function of the incident illumination at zero bias to a logarithmic function for large load resistance values (open circuit operation). Cell response time is generally in the range of from 1 to 100 microseconds for photovoltaic operation. Unbiased operation is of particular advantage for sensing low level DC light signals because of the absence of any dark

7-1

current in this mode of operation. Light signals with a minimum detectable power as low as 10^{-13} watts can be sensed in the unbiased photovoltaic mode.

Photodiodes operated in the back-biased or photoconductive mode behave like constant current generators with output current directly proportional to the incident light intensity. The response function exhibits excellent linearity and cell responsivity can be maximized in this mode of operation. In addition, cell response times on the order of 10 nanoseconds can be achieved and these devices do not exhibit hysteresis. Therefore, back-biased photodiodes are excellent for most scanning applications.

Typical 50% response points are at 550 nm and 1.0 μm, with peak response at about 850 nm. Sensitivity at the spectral peak is 0.4 microamps per microwatt of incident radiation at the spectral peak (850 nm).

Specially shaped photodiode arrays can be supplied by several manufacturers. Cells have been constructed in a variety of geometric forms with lengths to ten inches, diameters to two inches, and in arrays with densities to 150 elements per linear inch.

7.2   PHOTODIODE PARAMETERS

Responsivity

The generation of current by light in a silicon cell is a quantum effect, i.e., one incident photon produces one electron-hole pair. The incoming light beam thus represents a stream of electrons or electrical current. The photon current flow has units of watts, since each photon is represented by a unit of energy expressed in joules and a watt is the flow per second of a joule of energy. Responsivity is a measure of the effectiveness of the light current transduction process in a silicon cell. The responsivity will vary with changes in wavelength of the incident light and will also vary slightly with changes in the applied voltage and with changes in temperature. The reason for the responsivity change with

wavelength is that the light reflection and absorption coefficients of silicon change with wavelength. The applied voltage affects the collection process of the photogenerated electron-hole pairs within silicon and thus alters the responsivity. Temperature changes affect both the optical constants of the silicon cell and the collection process, also varying the responsivity. For photodiodes operated in the photoconductive mode, responsivity:

(1) Increases an average of 0.1% per volt of applied reverse bias.
(2) Increases an average of 0.2% per °C of temperature rise.

Responsivity variation with wavelength is called the spectral response. A typical spectral response curve for a planar diffused photodiode is shown in Figure 7-1.

Response Time

The construction of a planar diffused diode is shown in Figure 7-2. Oxide is grown on the silicon wafer, a hole is etched in the oxide, and an impurity diffused into the silicon through the oxide that forms a junction. The back side of the slice is then diffused with an ohmic plus contact. The relationship between electric field and penetration or depletion depth and applied voltage is $d = \frac{1}{2}\sqrt{\rho V}$, where V is the applied voltage, ρ is the resistivity of silicon, and d the depth in microns.

If a light beam is instantaneously turned on a photodiode, it takes a certain time for photogenerated current carriers to flow in the external circuit. This is called the rise time (T_r) of the detector. If the light beam is instantaneously turned off, it takes a certain time for the photogenerated current to stop flowing. This is called the decay time (T_d) of the detector. The three basic factors governing response time are:

7-3
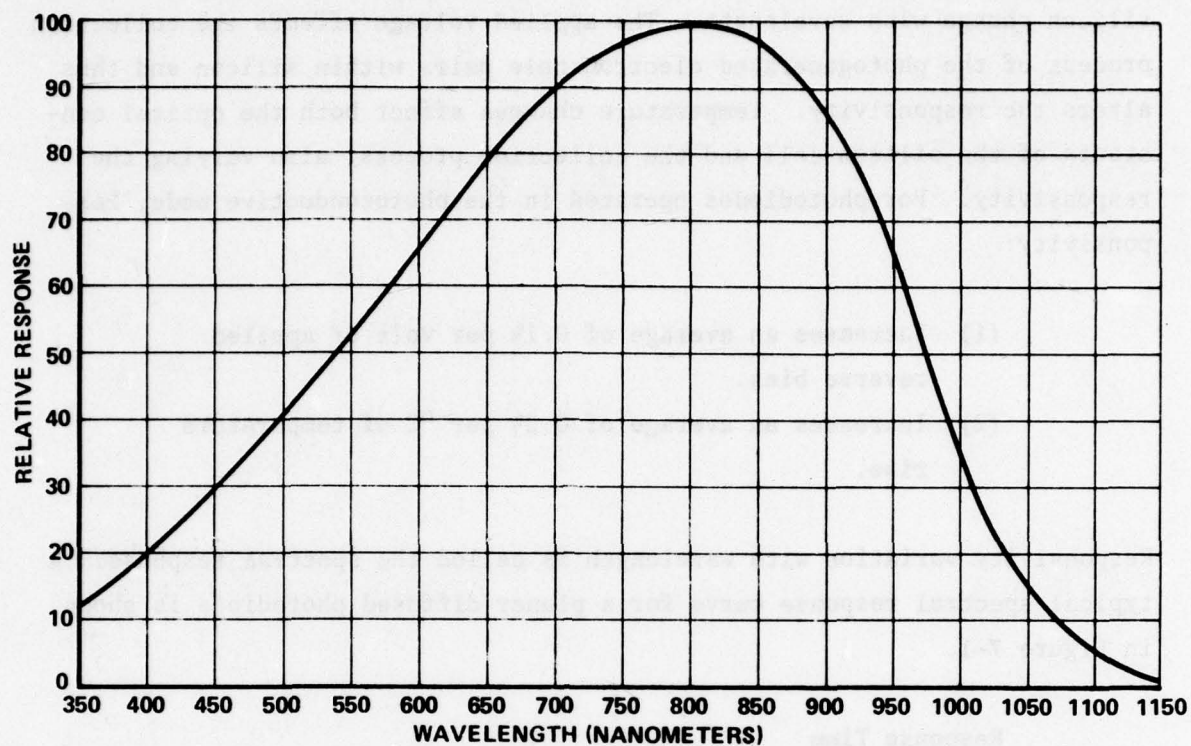
Figure 7-1 PHOTODIODE SPECTRAL RESPONSE
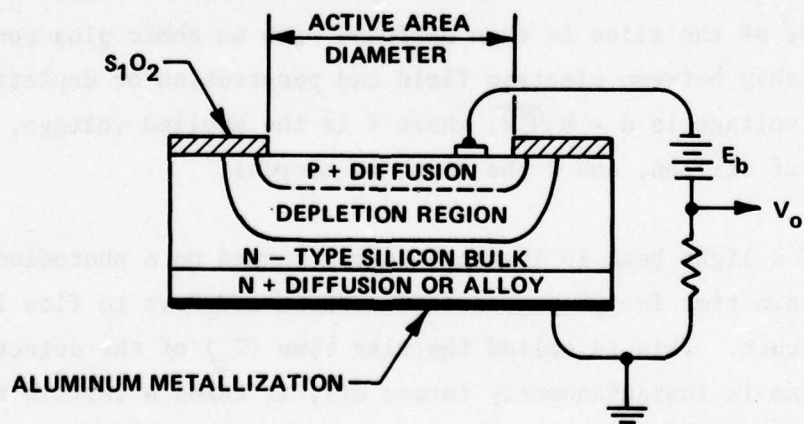
Figure 7-2 PLANAR DIFFUSED PHOTODIODE

(1) Transit time of the photogenerated carriers within
    the silicon crystal.
(2) Equivalent circuit (RC) rise and decay time.
(3) Trapping of photogenerated carriers within the
    silicon crystal.

The transit time is the sum of the times it takes the photodiode generated
minority carrier to move to the junction and the photogenerated majority
carrier to move to the ohmic contact. The transit time will be very short
if the photodiode collects the photogenerated carriers in a strong electric
field. A transit time of 1 nanosecond (ns) per mil of travel can be ob-
tained in high speed photodiodes. Thus a photodiode 5 mils thick could
have a transit time of 5 ns if the applied external voltage were enough to
deplete the detector fully. If the RC time constant and trapping time were
less than 5 ns, then the observed rise and decay times would be 5 ns. The
trapping effect of photogenerated carriers by deep lying energy centers in
the silicon can be reduced to negligible levels by proper selection of the
starting material and final device checkout. However, response time for
high speed photodiodes in scanning applications is determined primarily by
the external circuit rather than the actual device parameters. The equiva-
lent circuit for a high speed photodiode is shown in Figure 7-3.
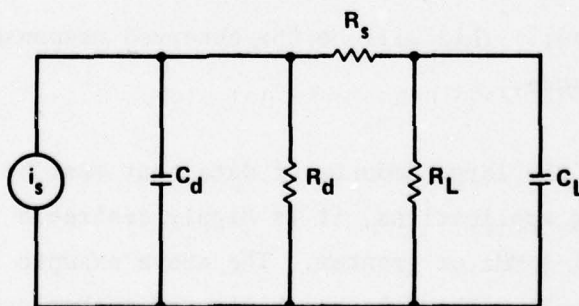
Figure 7-3   PIN PHOTODIODE EQUIVALENT CIRCUIT

where i_s = signal current

         C_d = depletion layer capacitance

R_d = depletion layer resistance

R_s = series resistance in the silicon and leads

R_L = load resistance

C_L = load capacitance

Typically, R_s is on the order of 100 ohms, R_d is on the order of 10^7 ohms, and R_L is on the order of 10^3 ohms, so that the rise time is determined primarily by the time it takes to charge and discharge the depletion layer capacitance C_d and load capacitance C_L through the load resistance, R_L. C_d is typically in the range of from 100 pf to 1000 pf, depending upon the size of the photodiode. C_L can be kept small by proper care in the fabrication of the external circuit, so that the network time constant is:

$$T_{RC} = R_L C_d$$

This is the time it takes for the load voltage to change by 63% of its final steady state value. Therefore, if the load resistance is 10^3 ohms, and the load capacitance 100 pf, the network time constant for a typical cell is:

$$T_{RC} = 10^3 \times 10^2 \times 10^{-12} = 10^{-7} \text{ seconds}$$

or 0.1 μs (microsecond). This will be the observed response time for the selected load resistance.

Because of the large amounts of data that must be processed in cartographic scanning applications, it is highly desirable to scan at data rates on the order of 1 MHz or greater. The above example indicates that this requirement is well within the capability of technology that can be utilized to fabricate specially shaped arrays for cartographic scanning.

There is a tradeoff to be made in the selection of load resistance for both fast response and high photodiode sensitivity. Fast response requires low load resistance, while high sensitivity requires high load

resistance.

Sensitivity

Diode sensitivity is determined by the amount of light required to produce a signal equal to the internally generated noise of the photodiode. The two sources of noise are shot noise in the photodiode and thermal noise in the load resistor. Shot noise voltage across R_L is given by:

$$V_S = (2eI_0B)^{\frac{1}{2}}R_L$$

The thermal noise generated in R_L is:

$$V_T = (4KTBR_L)^{\frac{1}{2}}$$

and the signal-to-noise ratio is:

$$S/N = \frac{i_iR_L}{(V_S^2 + V_T^2)^{\frac{1}{2}}} = \frac{i_i}{\left(2eI_0B + \dfrac{4KTB}{R_L}\right)^{\frac{1}{2}}}$$

where e = electron charge, 1.6×10^{-19} coulomb

k = Boltzman's constant, 1.38×10^{-23} joules/^oK

T = temperature, ^oK ($68\ ^oF = 293^oK$)

B = bandwidth of the measuring system, typically 100 KHz

I_0 = photodiode dark current

i = photogenerated signal current

For values of load resistance less than 10K ohms, the thermal noise voltage is considerably greater than the shot noise. Since high speed response is desired for cartographic scanning, the load resistance selected should be much smaller than 10K ohms. Then the noise equivalent power of the photodiode is given by:

$$P_N = R^{-1}(2eI_0B + \frac{4KTB}{R_L})^{\frac{1}{2}}$$

where R is the photodiode responsivity in amps/watt and the terms within the brackets represent equivalent noise currents from the shot noise and thermal noise sources. Peak responsivity is 0.3 to 0.4 amps/watt. Therefore, for high speed scanning $(V_S << V_T)$, the noise equivalent power is:

$$P_N = R^{-1}\frac{4KTB}{R_L}^{\frac{1}{2}} \approx 0.4 \frac{2}{amps/watt}\left(\frac{1.38 \times 10^{-23} \frac{joules}{^\circ K} \times 2.93 \times 10^2 \; ^\circ K \times 10^5 \; sec^{-1}}{10^3 \; ohms}\right)^{\frac{1}{2}}$$

or $\quad P_N = 5 \; (4.05 \times 10^{-21})^{\frac{1}{2}}$ watts

$$= 3.2 \times 10^{-12} \text{ watts}$$

For comparison, moonlight illumination is on the order of 5×10^{-7}.

Linearity

Back-biased silicon photodiodes behave like constant current generators with the amount of current proportional to the incident light. Maximum deviation from a straight line for United Detector Technology photodiodes is 5% over a range of intensity from the limit of detectability, 10^{-13} watts/cm^2, to 10^{-3} watts/cm^2 with typical deviation on the order of $\frac{1}{2}$%. At light intensities greater than 10 milliwatts/cm^2, major deviations in the linearity begin to occur. For comparison, a 60 watt tungsten bulb at 1 foot produces an illumination of approximately 2.5 mw/cm^2.

7.3 PHOTOSENSOR ARRAYS

Discrete photodiodes discussed in the previous section can be obtained in both custom and linear array configurations. External signal processing circuits must then be supplied for each photodiode in the array.

There are three other currently available array technologies which can be used for scanning applications:

    (1) Self-scanned photodiode arrays
    (2) Charge-coupled devices (CCD)
    (3) Charge injection devices (CID)

The self-scanned MOS photodiode sensor is essentially a high performance diode scanning circuit built with standard photodiode and either metal or silicon gate technology. The scanning circuit is made up of MOS transistors that are imbedded in the same monolithic structure containing the array of photodiodes. After an object is imaged onto the surface of the photodiode array, the MOS scanning circuit shifts the signals off the chip by accessing the diodes sequentially through an analog switch to a common bus line.

A CCD sensor is essentially an analog-signal shift register or delay line fabricated from a closely spaced array of MOS capacitors built using silicon gate buried layer technology. The input signal takes the form of minority carriers generated in the semiconductor beneath the capacitor plates by the absorption of incident light. The signal charge consisting of minority carriers is stored in packets beneath the capacitor plates. The charge packets are transferred from capacitor to capacitor throughout the array by the application of a sequence of biasing pulses. Since the signals are stored in packets, they appear at the output as sampled signals with each sample representing a packet of charge.

CID sensors employ intracell transfer and capacitive storage similar to CCD's. Charge injection is used to sense the photon-generated charge at each sensing site and readout can be performed using sequential injection, parallel injection, or random site selection. In sequential injection, the charge is injected into the substrate and the resulting displacement current sensed. In parallel injection, the functions of signal charge detection and injection are separated. The injection operation is used to reset or empty the charge storage capacitors after line readout

7-9

has been completed. Non-destructive readout is possible by deferring the injection operation. The X-Y coincident voltage configuration of the CID is also easily adaptable to special scan formats in which each sensing site is directly accessible without regard to its time or spatial sequence with respect to other sites in the array. In many respects, image site selection in the CID resembles MOS memory addressing and many of the decoding techniques developed for addressing MOS memories can be applied to random-access imaging.

Linear self-scanned photodiode arrays are available in configurations containing from 16 to 1872 photodiodes. CCD arrays include linear sensors containing as many as 1728 cells and off-the-shelf rectangular arrays as large as 512 x 320 cells in devices designed to generate 525 line standard interlaced television picture frames. Therefore, the technology is highly developed. Off-the-shelf linear arrays have several significant advantages over the larger rectangular arrays in cartographic scanning applications. In particular:

(1) The linear array is much simpler because of fewer cells. Therefore, quality control tends to be superior with better control over cell imperfections and nonuniformities at lower cost.

(2) It is much easier to calibrate a linear array containing 1024 cells and correct for cell-to-cell nonuniformity than it would be for a rectangular array containing 100,000 or more cells. Storage and manipulation of factors to correct the $^+_-6$% to $^+_-10$% cell-to-cell non-uniformity is also much simpler for a linear array.

(3) Circuitry for first stage processing of the photodiode sensor data at high scanning rates is much simpler for linear arrays.

Fairchild CCD arrays of 1024 or 1728 elements appear to be the most attractive for general purpose cartographic scanning applications,

primarily because of their wider dynamic range and lower saturation exposure. For example, compared to the Reticon H-series self-scanned linear arrays, the CCD sensors have a much greater dynamic range and require from one-fourth to one-half the energy for saturation. The Fairchild CCD 131 array contains 1024 elements, 0.51 mils square on 0.51 mil centers and can be operated at an average pixel scanning rate of 20 MHz if supplied with enough light to provide good image contrast. The 500:1 dynamic range of the CCD 131 is sufficient to generate more than 8 bits of gray level. Further improvement in device performance can be obtained by decreasing the integration time. For example, the average dark signal in the CCD 131 is approximately 10 mv at 25°C for a 1 ms integration time with the dark signal nonuniformity on the order of 3% of the saturation voltage (device test parameters from the data sheet). With these parameters, the dynamic range ·is 500:1. However, since average dark signal current is a linear function of the integration time, it can be reduced by a factor of 10 (i.e., to 1 mv) by cutting the integration time by a factor of 10 (to 100 μs). This is still well within the 20 MHz capability of the linear array.

There is no geometric distortion in the actual arrays since cell geometry is typically accurate to within 1 micron. Sensor spectral response ranges from 0.1 a/w to 0.3 a/w for wavelengths of 450 nm to 1.0 μm peaking at approximately 700 nm. Therefore, the CCD 131 can be used very effectively for multispectral scanning by filtering the light source to eliminate the infrared energy and by using filters over the array to select the desired red, green, or blue color band.

The light source can be mounted in a fixed position relative to the sensor so that the light reflected from the document will always strike the sensor at the same angle permitting a set of dichroic filters to be used over the sensor to provide color separation. High quality dichroic filters transmit an average of more than 80% of the selected red, green, or blue spectral band.

7.4   DOCUMENT ILLUMINATION

An analysis of sensor characteristics and the application of available technology to cartographic scanning also requires a consideration of available illumination sources. It is essential to provide intense uniform illumination with an irradiance sufficient to saturate the selected specially shaped array or self-scanned array. Auxiliary optics are needed to provide efficient uniform illumination. The most commonly used light sources for this type of application are quartz-halogen lamps with a color temperature of $3000^{\circ}K$. A standard 100-watt quartz-halogen lamp with a condensing lens assembly, spherical rear reflector, and stabilized power supply is available as a packaged subsystem. It will deliver a uniform 1.5" diameter collimated beam but the rated lamp life at the full operating voltage (12 V) is only 50 hrs. The rated life can be increased to 250 hrs. by operating the lamp at 10 V, but the light output is sharply reduced at the lower voltage. Quartz-halogen lamp irradiance also drops off sharply at lower wavelengths (Figure 7-4).

In contrast, 150 W Xenon lamps exhibit a typical output that is much more uniform over the visible spectra. It will therefore be a much better source for multi-spectral scanning. The color temperature of a Xenon lamp is approximately $6000^{\circ}K$. This lamp can also be obtained as a packaged subsystem with a 68 mm (3") diameter aspheric 4-element 0.7 Pyrex condensing lens. This lens exhibits less than 0.25% spherical aberration in a collimated beam. A solid state regulated DC power supply, included with the subsystem, maintains light output within $\pm$1% for $\pm$10% variation in line voltage. Light ripple is less than ½% RMS. In addition, constant wattage is maintained as lamp impedance increases with age. The lamp assembly can be used with either Xenon or Mercury arc lamps. Average Xenon lamp life at the rated voltage (20 V) is 1200 hrs. The explosion proof lamp housing also provides forced air cooling and independent horizontal and vertical adjustments for the spherical rear reflector.

SPECTRAL IRRADIANCE - Microwatts/cm² - Nanometer at 50 cm distance

WAVELENGTH (NANOMETERS)

200 WATT MERCURY LAMP

150 WATT XENON LAMP

100 WATT QUARTZ HALOGEN (FILAMENT) LAMP

50 WATT DEUTERIUM LAMP
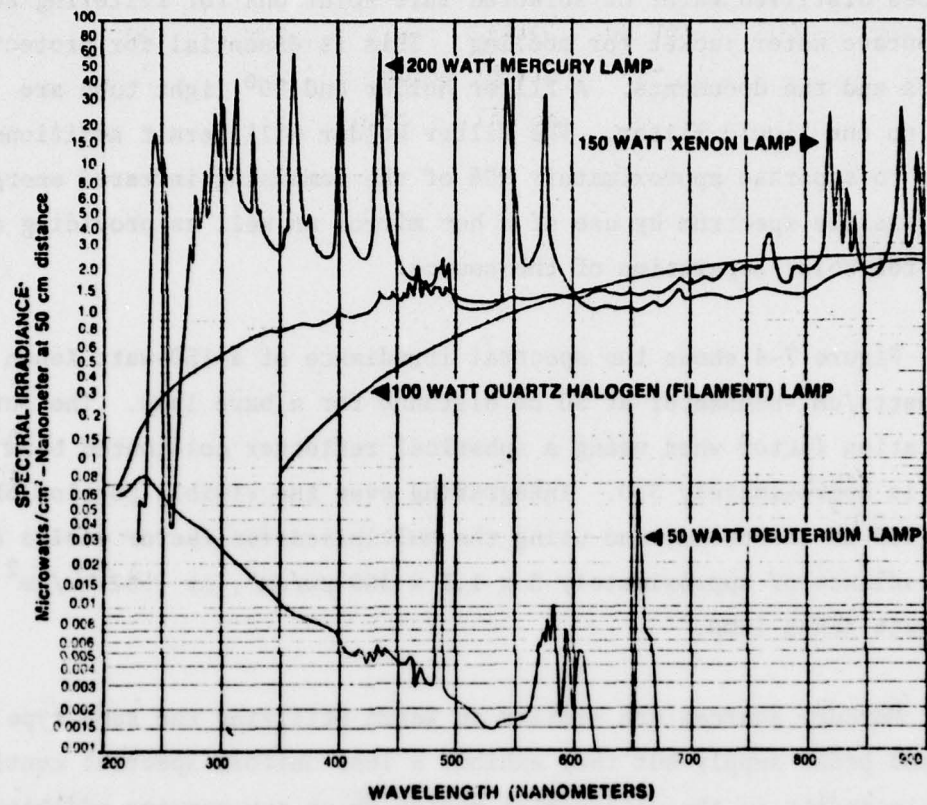
Figure 7-4   TYPICAL OUTPUT SPECTRA

A series of accessories are required for either lamp assembly (Figure 7-5). Adjacent to the housing is a liquid filter to reduce unwanted infrared energy and corresponding heat by 60%. The liquid filter holder uses distilled water or selected salt solutions for filtering and has a separate water jacket for cooling. This is essential for protection of filters and the documents. A filter holder and 90° light tube are attached to the liquid filter. The filter holder will permit additional filtering to separate approximately 90% of the remaining infrared energy from the visible spectrum by use of a hot mirror as well as providing a facility for color separation of the source.

Figure 7-4 shows the spectral irradiance of a 150-watt Xenon lamp in microwatts/cm^2-nanometer at 50 cm distance for a bare lamp. The output multiplication factor when using a spherical reflector collimated beam and 0.7 lens is approximately 3.0. Integrating over the visible portion of the spectra (400 nm to 760 nm) and using the multiplication factor yields a total irradiance of approximately 3 x 1.5 x 360 μw/cm^2, or 1.62 mw/cm^2 for the 150-watt Xenon lamp.

Mercury sources are similar to Xenon utilizing the same type of housing and power supply but they exhibit a less uniform spectral continuum and high intensity in the ultraviolet region which may require additional filtering. Mercury source advantages over Xenon include more compact packaging.

7.5   ADDITIONAL DESIGN CONSIDERATIONS

Scanner Configuration

Drum scanners can be utilized effectively with multiple single element sensors to achieve simultaneous color separation of any three selected color bands. They are severely limited in their random access capability and are inconvenient for aligning or registering a map to a photograph. Furthermore, multiple single element sensors place a

7-14

XENON SOURCE

68 mm DIAMETER
ASPHERAB 4 ELEMENT f0.7 PYREX CONDENSING LENS

LIQUID FILTER

COOLING FLOW-IN
COOLING FLOW-OUT

90° LIGHT TUBE

FILTER HOLDER
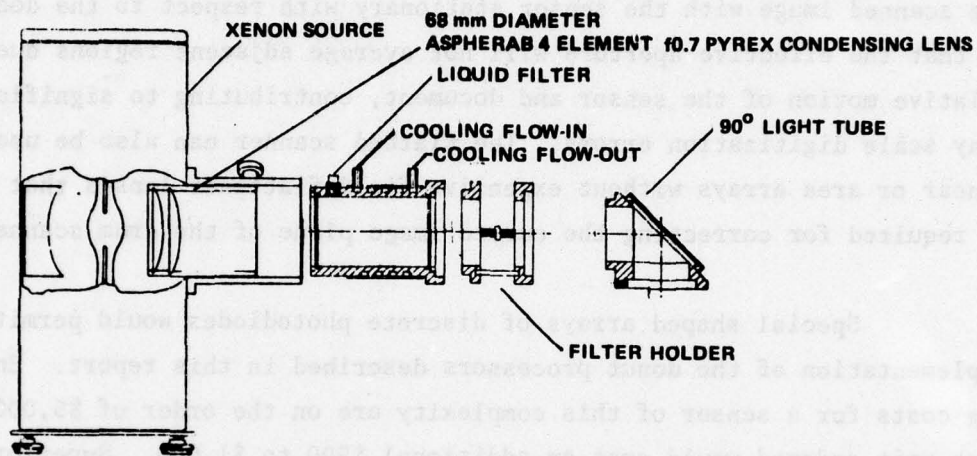
Figure 7-5   XENON LAMP SOURCE AND ACCESSORIES

7-15

considerable burden on the peripheral support equipment because of the relatively high data rates and storage required for simultaneous color separation.

Because of these limitations, a flatbed image scanner is recommended using separate scans for each color band to reduce the scanner complexity. A flatbed image scanner also will permit light integration of the scanned image with the sensor stationary with respect to the document, so that the effective aperture will not average adjacent regions due to relative motion of the sensor and document, contributing to significant gray scale digitization errors. The flatbed scanner can also be used with linear or area arrays without expensive field flattener lenses that would be required for correcting the curved image plane of the drum scanner.

Special shaped arrays of discrete photodiodes would permit direct implementation of the donut processors described in this report. Engineering costs for a sensor of this complexity are on the order of $5,000 and each unit ordered would cost an additional $500 to $1,000. Superior sensor sensitivity can be achieved in discrete photodiode designs, however, sufficient illumination can be obtained from properly designed sources to achieve satisfactory results with any of the array technologies.

There is a significant advantage to using multiple small diodes to cover a region of the document rather than a larger single specially shaped sensor. When a light spot less than 100 mils in diameter is moved over the surface of a photodiode, deviations are observed in the signal current. The magnitude of these deviations is an inverse function of the beam diameter. With a 50 mil diameter light spot, the mean deviation in DC output over the surface of the active area is typically $\pm$2% for large planar, diffused photodiodes and with a 1 mil diameter light spot, the mean deviation is 8%. This problem will be minimized in scanning applications if the area of each photodiode in an array is of the same order of magnitude as the smallest detail in the cartographic document.

CID development has been carried out by the General Electric Company and arrays are only available in TV camera systems from G.E. The random addressing capability available with this technology could be used to great advantage to simulate any special purpose array by proper selection of diodes within the array structure. Selected diodes could be addressed in any desired sequence and the remaining diodes ignored. This technique could achieve the advantages of the special purpose array in greatly reducing the required data processing of the gray level image. However, it would be necessary to persuade G.E. to provide the required customizing and sell the sensor as a separate unit.

7.6   CONCLUSIONS

The best choice of sensor for cartographic scanning at the present time appears to be the Fairchild CCD 131 linear array which can be purchased in a complete line scan camera system. This system can be used most effectively in a flatbed scanner configuration utilizing a Xenon light source with dichroic filters for color separation. Color separation would be provided by separate scans of the entire image.

Section 8
GEOMETRIC ARRAY IMPLEMENTATION

The function of the Donut Processor is to determine X and Y coordinates of points located along lines on a cartographic or topographic map. Inherent to the point digitizing process, the Donut Processor provides line direction information that subsequently is used to track and follow the lines. As a map contains many lines which can intersect and have branches, the line following algorithm has to be sufficiently sophisticated to avoid breaking track or providing misrepresented (inaccurate) coordinate information.

Essentially the processing requirements to implement a donut in either hardware or software involve the acquisition of a number of points surrounding the center point of the donut, combining points located along specific directions into quantities representative of the total intensity along each direction and performing mathematic operations on these quantities to determine which direction the line segment within the donut actually travels. The direction information is subsequently used to relocate the donut to the next position on the line.

The Donut Processor is currently implemented in software on a Digital Equipment Corporation PDP-9 minicomputer. While this implementation is entirely satisfactory for laboratory experiments, the processing rate is too slow to meet any reasonable rate of production. Alternate methods of implementation of the Donut Processor might utilize an array processor, a bit-slice microprocessor, or special purpose hardware. These, in turn, would be interfaced to a host processor.

8.1   ARRAY PROCESSOR

One method that can be used to increase the operational speed of the Donut Processor is to implement the algorithm using an array processor.

These devices are particularly well suited to perform large numbers of iterative multiplications and additions required in digital signal processing, matrix arithmetic, statistical analysis and numerical simulation.

Programmable array processors achieve their rapid data handling by methods similar to those used in custom hardware designs:

(1) Separate memories for program storage, constants and data.

(2) Program memory utilizies large words so that multiple instructions can be fetched in one word.

(3) Multiprocessors operate in parallel.

(4) Extensive pipelining allows overlapping of computations.

(5) Many registers available for temporary storage of intermediate results.

(6) Separate arithmetic units to accomplish counting, address indexing and branch decision making.

(7) Multiple data paths between system elements so data transfers can occur in parallel.

Figure 8-1 shows the internal architecture of a typical array processor.

The highly parallel architecture of an array processor allows the "overhead" of array indexing, loop counting, and data fetching from memory to be performed simultaneously with arithmetic operations on the data. This allows much faster execution than on a typical general-purpose computer, where each of the above operations must occur sequentially.

In general, the approach to implementing the donut algorithm using an array processor would be as follows:

The array processor would be equipped with sufficient random access memory (RAM) to hold a reasonably large sector of the digitized image in order to reduce the overhead of repeated filling of data buffers. In order to conserve memory space the pixel information would probably be

HOST
CPU

I/O   DMA

INTERFACE

MULTIPLE
DATA PATHS

TABLE
MEMORY

REGISTER
SET 1

REGISTER
SET 2

MAIN
DATA
MEMORY

MULTIPLE
DATA PATHS

M1   M2

STAGE 1   MULTIPLIER
PIPELINE
STAGE 2

STAGE 3

A1   A2

STAGE 1   ADDER
PIPELINE
STAGE 2

MULTIPLE PATHS
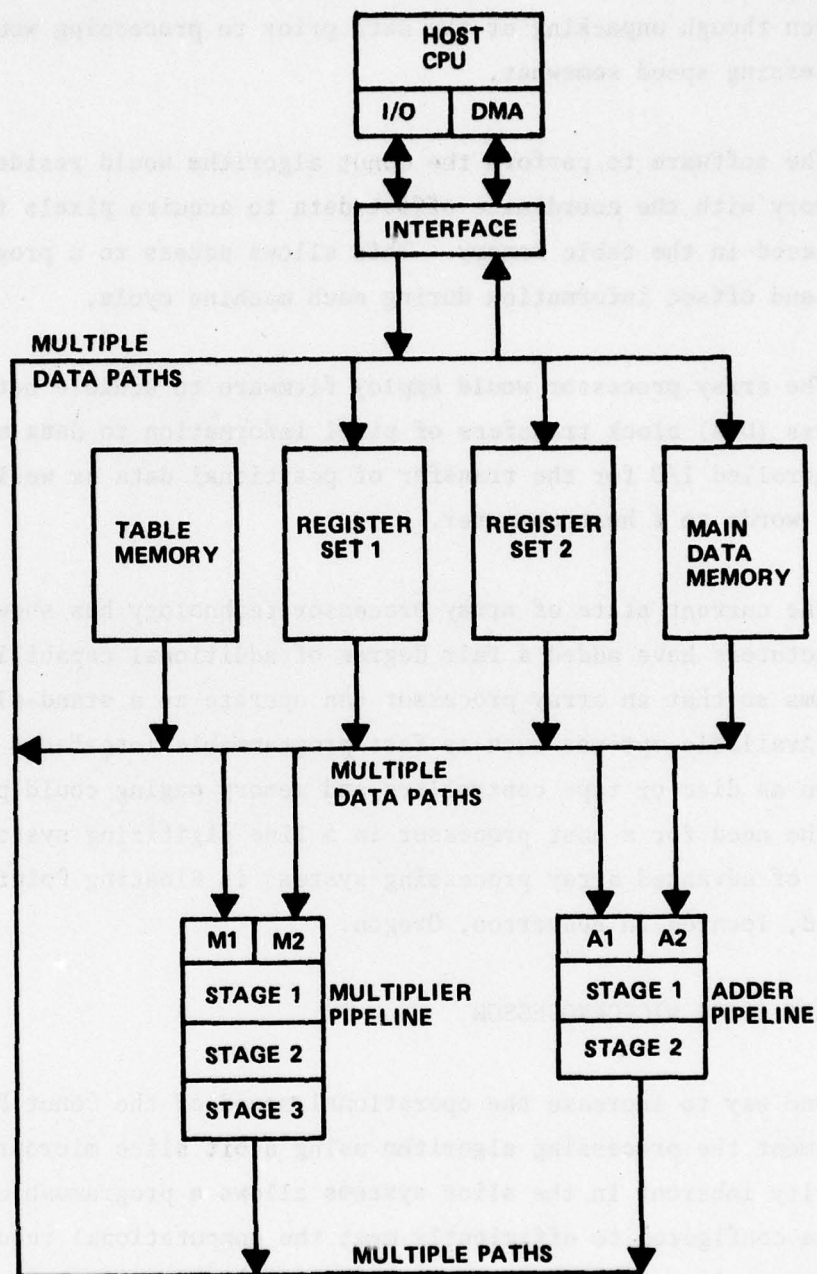
Figure 8-1   ARCHITECTURE OF A TYPICAL ARRAY PROCESSOR

packed into memory on half-byte boundaries (if four bit gray scale is maintained), even though unpacking of the data prior to processing would slow up the processing speed somewhat.

The software to perform the donut algorithm would reside in program memory with the coordinate offset data to acquire pixels for each aperture placed in the table memory. This allows access to a program word, pixel data and offset information during each machine cycle.

The array processor would employ firmware to achieve both direct memory access (DMA) block transfers of pixel information to data memory and program controlled I/O for the transfer of positional data as well as status and control words to a host computer.

The current state of array processor technology has shown that some manufacturers have added a fair degree of additional capability to their systems so that an array processor can operate as a stand-alone computer. Available options such as fast programmable interfaces which can function as disc or tape controllers and memory paging could potentially eliminate the need for a host processor in a line digitizing system. One such vendor of advanced array processing systems is Floating Point Systems, Incorporated, located in Beaverton, Oregon.

8.2   BIT SLICE MICROPROCESSOR

One way to increase the operational speed of the Donut Processor is to implement the processing algorithm using a bit slice microprocessor. The modularity inherent in the slice systems allows a programmable processor to be configured to efficiently meet the computational requirements for any given application. Some of the attributes of a slice system that allow the tailoring to a specific need are outlined below:

(1) The slice system components are in themselves very fast. Fabricated using either Schottkey bi-polar or emitter-

coupled-logic techniques, a slice system having micro-
instruction execution times of less than 100 nano-
seconds can be realized.

(2)   Because of the modularity of the system, the word
        length can be tailored to the size required by the
        particular application.

(3)   A slice system is characterized as being micro-
        programmed. This means that a system instruction set
        optimized for a required application can be generated
        by programming a block of high speed memory (micro-
        program control storage) with microinstructions.
        Machine instructions are then performed by sequencing
        through the microprogram memory. With proper coding of
        the control storage it is possible to have any number
        or combination of machine instructions.

Figure 8-2 illustrates one configuration of a microprogrammed processor.

        In general, the bit-slice approach to implementation of the Donut
Processor would be as follows:

        The system would be configured with enough fast random access
memory (RAM) to hold a sizeable sector of the digitized gray level image.
This will reduce the overhead of loading the memory allocated for image
storage. Because the word length of the memory can be tailored to the
number of bits of gray scale from the scanner (4 bits as currently imple-
mented), the information can be stored as one point per memory location
without being wasteful of memory. This then eliminates the need for
unpacking data and would greatly simplify the acquisition of points surround-
ing the center of the donut.

        The system would also contain a register file for storage of the
directional intensities formed by combining sets of gray scale points and
storage of results from intermediate computations. The word length of the
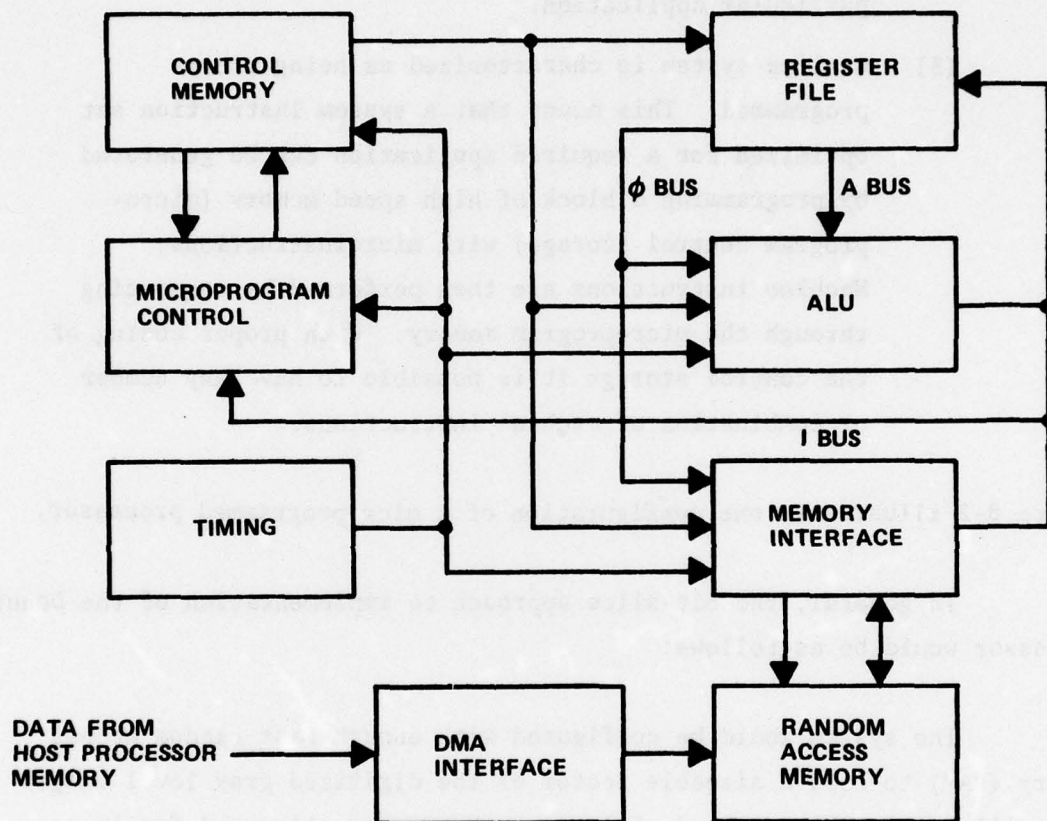
Figure 8-2   TYPICAL MICROPROGRAMMED PROCESSOR

register file would be sufficient to contain the results of the computations and can be of different length than the high speed RAM.

The bit slice system would also have firmware to enable loading of imagery data into its high speed RAM and to transfer answers back to a host computer. The former would probably be a direct memory access (DMA) block transfer between the two machines while the latter would be under program control.

Lastly, a machine instruction set that could efficiently perform the computations and data manipulations required by the donut algorithm would be generated using the microprogramming feature of the bit slice architecture.

8.3   SPECIAL PURPOSE HARDWARE

When processing speed is very critical special purpose hardware can be introduced into a system. Although hardware implementation usually imposes a limitation on processing flexibility it can greatly reduce the time required to perform a computation. Generally, the more dedicated the special purpose hardware is allowed to be, the faster (up to a point) it can be made to operate. As the donut processing algorithm will be a fixed computation, it would lend itself to hardware implementation with an obtainable execution speed dependent upon the degree of parallelism designed into the hardware circuitry.

Hardware processors achieve high computational speed by a number of techniques. Some of these are listed below:

(1) Extensive use of table look-ups.

(2) Arithmetic units tailored to word size.

(3) Pipelining between stages increases effective throughput rate.

(4) Highly parallel-multiple subsystems to achieve required

8-7

computational speed.

(5) Controllers dedicated to performing one function very
     efficiently.

(6) Custom integrated circuits sometimes used.

The required processing speed of 1000 lineal inches per hour
implies a processing time of 1.8 millisecond per donut under worst case
combinations of step size and resolution.   An economical approach to the
hardware design would be to implement sufficient parallel processing capa-
bility to meet but not greatly exceed the processing speed requirement.
One possible approach is illustrated in the block diagram of Figure 8-3.

Image information from the host processor is entered into high
speed random access memory (RAM) via a DMA channel. Unpacking of the data
occurs concurrently with the data transfer. The host processor supplies
coordinate information to center the donut over a particular location in
the imagery data. The hardware then acquires pixels for each aperture by
sequencing through a read only memory (ROM) to obtain coordinate offsets
and adding these to the central coordinate of the donut to address locations
in RAM. The intensity value for each pixel in an aperture is added by an
accumulator and the intensity sum stored in a register (a separate register
is provided for each aperture).

Computations are now performed upon the aperture intensities to
provide direction information about line segments contained within the
donut. Operations typical of the donut algorithms are:

(1) Normalization of intensity values to compensate for
     apertures formed using different numbers of pixels.

(2) Determination of the maximum and minimum intensity.

(3) Calculation of the difference between the maximum and
     minimum intensities.

8-8
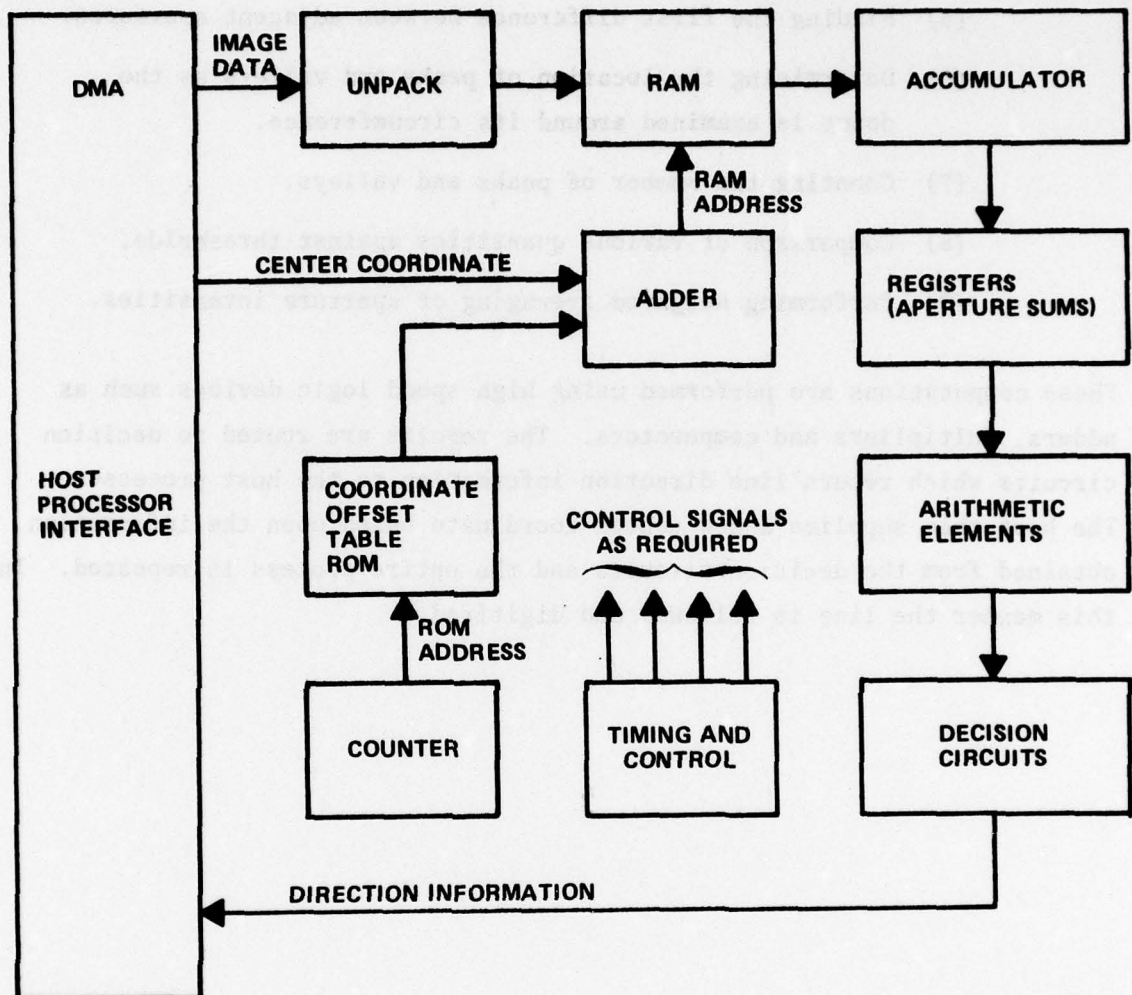
Figure 8-3   HARDWARE IMPLEMENTATION OF DONUT ALGORITHM

8-9

(4) Determination of the average intensity of all apertures in the donut.

(5) Finding the first difference between adjacent apertures.

(6) Determining the location of peaks and valleys as the donut is examined around its circumference.

(7) Counting the number of peaks and valleys.

(8) Comparison of various quantities against thresholds.

(9) Performing weighted averaging of aperture intensities.

These computations are performed using high speed logic devices such as adders, multipliers and comparators. The results are routed to decision circuits which return line direction information to the host processor. The host then supplies a new center coordinate based upon the information obtained from the decision circuits and the entire process is repeated. In this manner the line is followed and digitized.

Section 9
CONCLUSIONS AND RECOMMENDATIONS

The objective of this study was to determine the feasibility of scanning cartographic documents by large linear arrays and by specially shaped geometric arrays. The Calspan flatbed image scanner with its linear array sensor was used with supporting computer software to scan and process small sections of the USAF's Cartographic Test Standard (film version). Two different geometric array configurations were simulated in software.

The results show that good quality imagery is obtained by the sensor and that line directions are consistently and correctly found. Both of these conclusions are qualified by a resolution requirement. The lines must be wide enough for the scanner to see about 2½ resolution elements wide, and the lines must fall within the range of line widths processable by the geometric array for correct directions to be found. Although the first resolution requirement mentioned above holds in general, narrower lines, when isolated in a high contrast field, will be detected.

The scanner has a resolution which is adjustable from 1 mil to 6 mils. By changing the optics the resolution could be increased to scan 2 mil lines or even 1 mil lines. However, optical diffraction is expected to limit the practical resolution, particularly when several lines are close together. At 1 mil resolution this may be a problem.

The geometric arrays were evaluated by simulation using imagery data generated by the large linear array. The behavior of the arrays was examined by looking at the line directions computed as they crossed lines and combinations of lines. The DIGIMAP array behaves well in finding the correct line direction. It does this even where lines are close together. It also points at nearby lines which in most applications is undesirable. This characteristic could be eliminated by adding a central aperture to

9-1

the array and using it for a threshold test which would establish whether or not the center of the array is within the boundaries of a line.

The TOPS geometric array finds line directions well but sometimes misses one of the two directions when on the edge of a line. It rarely points at a line as it has a central aperture based threshold test in its processing sequence.

The geometric array has been defined as consisting of two parts: (1) a sensing part and (2) a computational part. The state-of-the-art of the technology in each of these areas was evaluated and has been reported in Sections 7 and 8 of this report. In Section 7 a specific CCD array, light source, and filter set was recommended for the cartographic scanning application. In Section 8 it was described how the computation required by a geometric array can be implemented for high speed. The choice of which of the three methods to use depends on the system specifications for the particular application being filled.

A detailed evaluation has been made of existing capabilities of solid state array scanning and supporting computational algorithms. The next step is to establish how far these capabilities can be extended. The key technical areas are those of color response and discrimination, resolution limits, and scanning and processing speeds.

Section 10
COMPUTER SOFTWARE DOCUMENTATION

The experimental software system consists of three computer
software packages. Two geometric array simulation packages and an imagery
printout package have been implemented. To form a geometric array package
each set of simulation routines is combined with support routines by the
CHAIN utility to create an EXECUTE file. One EXECUTE file exists for each
of the geometric array configurations: DØ1Cnn for the DIGIMAP donut,
and DØ2Cnn for the TOPS donut, where nn is the current revision number.
The operator may then experiment with a selected geometric array by using
the appropriate EXECUTE file. The third package is chained as an EXECUTE
file named DMPLND. This package produces a formatted dump of the imagery
data.

The LANDSCAPE experimentation software is a combination of new
routines plus modifications and extractions from the Calspan DIGIMAP system.
The new routines and the modified DIGIMAP routines used in the LANDSCAPE
software system have been documented. Each routine is documented by program
name and description and by a flow chart. Program constants and variables
are documented in the program listings. (The listings are contained in a
separate document.)

A logic diagram of program flow for the geometric array simu-
lations is shown in Figure 10-1. Program inputs and outputs are documented
in the program writeups. A list of accumulator switch settings precedes
the individual routine descriptions.

10-1
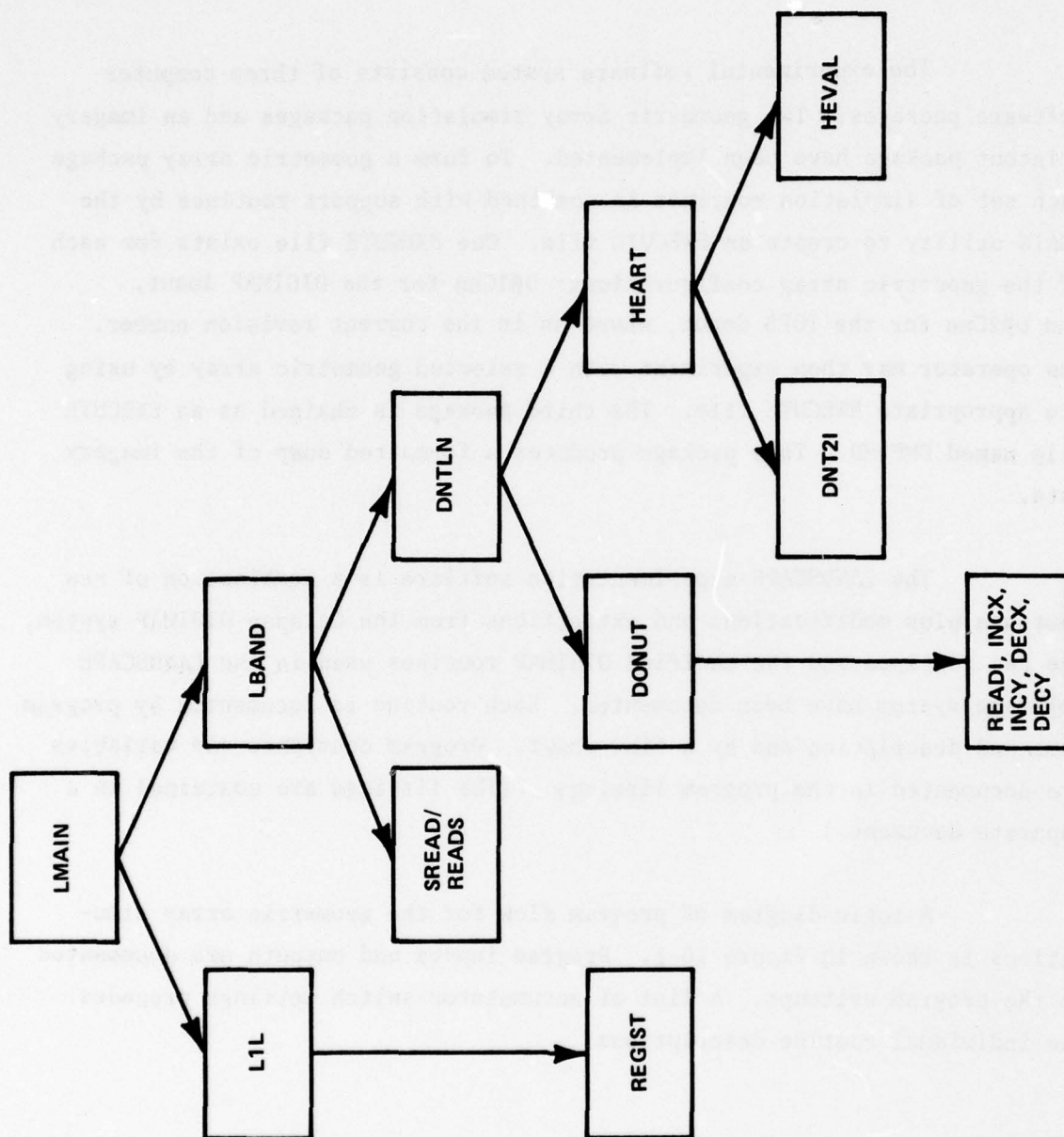
Figure 10-1 COMPUTER PROGRAM LOGIC DIAGRAM

Accumulator switch settings which affect the operation of the LANDSCAPE system:

Switch 0: Used to delay processing of a map segment. The map segment processing is not started unless, and until switch 0 (zero) is off (down).

Once map segment processing has started, switch 0, when on, will cause a short delay before the geometric array processing at each point the array is processed.

Switch 1: When this switch is on, a circle is drawn around the circumference of the geometric array being processed.

Switch 4: When this switch is on, image data buffer is dumped each time a bi-strip is obtained by SREAD. Turning this switch off terminates the current buffer dump, and buffer dumps are not given until this switch is again turned on.

Switch 9: Geometric array printouts are generated when this switch is on. The operator may suppress array printouts by turning this switch off.

Switches 11 and 12:

These switches control the creation and reading of LNDRCD data tapes.

11 off allows normal processing of data from the scanning array.

11 and 12 on cause the creation of a LNDRCD data tape while performing normal processing of data from the scanning array.

11 on and 12 off cause data to be obtained from a LNDRCD data tape instead of the scanning array.

Switch 14: This switch implements a slow scan mode. When this switch is on, there is a 1.5 second delay after moving the scanning array before the array is sampled. This allows various vibrations to completely settle out that may cause slight variations in scanner direction. The slow scan delay mode takes about 25 minutes to complete a scan of the map segment.

When this switch is off, the scanner array is sampled immediately after the array is positioned.

Switch 16: This switch must be on to obtain geometric array printouts.

Program Name: CCHK

Program Description: This routine checks that a point is within current bi-strip buffer. Called by DNTLN.

Logic Diagram: See Figure

Program Constants: See program listing.

Program Variables: See program listing.

Inputs DXC: X coordinate
      DYC: Y coordinate
      BXC: right hand boundary of bi-strip

Outputs: Next instruction is executed if point is outside bi-strip. Next instruction is skipped if point is within bi-strip.

CCHK

IS COORDINATE
WITHIN CURRENT
BI-STRIP IN
BUFFER

N

Y

INCREMENT RETURN
POINT

RETURN

Figure 10-2   CCHK

10-6
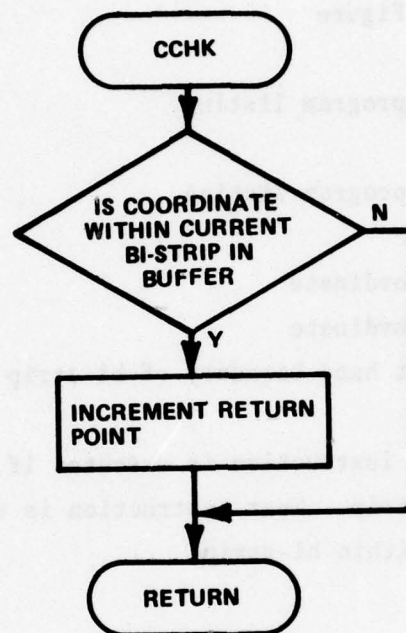
Program Name: DECX

Program Description: Obtain intensity for decremented X coordinate
                       relative to last data point sampled by READI, INCX,
                       DEXC, INCY, or DECY. This routine is an entry point
                       in READI, and is called from the geometric array
                       simulation routines.

Logic Diagram: See Figure

Program Constants: See program listing.

Program Variables: See program listing.

Inputs: Coordinate buffer pointers of last intensity are
                       used to determine new coordinate buffer pointers.

Outputs: Intensity data value.

(See Figure 10-17)

Figure 10-3   DECX

Program Name: DECY

Program Description: Obtain intensity for decremented Y coordinate
                       relative to last data point sampled by READI, INCX,
                       DEXC, INCY, or DECY. This routine is an entry point
                       in READI, and is called from the geometric array
                       simulation routines.

Logic Diagram: See Figure

Program Constants: See program listing.

Program Variables: See program listing.

Inputs: Coordinate buffer pointers of last intensity are
                       used to determine new coordinate buffer pointers.

Outputs: Intensity data value.

(See Figure 10-17)

Figure 10-4   DECY

10-10

Program Name:	DMPLND
Program Description:	This program produces a formatted dump printout of the imagery data on a LNDRCD data tape.
	The operator inputs the character to be printed for each gray level of imagery data. Multiple passes are then made of the LNDRCD data tape to produce a formatted dump of the imagery data on the line printer.
Logic Diagram:	See Figure
Program Constants:	See program listing.
Program Variables:	See program listing.
Inputs:	The operator inputs sixteen characters to represent the gray levels of the imagery data. For a normal hexidecimal dump the characters FEDCBA9876543210 are entered.
	LNDRCD imagery data is obtained from the LNDRCD magnetic tape, as recorded by READS. The format of the LNDRCD tape is described in the READS program outputs section.
Outputs:	A formatted dump is printed with the characters selected to represent the gray levels. A heading and footing for each pass indicates the position along the linear array. The scan number is printed at the left and right sides. Five passes of the data are made in order to print all 512 imagery data points.

Figure 10-5 DMPLND

10-12

10.5
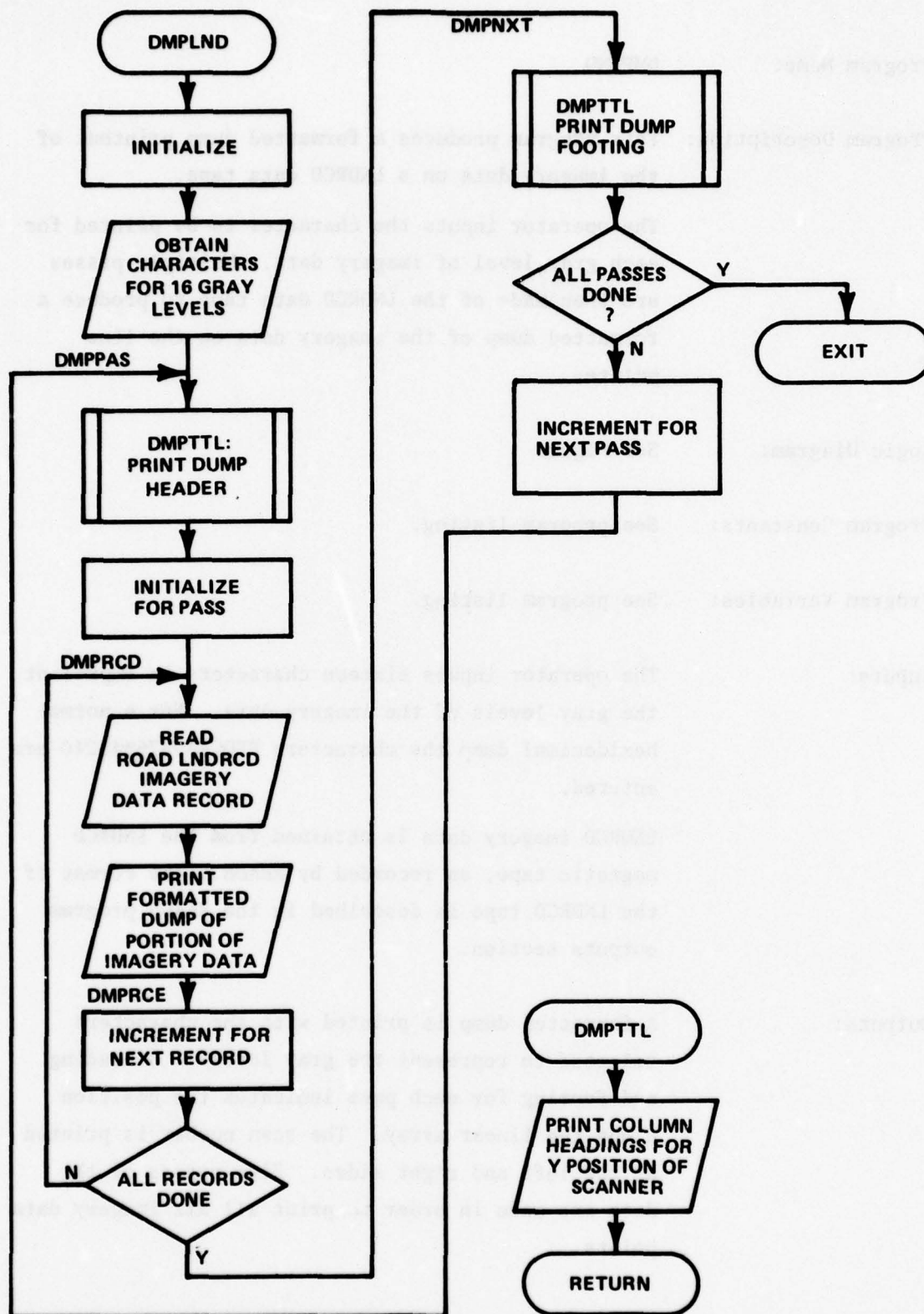
Program Name:	DNTLN
Program Description:	DNTLN is called from LBAND to position a geometric array at points along a line segment. The points are checked to see if they are contained in the current buffer. When a point is contained in the current buffer a geometric array simulation routine is called. The geometric array process being simulated is dependent on which program is being executed.
Logic Diagram:	See Figure
Program Constants:	See program listing.
Program Variables:	See program listing.
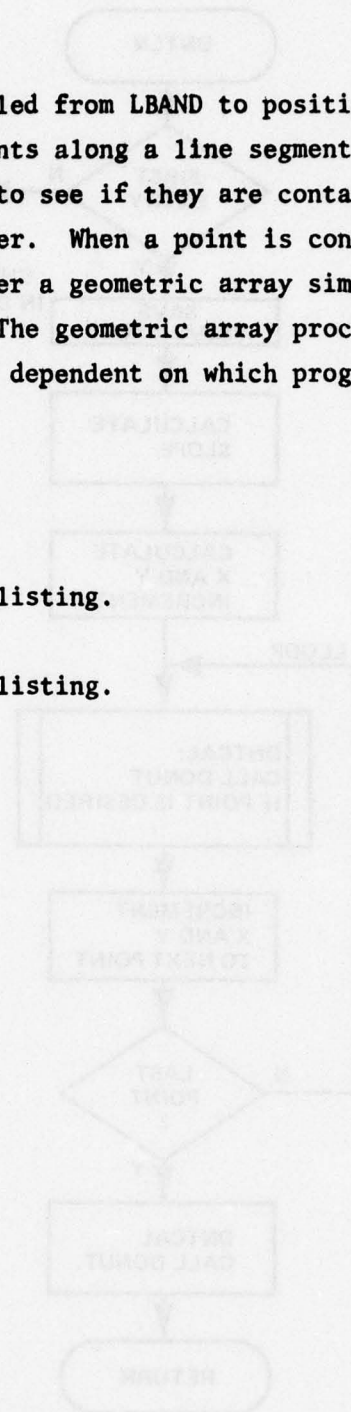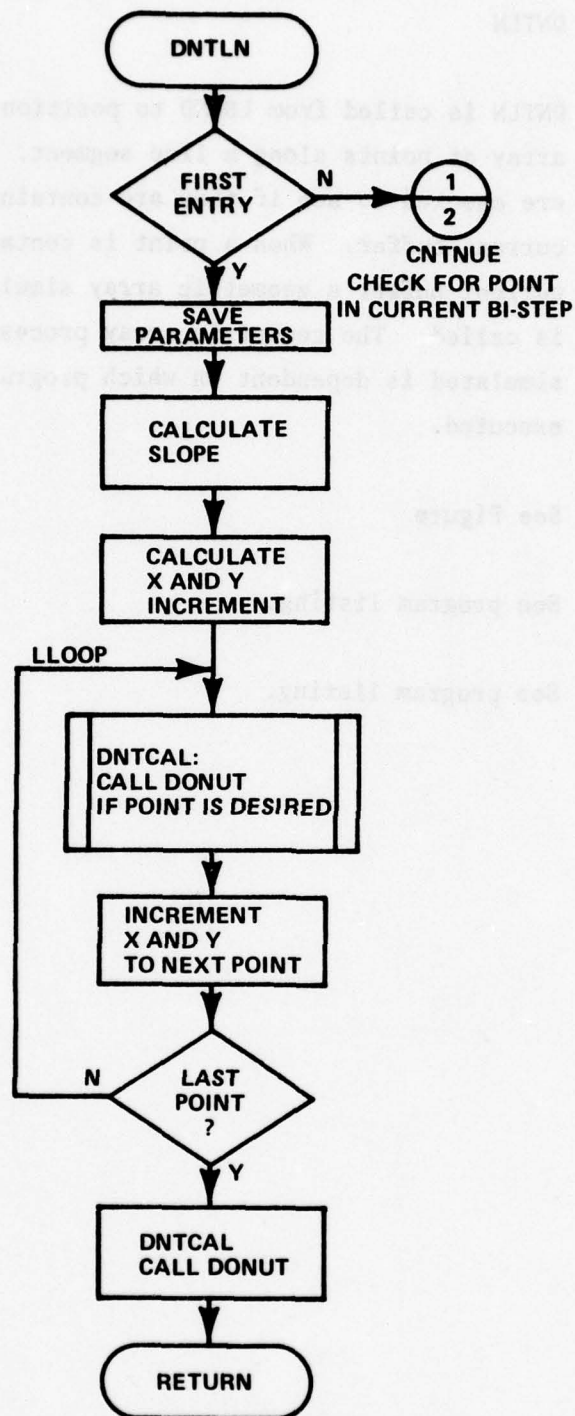
Figure 10-6   DNTLN (Page 1 of 2)
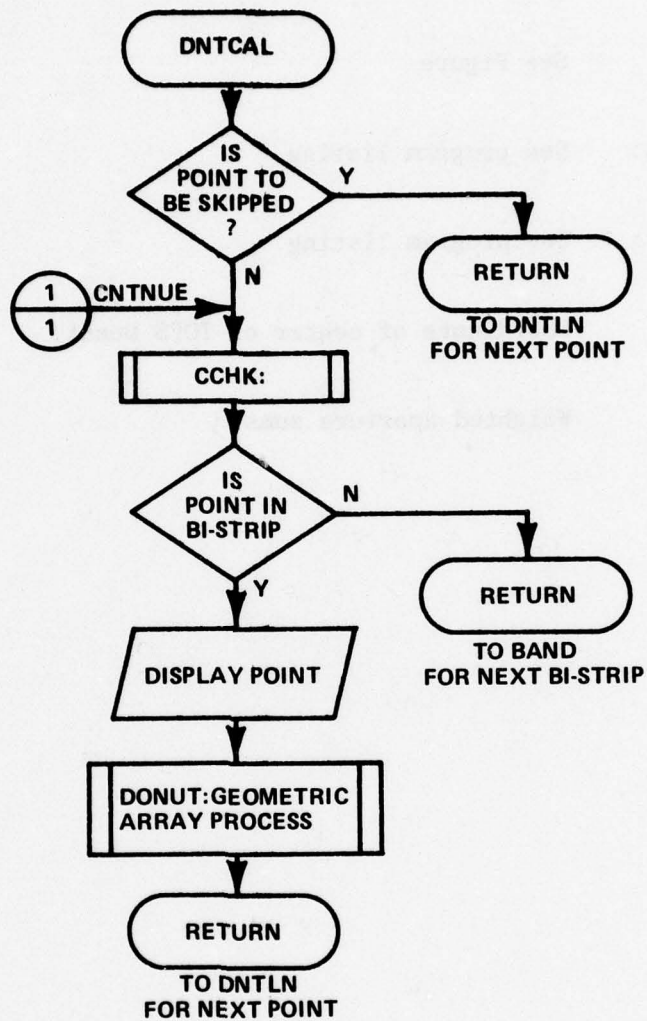
Figure 10-6   DNTLN (Page 2 of 2)

10-15

Program Name: DNT2I

Program Description: This routine is called by HEART to obtain the
                       weighted aperture sums for the TOPS Donut.

Logic Diagram: See Figure

Program Constants: See program listing.

Program Variables: See program listing.

Inputs: Coordinate of center of TOPS Donut.

Outputs: Weighted aperture sums.

```
                    ╭──────────────╮
                    │    DNT2I     │
                    ╰──────┬───────╯
                           │
                           ▼
                ┌──────────────────────┐
                │ OBTAIN               │
                │ INTENSITIES          │
                │ FOR ALL              │
                │ APERTURES            │
                └──────────┬───────────┘
                           │
                           ▼
                ┌──────────────────────┐
                │ NORMALIZE            │
                │ INNER                │
                │ RING 1               │
                └──────────┬───────────┘
                           │
                           ▼
                ┌──────────────────────┐
                │ NORMALIZE            │
                │ MIDDLE               │
                │ RING 2               │
                └──────────┬───────────┘
                           │
                           ▼
                    ╭──────────────╮
                    │   RETURN     │
                    ╰──────────────╯
```
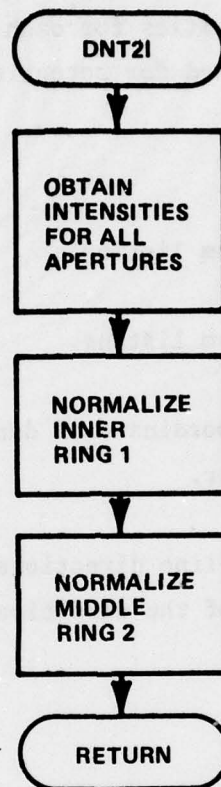
Figure 10-7   DNTL

10-17

Program Name: DONUT

Program Description: This routine is called by LBAND to implement the
simulation of the DIGIMAP donut. This routine
calls READI and INCX, INCY, DECX and DECY to sum
the intensities for each aperture. The apertures
are searched for potential line directions.

Logic Diagram: See Figure

Program Constants: See program listing.

Program Variables: See program listing.

Inputs: X and Y coordinate of donut position, and scanner
data buffer.

Outputs: Number of line directions out of the donut, and
an array of the directions, if any.
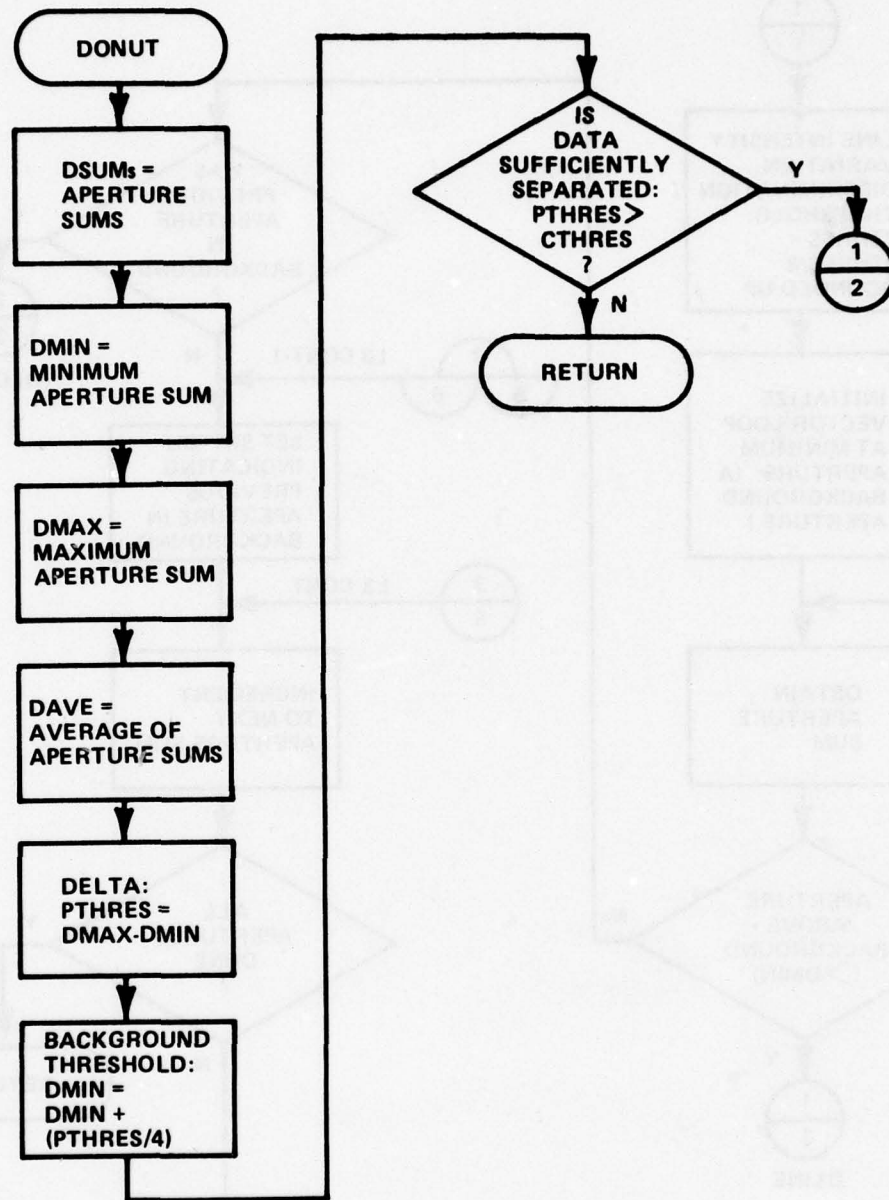
Figure 10-8   DONUT (Page 1 of 8)

Figure 10-8   DONUT (Page 2 of 8)

DLINE

① / ②

DLCONT

② / ②

WAS LAST VECTOR ABOVE BACKGROUND ?

Y

N

INITIALIZE APERTURE SUM PSUM, APERTURE POSITION SUM PPSUM, LAST APERTURE DIFFERENCE LDIF, AND LAST APERTURE SUM LINT.

INITIALIZE LOCAL MAXIMUM AND MINIMUM APERTURE SUM AND APERTURE POSITION ARRAYS.

DIF = DIFFERENCE BETWEEN THIS APERTURE SUM AND PREVIOUS APERTURE SUM

DETERMINE IF A LOCAL MAXIMUM OR MINIMUM

SIGN OF PREVIOUS DIFFERENCE AND CURRENT DIFFERENCE DIFFERENT ?

N

① / ⑤

DLSUM

Y

① / ④

Figure 10-8   DONUT (Page 3 of 8)

10-21

LOCAL MAXIMUM
OR MINIMUM APERTURE

$\frac{1}{3}$

SAVE
DIRECTION
AND
APERTURE SUM

INCREMENT
COUNT OF
LOCAL
MAX & MIN
APERTURE SUM

MORE
THAN 6
LOCAL
MAX & MIN
APERTURE
SUMS

N

$\frac{1}{5}$

DLSUM

Y

CLEAR COUNT
OF DIRECTIONS

RETURN

Figure 10-8   DONUT   (Page 4 of 8)

10-22

Figure 10-8   DONUT   (Page 5 of 8)

10-23

EXAMINE LOCAL
MAX & MIN BUFFER
TO DETERMINE IF
SUFFICIENT DIFFERENCES
TO DISCRIMINATE LINES

DNODE

1/5

INITIALIZE
FOR FIRST
MAX & MIN
PAIR

2/7

DOLP4

DIFFERENCES
BETWEEN
MAX & MIN
>
PTHRES

N

1/7

DELETE HIGHER
MINIMUM

L4CONT   Y

INCREMENT
TO NEXT
LOCAL MAX & MIN
OR MIN & MAX
PAIR

ANY
ENTRIES
LEFT
?

N

2/2

L3CONT-1

N

ALL
LOCAL MIN & MAX
DONE
?

Y

Y

SAVE
DIRECTIONS
OF
MAXIMUMS

Y

ANY
PAIRS
DELETED
?

N

2/2

L3CONT-1

Figure 10-8   DONUT   (Page 6 of 8)

10-24

DELETE HIGHER
MINIMUM

①/⑥

IS
FIRST
APERTURE OF
PAIR A
MAX

Y →

IS
THIS (+0) MAX
> NEXT (+2) MAX
?

N

N ↓

DP1

DPSUB:
SAVE
SMALLER
OF THIS (+0)
AND NEXT (+2)
MINIMUM
DELETING (+1)
MAXIMUM.

Y ↓

DP2

DPSUB:
SAVE
SMALLER
OF PREVIOUS (-1)
AND NEXT (+1)
MINIMUMS

DELETE THIS (+0) MAX
AND NEXT (+1) MIN.

DPBACK

DELETE SELECTED
MAX AND
HIGHER MIN
AND THEIR
POSITIONS

ONLY
ONE MAX
LEFT
?

Y →

②/⑤

PSUM-5
USE WEIGHTED
LINE DIRECTION

N ↓

②/⑥

DOLP4
PROCESS NEW
MAX/MIN OR
MIN/MAX PAIR

Figure 10-8   DONUT (Page 7 of 8)

DPSUB: SAVE SMALLER OF TWO SELECTED LOCAL MINIMUMS
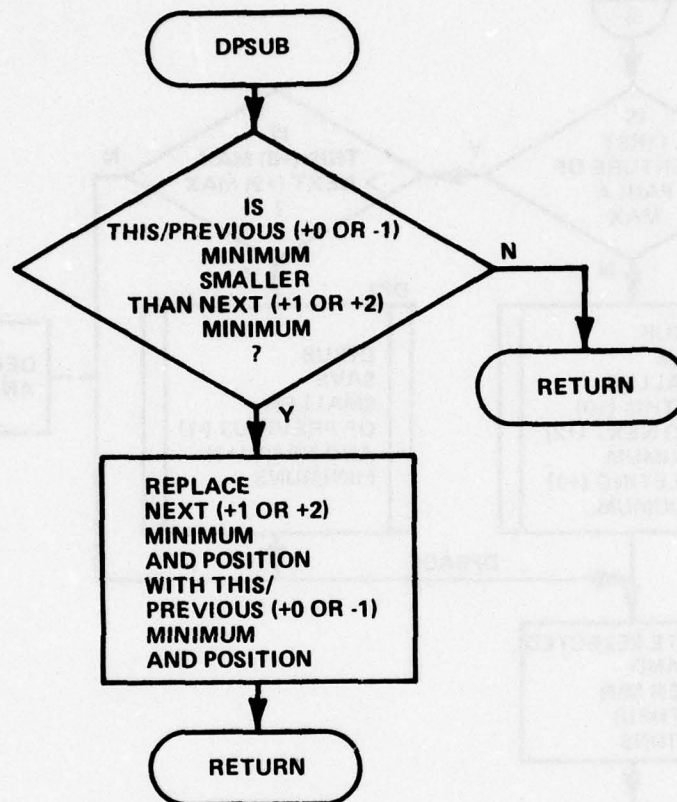
Figure 10-8   DONUT (Page 8 of 8)

Program Name: HEART

Program Description: This routine is called by LBAND to simulate the
                          TOPS Donut. This routine calls DNT2I to obtain
                          the weighted aperture sums. The inner ring average
                          is tested to see if the donut is on a line. When
                          the donut is on a line, the middle ring is searched
                          for possible directions. When possible directions
                          are found in the middle ring, routine HEVAL is
                          called to determine the direction of the line out
                          of the donut. This routine will return the number
                          of directions found, and a list of the directions
                          found.

Logic Diagram: See Figure

Program Constants: See program listing.

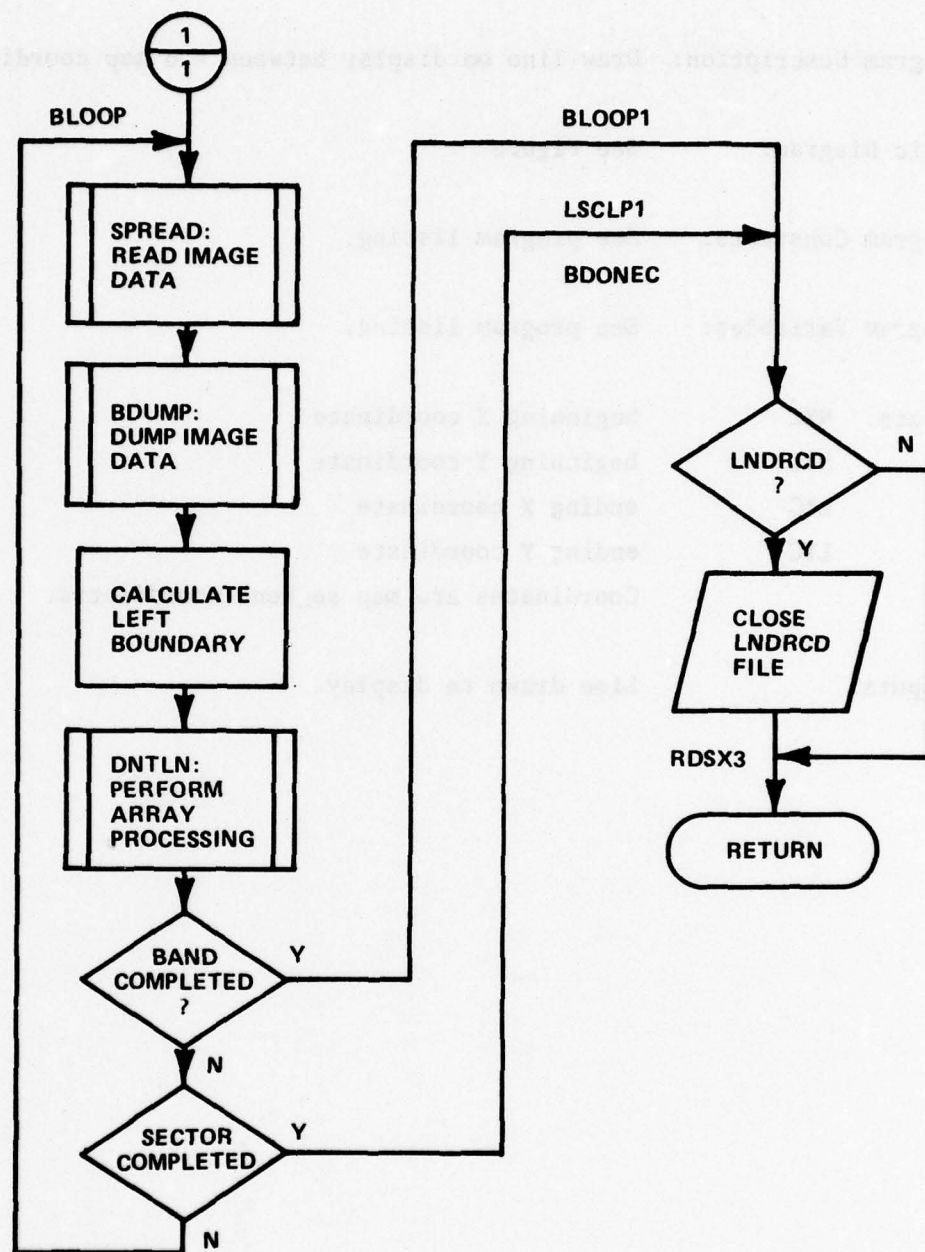Program Variables: See program listing.

Inputs: Coordinate of center of donut.

Outputs: Number of the directions found, and a list of the
                          directions found, if any.

Figure 10-9   HEART (Page 1 of 5)

NINTF
1
1 4

INITIALIZE
MIDDLE RING
SEARCHES

2
3   LOOP 2

SEARCH FOR
BACKGROUND
LEVEL
APERTURE

NOZRO

SEARCH FOR
APERTURE
ABOVE THRSH
BACKGROUND

LOOP 3

IS
MIDDLE RING
APERTURE
ABOVE
THRSH
?

N

APERTURE
ABOVE
THRSH
?

Y

Y

N

1
3

PEAK

INCREMENT
TO NEXT
MIDDLE RING
APERTURE

INCREMENT
TO NEXT
MIDDLE RING 1
APERTURE

FOUND
APERTURE
ABOVE
BACKGROUND
THRSH

N

MIDDLE
RING 1
DONE
?

N

MIDDLE
RING 1
DONE
?

Y

Y

2
5

DONE

2
5

DONE

Figure 10-9   HEART (Page 2 of 5)

10-29

Figure 10-9   HEART   (Page 3 of 5)

**TRYITH: TRY INCREASING
BACKGROUND THRESHOLD
THRSH**

①/③

INCREASE
BACKGROUND
THRESHOLD
THRSH BY
ONE PERCENT
OF INNER
RING AVERAGE
UNTIL
THRESHOLD
CHANGES

CLEAR COUNT
OF DIRECTIONS
FOUND

ANY
MIDDLE
RING 1
APERTURES
> THRSH

N

Y

①/②

NINTF

①/⑤
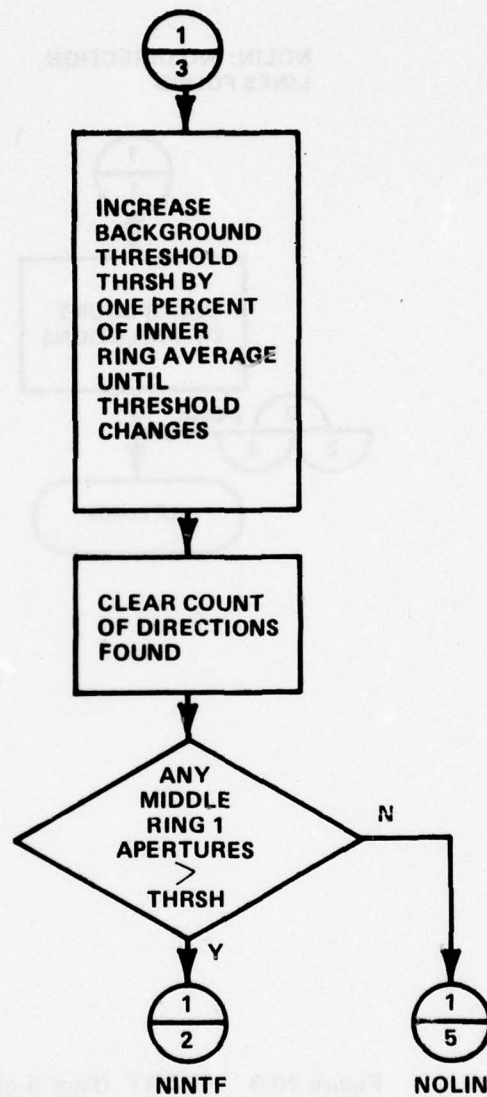
NOLIN

Figure 10-9   HEART   (Page 4 of 5)

10-31

**NOLIN: NO DIRECTION
LINES FOUND**

CLEAR COUNT
OF DIRECTIONS

DONE

RETURN
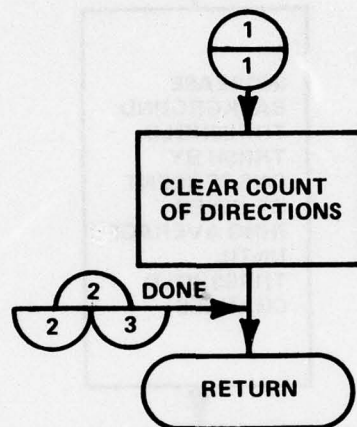
Figure 10-9   HEART   (Page 5 of 5)

Program Name: HEVAL

Program Description: This routine is called by HEART to determine the
                         direction of a line segment from the TOPS Donut.
                         The greater of two middle ring apertures is chosen.
                         The outer ring is examined at the points adjacent
                         to the chosen point to determine if the line is
                         present in the outer ring. If the line is in the
                         outer ring, the greatest of the outer ring apertures
                         is chosen for the line direction.

Logic Diagram: See Figure

Program Constants: See program listing.
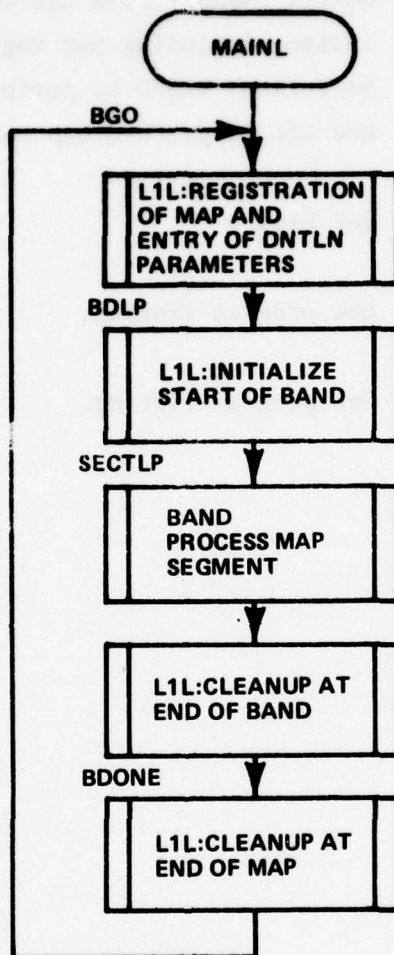
Program Variables: See program listing.

Inputs: Weighted aperture sums, and selected middle ring
                         apertures.

Outputs: Line direction.

EVALUATE MIDDLE RING 1 "DOUBLE"
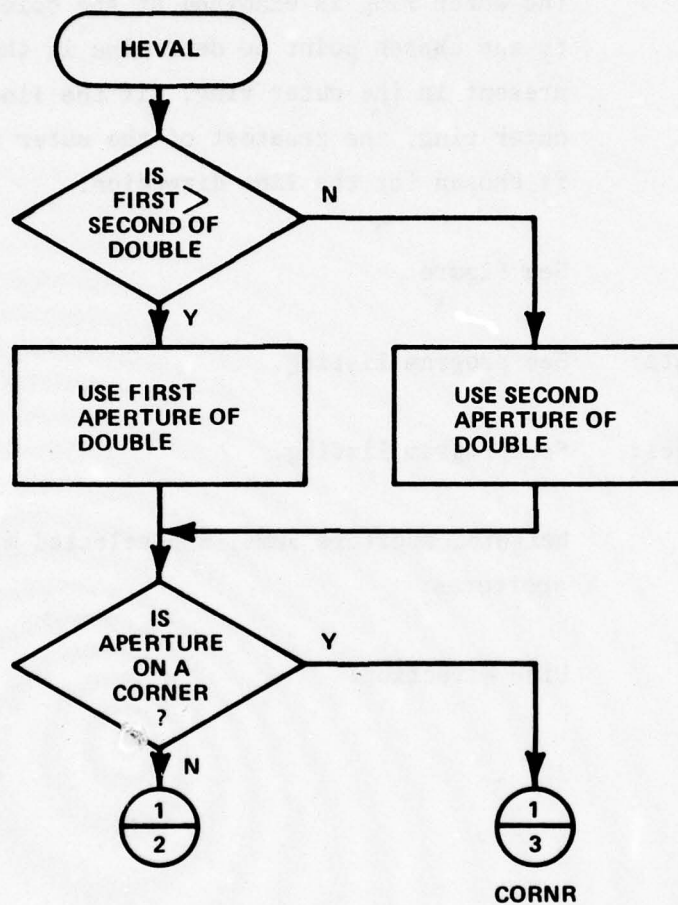
Figure 10-10   HEVAL (Page 1 of 3)

10-34

PEAK: MIDDLE RING 2 IS NOT ON A CORNER
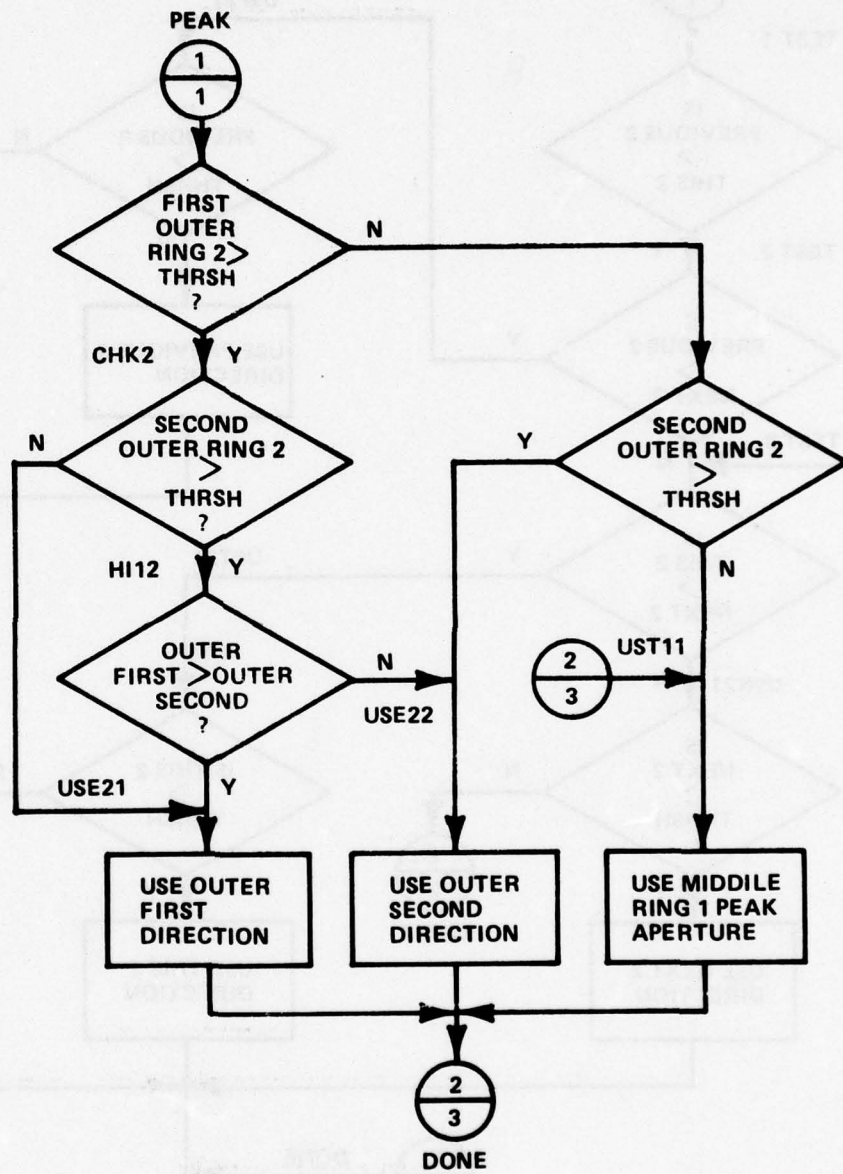
Figure 10-10   HEVAL (Page 2 of 3)

10-35

CORNR: PEAK MIDDLE RING 1 APERTURE IS A CORNER

DETERMINE MAX OF RING 2 PREVIOUS, THIS, AND NEXT APERTURES
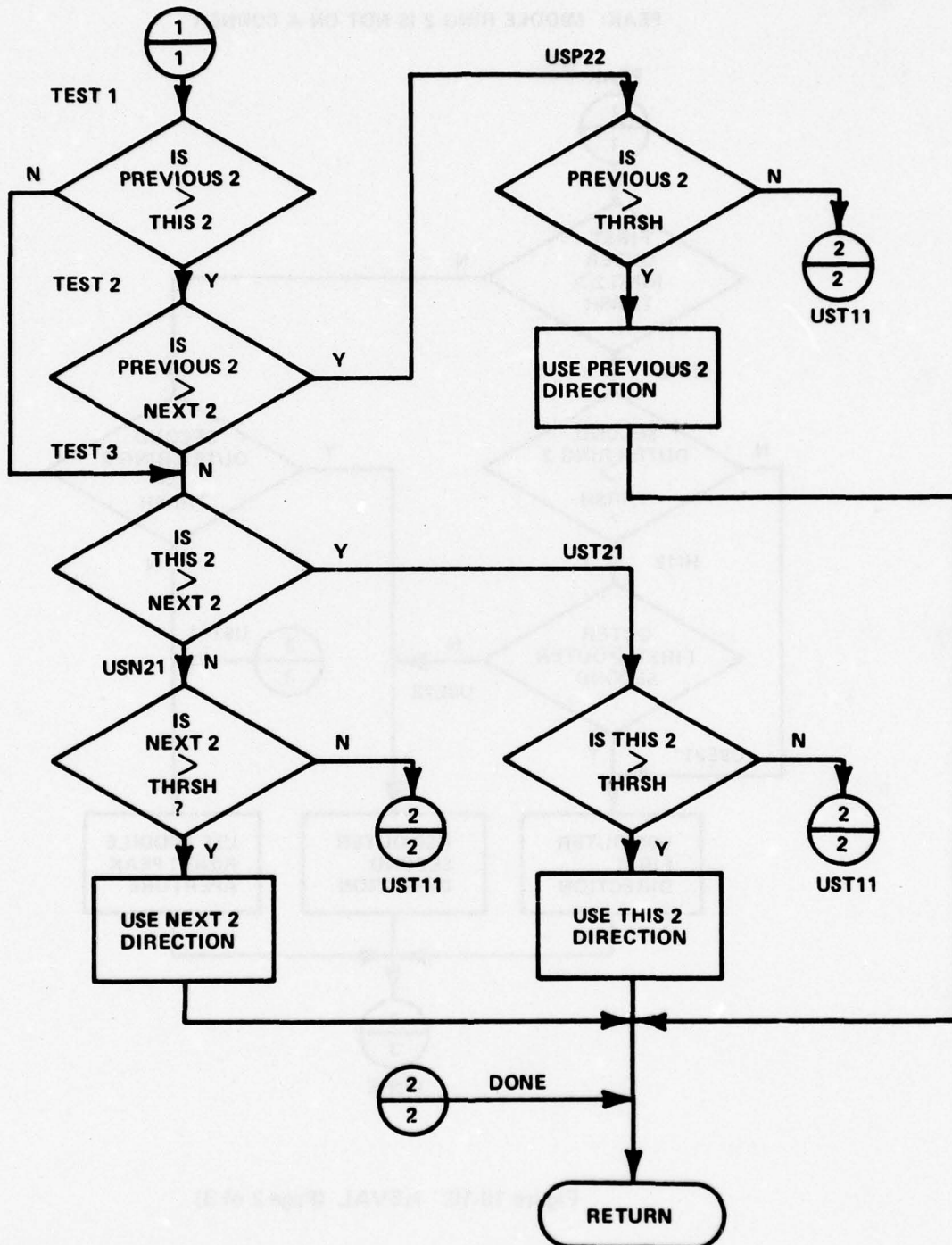
Figure 10-10   HEVAL (Page 3 of 3)

Program Name: INCX

Program Description: Obtain intensity for incremented X coordinate
                      relative to last data point sampled by READI, INCX,
                      DEXC, INCY, or DECY. This routine is an entry
                      point in READI, and is called from the geometric
                      array simulation routines.

Logic Diagram: See Figure

Program Constants: See program listing.

Program Variables: See program listing.

Inputs: Coordinate buffer pointers of last intensity are
                        used to determine new coordinate buffer pointers.

Outputs: Intensity data value.

(See Figure 10-17)

Figure 10-11   INCX

Program Name: INCY

Program Description: Obtain intensity for incremented Y coordinate
                       relative to last data point sampled by READI, INCX,
                       DECX, INCY, or DECY. This routine is an entry
                       point in READI, and is called from the geometric
                       array simulation routines.

Logic Diagram: See Figure

Program Constants: See program listing.

Program Variables: See program listing.

Inputs: Coordinate buffer pointers of last intensity are
                       used to determine new coordinate buffer pointers.

Outputs: Intensity data value.

(See Figure 10-17)

Figure 10-12   INCY

10.12

Program Name: LBAND

Program Description: The LBAND routine, called by MAINL, calls routine
                      SREAD to obtain scanner data across a map segment,
                      and DNTLN to position the simulated array along a
                      line segment.

Logic Diagram: See Figure

Program Constants: See program listing.

Program Variables: See program listing.
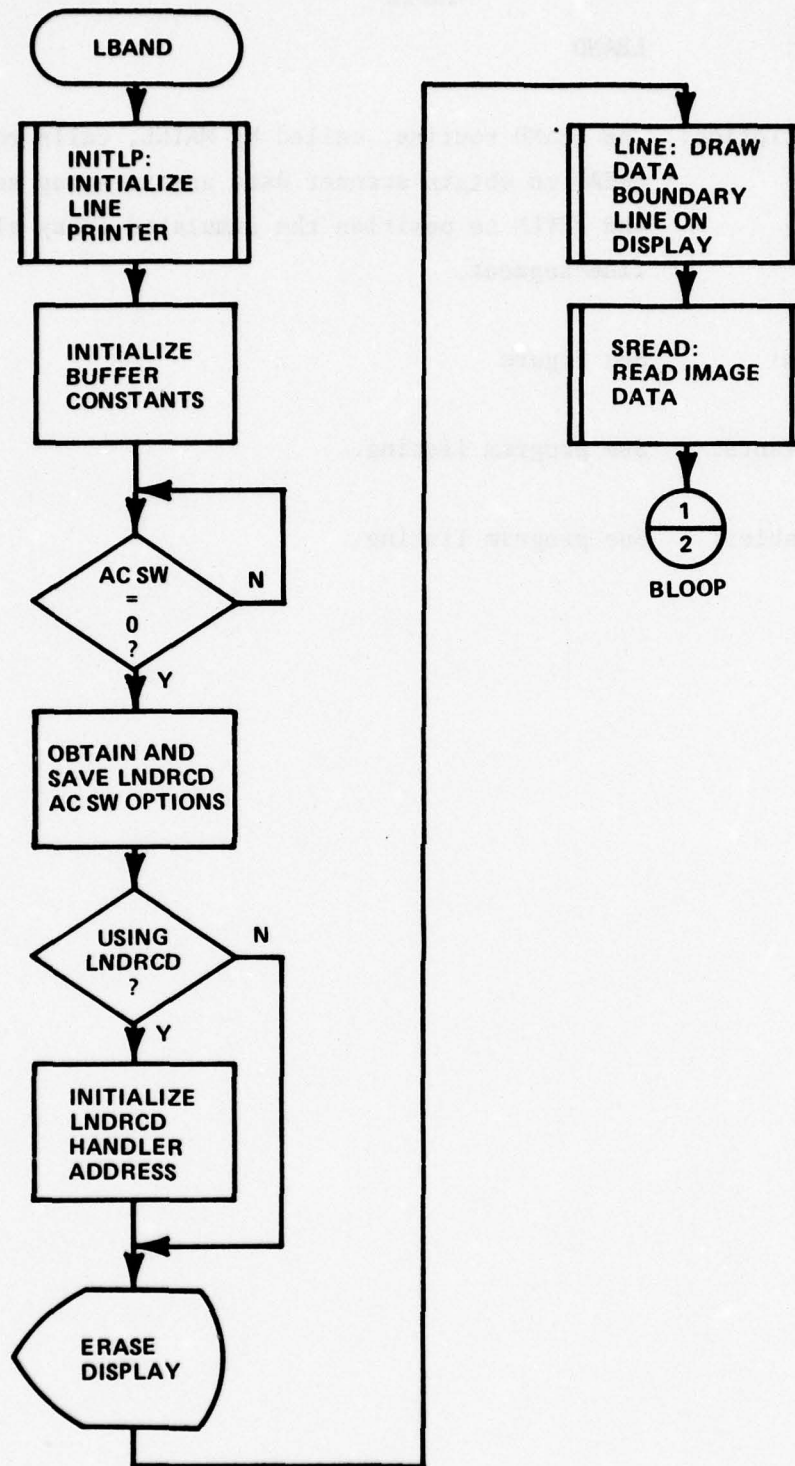
Figure 10-13   LBAND   (Page 1 of 2)

Figure 10-13   LBAND   (Page 2 of 2)

Program Name: LINE

Program Description: Draw line on display between two map coordinates.

Logic Diagram: See Figure

Program Constants: See program listing.

Program Variables: See program listing.

Inputs: NXC   beginning X coordinate
         NYC   beginning Y coordinate
         LXC   ending X coordinate
         LYC   ending Y coordinate
                      Coordinates are map segment coordinates.

Outputs: Line drawn on display.
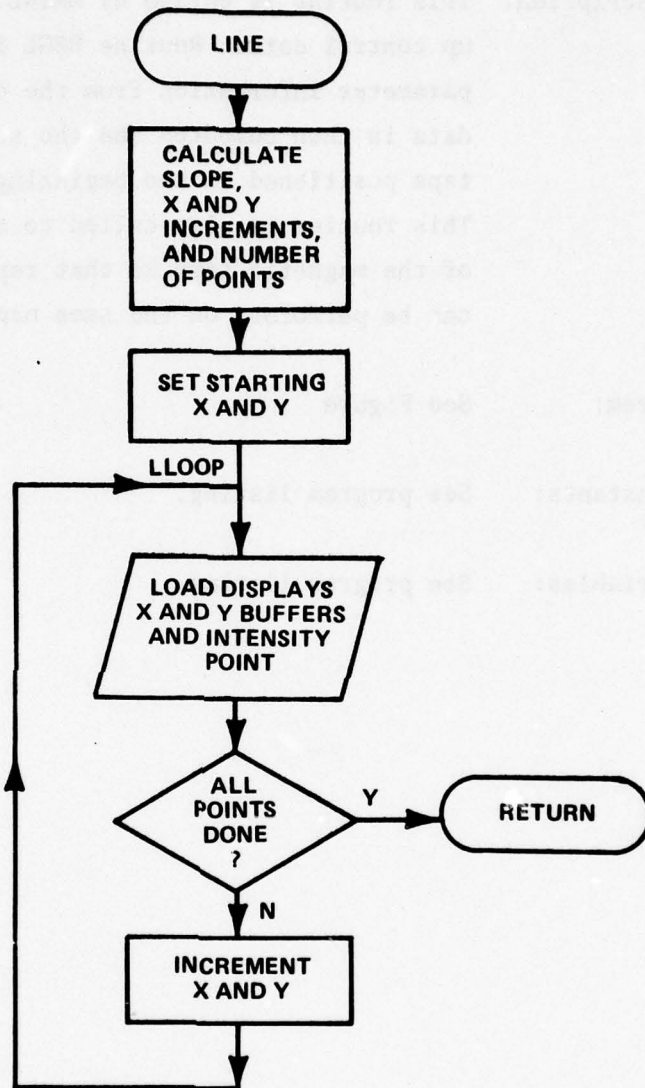
Figure 10-14   LINE

10.14

Program Name: L1L

Program Description: This routine is called by MAINL to obtain and set
                           up control data. Routine REGL is called to obtain
                           parameter information from the operator. Control
                           data is then computed and the scanner or magnetic
                           tape positioned to the beginning of the scan data.
                           This routine is also called to allow positioning
                           of the magnetic tape so that repetative passes
                           can be performed on the same map segment.

Logic Diagram: See Figure

Program Constants: See program listing.

Program Variables: See program listing.
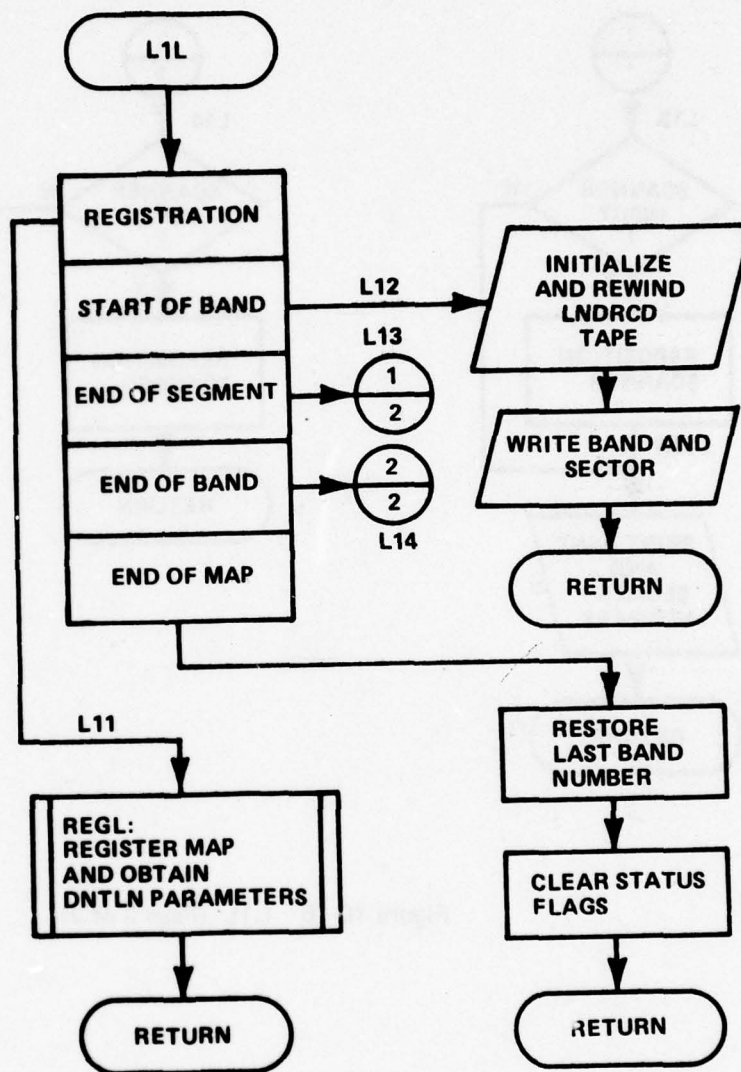
Figure 10-15   L1L   (Page 1 of 2)

10-47
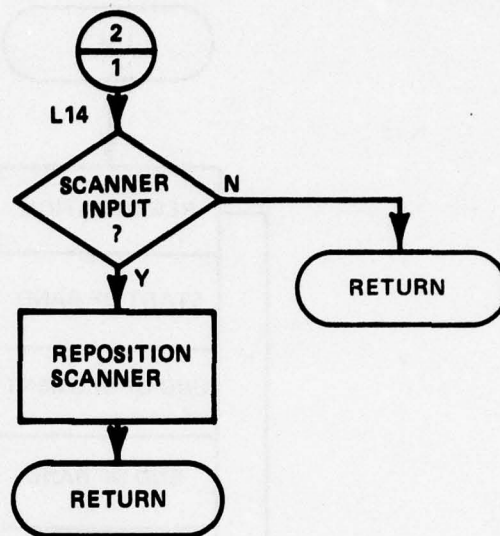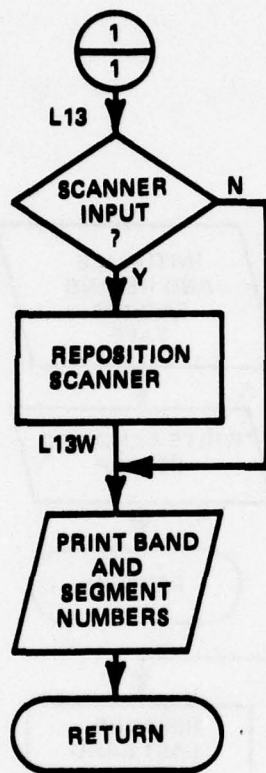
Figure 10-15   L1L   (Page 2 of 2)

10.15

Program Name:	MAINL
Program Description:	MAINL is the main supervisory routine for LAND-SCAPE. MAINL calls L1L to perform map initialization, including map registration and data selection; LBAND to perform map data processing; and L1L to perform map termination.
Logic Diagram:	See Figure
Program Constants:	See program listing.
Program Variables:	See program listing.

MAINL

BGO

L1L:REGISTRATION
OF MAP AND
ENTRY OF DNTLN
PARAMETERS

BDLP

L1L:INITIALIZE
START OF BAND

SECTLP

BAND
PROCESS MAP
SEGMENT

L1L:CLEANUP AT
END OF BAND

BDONE

L1L:CLEANUP AT
END OF MAP

Figure 10-16   MAINL

10-50

10.16

Program Name: READI

Program Description: Routine obtains intensity data from scanner data
                      buffer for specified point.

Logic Diagram: See Figure

Program Constants: See program listing.

Program Variables: See program listing.

Inputs: XPOS   X coordinate
         YPOS   Y coordinate

Outputs: Intensity data.
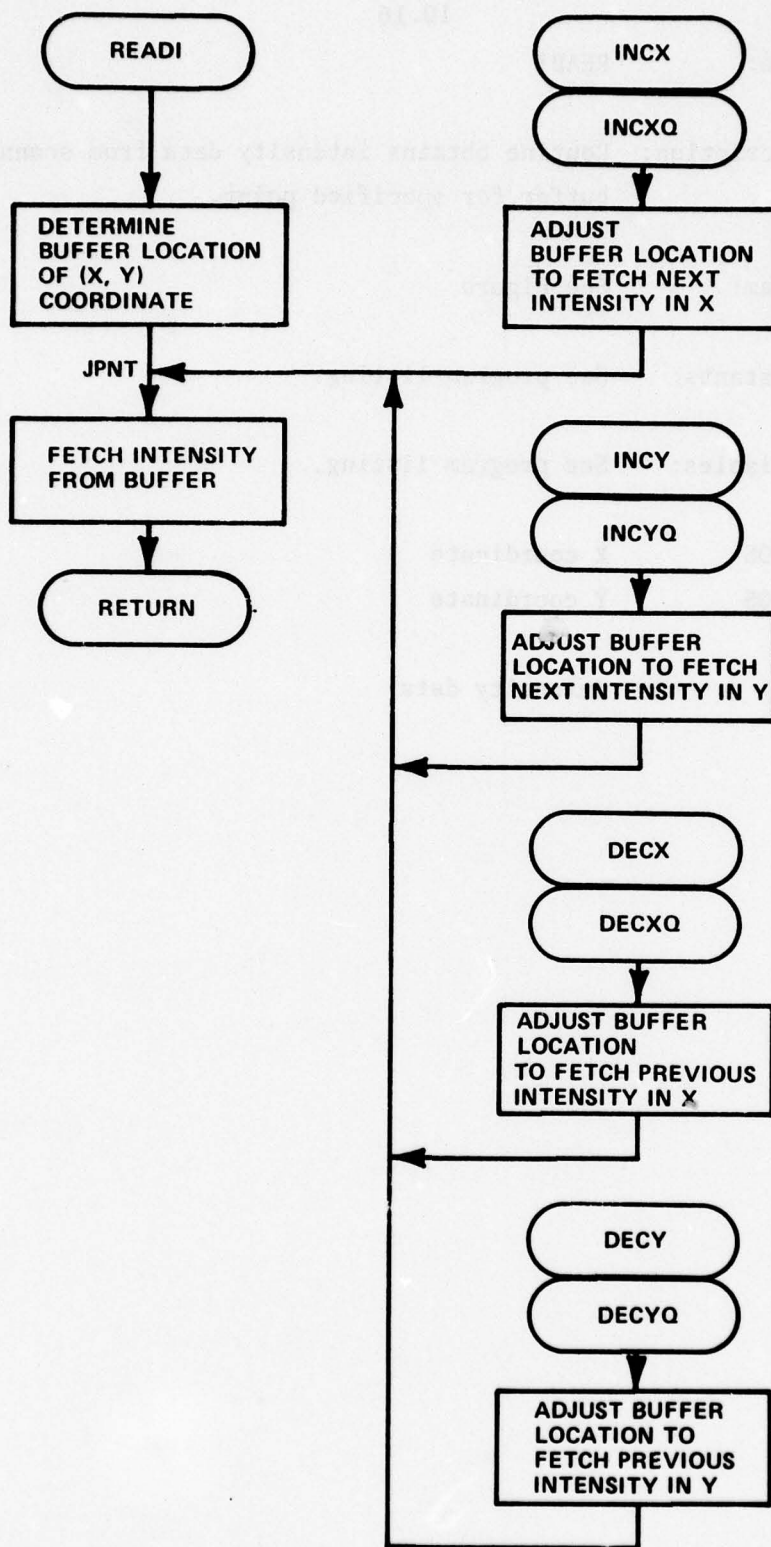
Figure 10-17   READI, DECX, DECY, INCX, INCY

10-52

10.17

Program Name: READS

Program Description: READS is called by SREAD to obtain one scanner line of data. READS determines whether data is to be obtained from the table scanner, and optionally recorded on a LNDRCD data tape; or if the data is to be obtained from a previously recorded LNDRCD data tape.

When data is to be obtained from the table scanner, the routine commands the table to increment to the next sample point and transfer the scanner sample to the proper area of a circular buffer. The scanner data is also displayed as set up by SREAD.

READS then checks to see if a LNDRCD data tape is being created. If so, then the scanner data is output to the LNDRCD data tape.

When data is to be obtained from the LNDRCD data tape, READS inputs a record from the data tape into the proper area of a circular buffer. The data is then displayed.

Logic Diagram: See Figure

Program Constants: See program listing.

Program Variables: See program listing.

Image Data Inputs: Image data is packed 4 intensities per word at 4 bits per intensity. The first intensity is in the least significant position in the word, with each following intensity occupying the next 4 bits

to the left of the previous intensity. The two
most significant bits of the word are not used.

0 1	2 3 4 5	6 7 8 9	10 11 12 13	14 15 16 17
unused	fourth	third	second	first

The image data is obtained from the scanner as
intensities from a linear array. The 512 array data
intensities, packed 4 intensities per word, occupy
128 words. The data words representing one linear
scan are stored by READS in a segment of a circular
buffer which can hold 32 scan lines. The buffer
segment is addressed by the modulus 32 of the X
coordinate of the scan data.

LNDRCD data is recorded as sequential records, each
consisting of the scanner data from a linear scan.
The LNDRCD data format is the same format as the
linear scanner array data format.

10-54
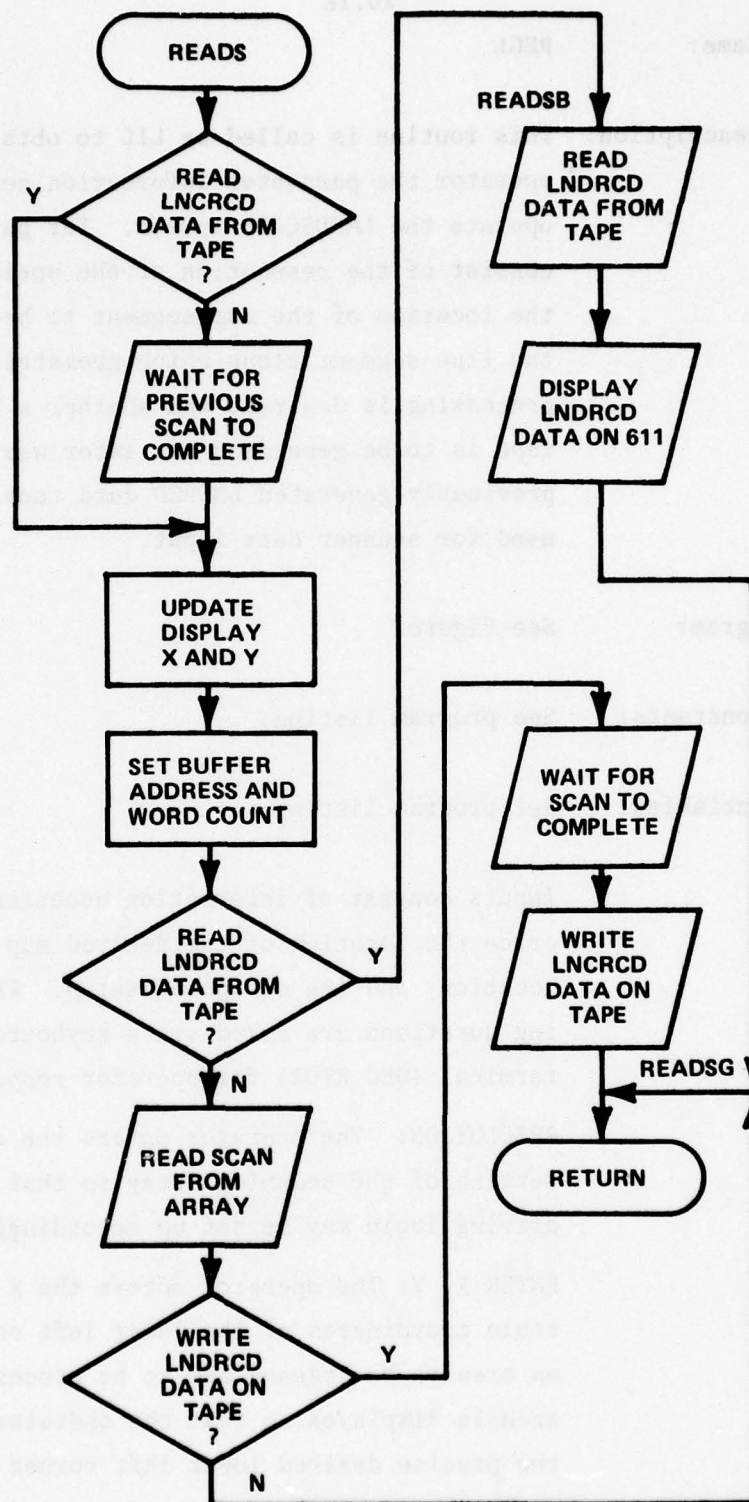
Figure 10-18   READS

Program Name: REGL

Program Description: This routine is called by LIL to obtain from the
                       operator the parameter information necessary to
                       operate the LANDSCAPE system. The parameters
                       consist of the resolution of the optics system;
                       the location of the map segment to be scanned;
                       the line segment along which geometric array
                       processing is desired; and whether a LNDRCD data
                       tape is to be generated for later use, or a
                       previously generated LNDRCD data tape is to be
                       used for scanner data input.

Logic Diagram: See Figure

Program Constants: See program listing.

Program Variables: See program listing.

Inputs: Inputs consist of information necessary to des-
                       cribe the location of the desired map segment
                       location, and the equipment setup. The follow-
                       ing questions are asked via a keyboard display
                       terminal (DEC RT02) for operator response:

                       RESOLUTION: The operator enters the resolution
                       setting of the scanning array so that the table
                       driving logic may be set up accordingly.

                       ENTER X, Y: The operator enters the X and Y
                       table coordinates of the lower left corner of
                       an area to be scanned and to be processed. This
                       area is displayed so that the operator may select
                       the precise desired lower left corner of the area
                       to be processed.

ENTER CORNER: The operator may move a track dot symbol on the displayed scan using the track ball. The track dot is placed at the lower left corner of the area to be processed. The send key is used with no data to indicate that the track dot is at the desired point.

If the displayed area does not contain the desired corner of the data, the operator may enter a minus one (-1) to allow reentry of X, Y coordinates.

ENTER X1, Y1: The coordinates of the left end of a line segment along which to process the geometric array are entered. If no array processing is to be done, then a minus one (-1) is entered. A zero, or no data, may be entered to display the coordinates of a track dot symbol, allowing the operator to find the coordinates of a point on the display.

ENTER X2, Y2: The coordinates of the right end of a line segment along which to process the geometric array are entered.

ENTER STEP SIZE IN POINTS: The stepping increment, N, between points along the line segment is entered. Every Nth point along the line segment is processed. The default step is one. A minus one (-1) may be entered to allow reentry of X1, Y1 and following entries.

REGL

OBTAIN
TABLE
RESOLUTION

LNDRCD
TAPE INPUT
?

Y

N

INITIALIZE TABLE

SET CONTROL
VARIABLES FOR
LANDSCAPE

LNDRCD
TAPE INPUT
?

N

Y

1/2

10

OBTAIN
LOWER
LEFT CORNER
OF MAP

MOVE TABLE
SCANNER TO CORNER

DISPLAY MAP
SECTION

OBTAIN
LOWER LEFT
REGISTRATION
POINT

REGISTRATION
OK
?

N

Y

1/2
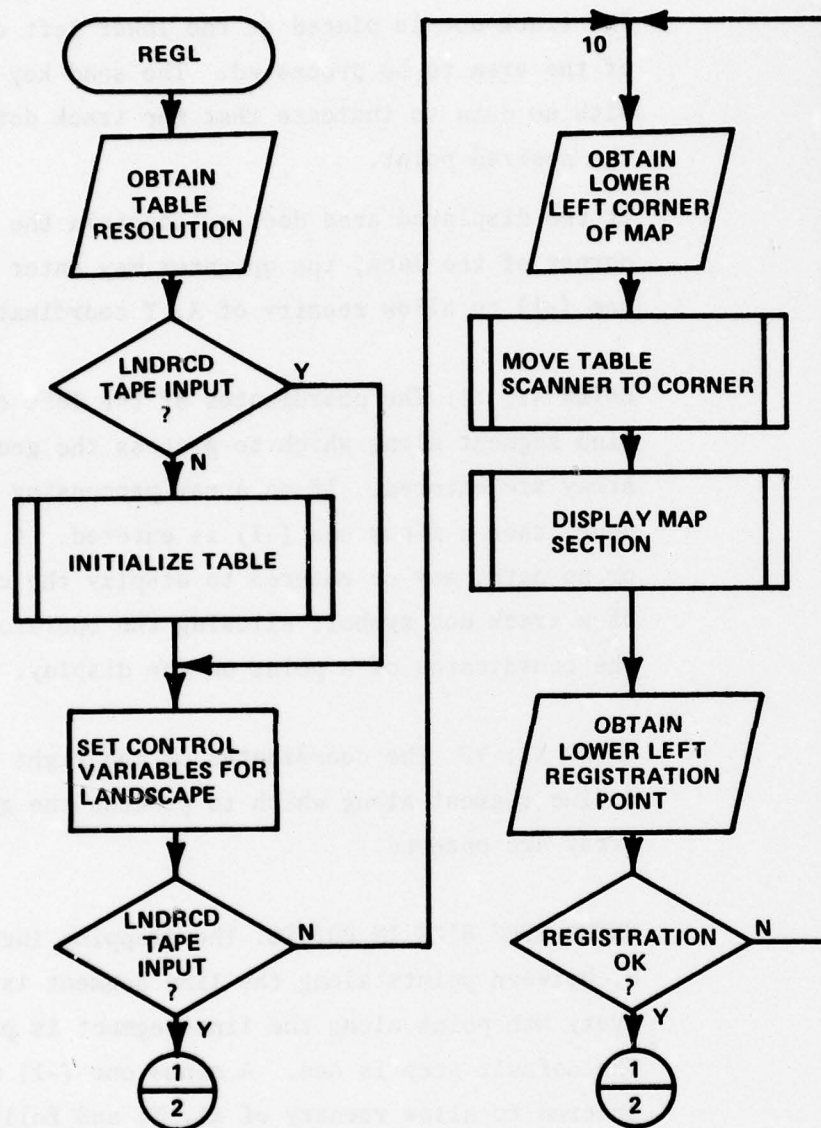
Figure 10-19   REGL   (Page 1 of 3)

10-58
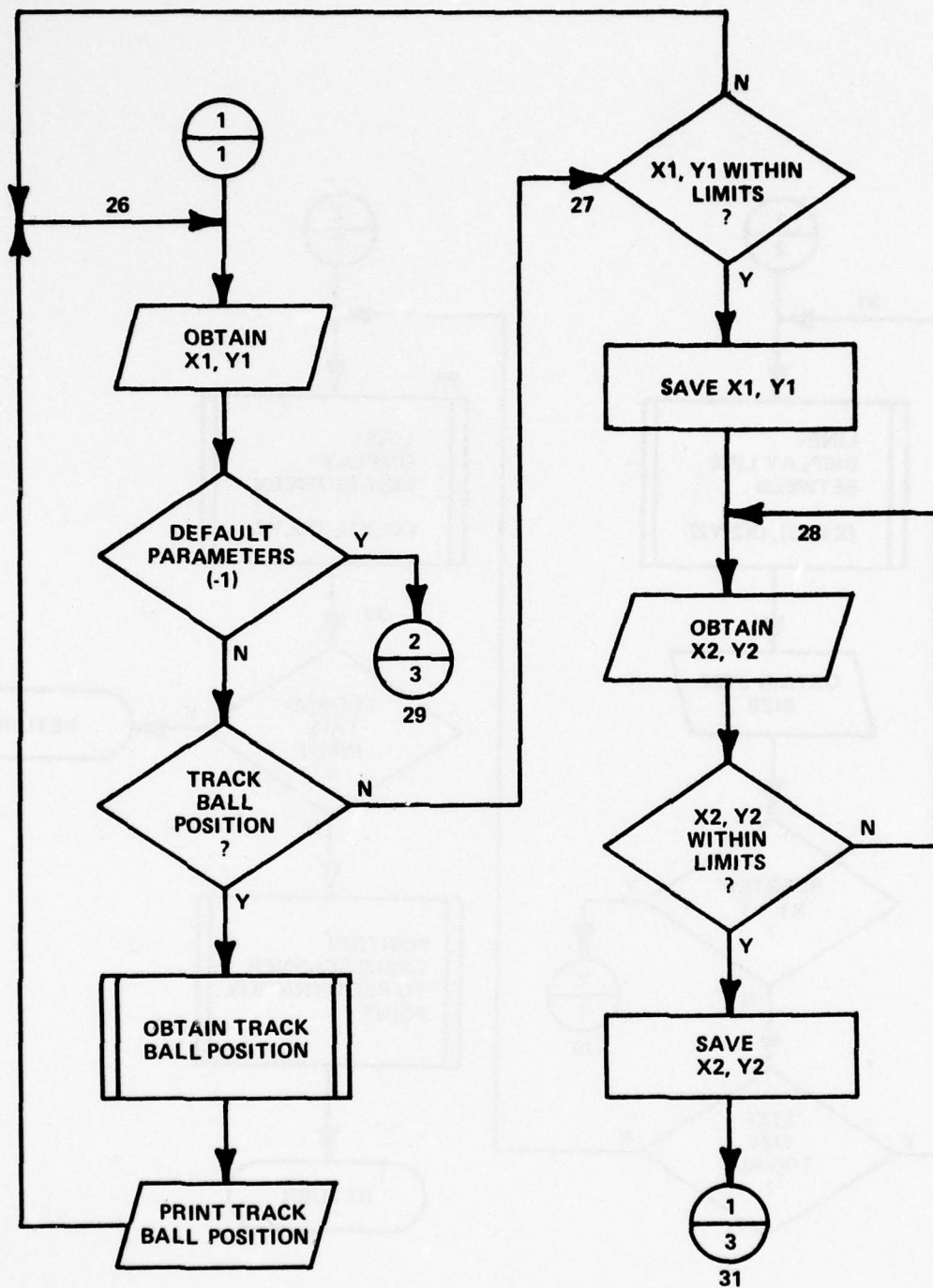
Figure 10-19 REGL (Page 2 of 3)
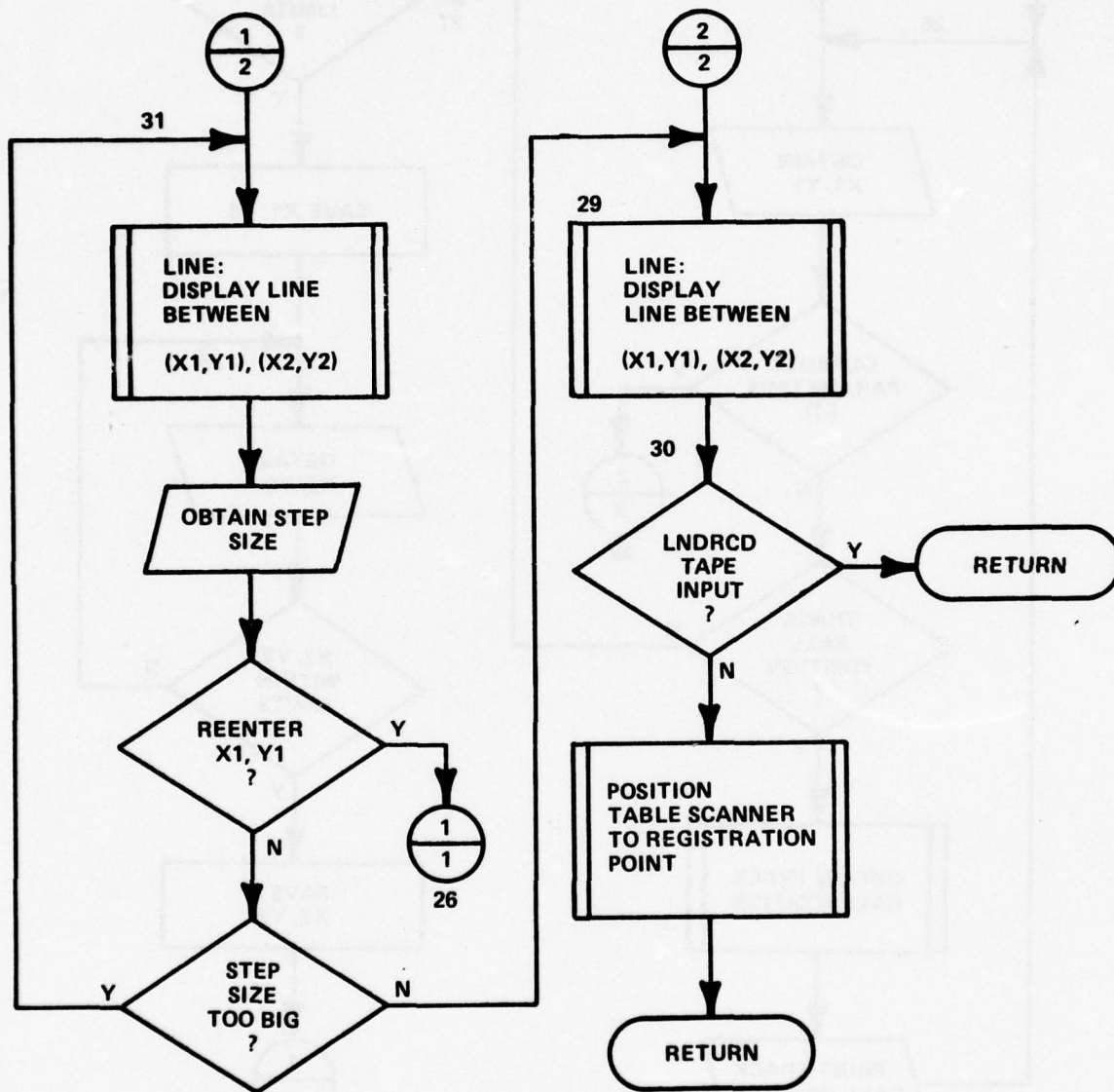
Figure 10-19   REGL   (Page 3 of 3)

10.19

Program Name: SREAD

Program Description: SREAD is called by LBAND to obtain data. SREAD
                       prepares the display to accept scanner data and
                       calls READS to obtain scanner data from either
                       the linear array or from the LNDRCD data tape.
                       SREAD then restores the display to a normal output
                       mode.

Logic Diagram: See Figure

Program Constants: See program listing.

Program Variables: See program listing.

10-61

SREAD

READ LNDRCD DATA FROM TAPE

Y

N

TURN ON TABLE INPUT FLAGS

SREADA

READS: READ SCAN

16 SCANS READ ?

N

Y

READ LNDRCD DATA FROM TAPE

Y

N

TURN OFF TABLE INPUT FLAGS

SREADB

RETURN

Figure 10-20   SREAD

10-62
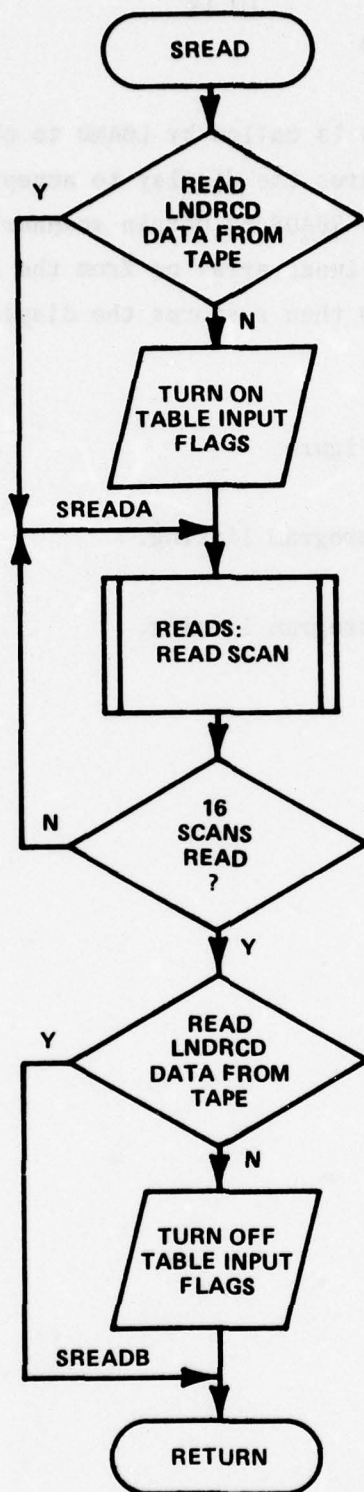
10.20

Program Name: XDIS

Program Description: Convert map X coordinate for the display.

Logic Diagram: See Figure

Program Constants: None

Program Variables: See program listing.

Input: Map X coordinate

Output: Display X coordinate
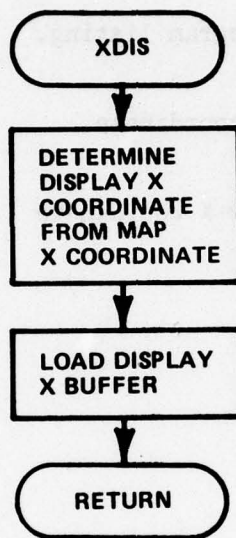
Figure 10-21   XDIS

APPENDIX A

LARGE LINEAR ARRAY SPECIFICATIONS

The scanning table utilizes a Reticon LC600 Solid State Line
Scan Camera for document scanning with an RL1024C monolithic linear
array of silicon photodiodes as the image sensor. Camera scan rates
are adjustable from 5KHZ to 1.05 MHZ. Gray level video for each line
scan is processed in the PDP-9 but external camera controls are used
for setting the video gain and thresholds. This Appendix contains
the manufacturer's specification sheets for the linear array.
Reticon's camera and systems product summary is also included.

RETICON® C SERIES SOLID-STATE LINE SCANNERS
128, 256, 384, 512, 768, 1024 ELEMENTS
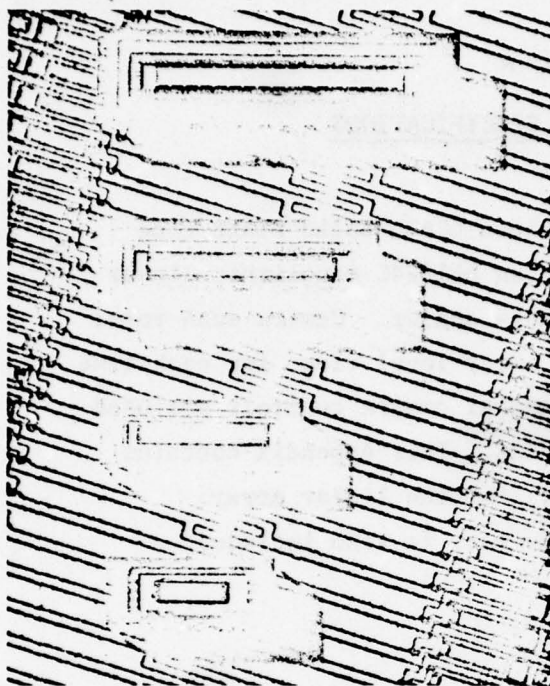
Reticon solid state line scanners are high density monolithic linear arrays of silicon photodiodes with integrated scanning circuits for serial readout. With a single basic design the "C" and "EC" series offers a choice of high resolution devices for page reading, film scanning and facsimile applications; lower resolution devices for OCR and pattern recognition; wide aperture high sensitivity devices for real time spectroscopy; and a wide selection of devices for various non-contact measurement and inspection applications. Some key features of these devices include the following:

- **High resolution—up to 1024 elements on 1 mil centers or 512 elements on 2 mil centers.**

- **On chip scanning for serial video output.**

- **Low power shift register scanning circuits—only 3 mwatts dissipation.**

- **Charge storage mode operation for high sensitivity.**

- **Wide range of scan rates—up to 10 MHz.**

- **Simple external circuitry using standard components.**

- **Standard dual-in-line packages with quartz windows.**

GENERAL DESCRIPTION

The Reticon "C" series is a family of monolithic self-scanning linear photodiode arrays. The devices in this series consist of a row of silicon photodiodes, each with an associated storage capacitor on which to integrate photocurrent and a multiplex switch for periodic readout via an integrated shift register scanning circuit. The part number of each device indicates the number of elements in the array while the letter(s) following the number indicate the center-to-center spacing and the required clock phases for driving the scanning circuit. "C" devices have sensors on one mil (25.4μ) centers and require 4-phase clocks while "EC" devices have sensors on two mil centers and require 2-phase clocks. The sensing area is defined by an aperture which is either one or 17 mils wide and runs the full length of the array. The 17 mil option is indicated by a /17 following the "C" or "EC" designation. For example, the RL-1024C/17 has 1024 elements on 1 mil centers and a 17 mil wide aperture. It is driven by a four-phase clock.

The devices are packaged in 16, 18, or 22 lead dual-in-line integrated circuit packages with ground and polished quartz windows. Pin configurations for the "C" devices are shown in Figure 1.

In the "EC" devices only common plus the left or the right row of pins is connected and devices may be supplied in either configuration. However, all devices may be made equivalent simply by connecting opposite pairs of pins on the socket.

TOP VIEW

RL256C
(RL128EC)

RL512C
(RL256EC)

RL768C, RL1024C
(RL384EC, RL512EC)
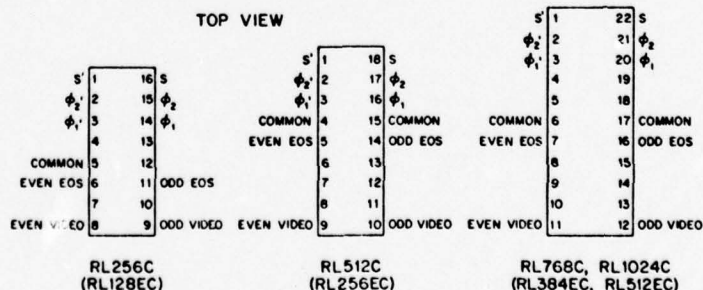
Figure 1. Pin configuration for "C" series line scanners. In the "EC" series only the left or the right row of pins is connected.

EQUIVALENT CIRCUIT

A simple equivalent circuit of an "EC" line scanner is shown in Figure 2. Each cell consists of a photosensor and a parallel storage capacitor and is connected through an MOS transistor switch to a common video output line. The switches are turned on and off in sequence by the shift register scanning circuit thereby periodically recharging each cell to 5 volts and storing a charge Q_{sat} on its capacitance. The shift register is driven by a two-phase clock with a periodic start pulse being introduced to initiate each scan. The cell-to-cell sampling rate is determined by the clock frequency and the total time between line scans is the interval between start pulses. During this line time the charge on each capacitor is gradually removed by the reverse current flowing in the associated photodiode. The reverse current is made up of two components: the photocurrent i_p and the dark leakage current i_d which is typically less than 1 pA at room temperature and can be neglected. The photocurrent is the product of the diode sensitivity and the light intensity or irradiance. During a line scan time the charge Q removed from each cell is the product of the photocurrent and the line time. This charge must be replaced through the video line when the diode is sampled once each scan. Thus, the output signal obtained from each scan of an N element array is a train of N charge pulses each proportional to the light intensity on the corresponding photodiode.

An equivalent circuit of a "C" line scanner is shown in Figure 3. These devices each consist of two "EC" circuits with the sensors interdigitated from either side to form a continuous row. By properly phasing the clock drives to the two shift registers all of the diodes can be sampled in proper sequence. The two video lines can then simply be connected together to provide a continuous train of output charge pulses.

SENSOR GEOMETRY

In the "C" and "EC" line scanners the light sensing area is a long, narrow rectangular region defined by an aperture in an opaque mask. Bar shaped photodiodes extend across the aperture and connect to the storage capacitors and multiplex switches which are buried under the mask. The entire aperture is photosensitive and photocurrent generated by light incident between the photodiodes will be collected by the nearest diode. Figure 4 shows the aperture geometry along with an idealized response function which would be obtained by scanning a point source of visible light along the length of the aperture.

The dimensions a, b, and c indicated in Figure 4 are as follows: The photodiode width a is 0.5 mils. The photodiode spacing b is 1 mil for "C" devices and 2 mils for "EC" devices. The aperture width c is optional. One mil and 17 mils are standard and devices with any intermediate aperture width can be produced with a nominal tooling charge.
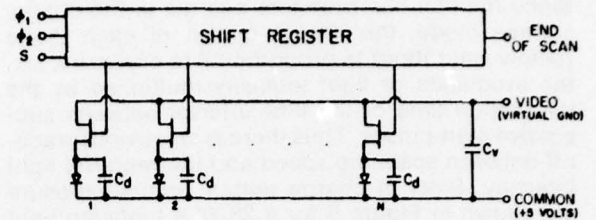
Figure 2. Equivalent circuit for "EC" series line scanner.
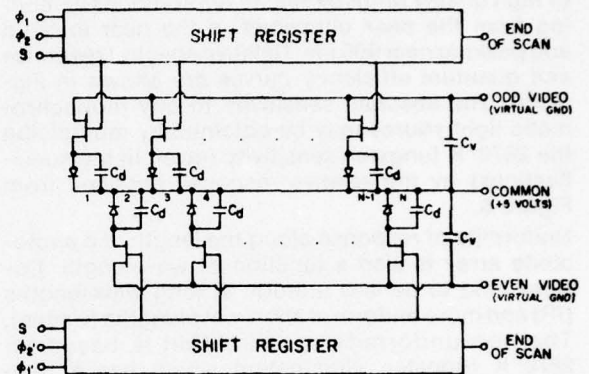
Figure 3. Equivalent circuit for "C" series line scanner.
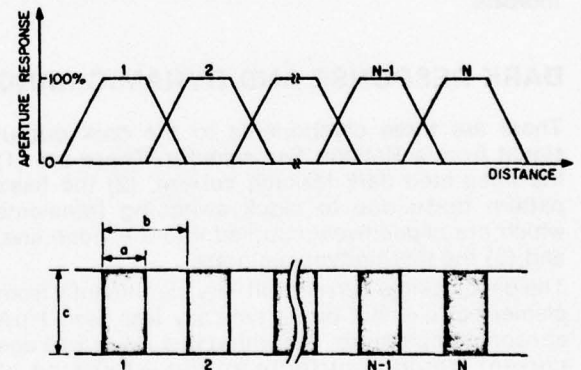
Figure 4. Sensor geometry and idealized aperture response function.

SENSITIVITY AND SPECTRAL RESPONSE

Since Reticon line scanners operate in the charge storage mode, the charge output of each diode (below saturation) is proportional to exposure, i.e., the irradiance or light intensity multiplied by the integration time or the time interval between successive start pulses. Thus there is an obvious trade-off between scanning speed and the required light intensity. Plots of charge output versus exposure are shown in Figure 5 for a 2870°K tungsten light source. The slope of these curves in the linear region is the sensitivity $S\left(\frac{pA}{\mu watt/cm^2}\right)$ while the saturated value is the saturation charge Q_{sat} (pcoul).

Spectral response of Reticon line scanners is typical of high quality diffused silicon photodiodes extending from the near ultraviolet to the near infrared and peaking near 900 nm. Relative spectral response and quantum efficiency curves are shown in Figure 6. The absolute sensitivity to any monochromatic light source may be obtained by multiplying the 2870°K tungsten sensitivity (given in the specifications) by the relative response obtained from Figure 6.

Uniformity of response along the length of a photodiode array is also a function of wavelength. Devices tend to be less uniform at long wavelengths (IR) and more uniform at short wavelengths (visible). The non-uniformity specification is based on 2870°K tungsten illumination which has a high percentage of its energy in the infrared. Therefore, when only visible light is used the uniformity will typically be better than the specifications would indicate.

Figure 5. Signal charge per cell as a function of exposure (light intensity x line scan time) for 2870°K tungsten source.
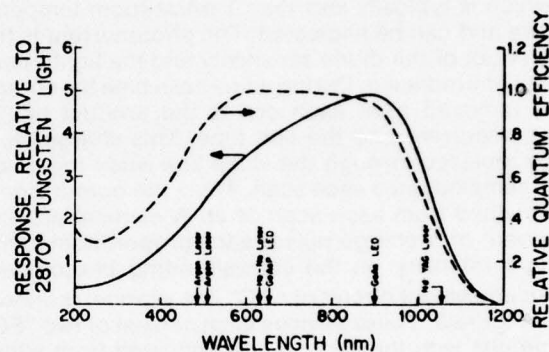
Figure 6. Dependence of sensitivity and quantum efficiency on wavelength.

DARK RESPONSE AND DYNAMIC RANGE

There are three components to the dark output signal from a Reticon line scanner. These are (1) the integrated dark leakage current, (2) the fixed pattern noise due to clock switching transients which are capacitively coupled into the video line, and (3) the thermodynamic noise.

The dark leakage current will vary significantly from element to element but is typically less than 1 pA at room temperature. Assuming this value, leakage current would contribute an output charge of 1 pcoul with a 1 sec line time or .04 pcoul with a 40 msec line time. Thus since $Q_{sat} \simeq 4$ pcoul, dark current will contribute about 1% of the saturated output signal for t_L = 40 msec, 0.1% for t_L = 4 msec and so on. The dark current is a very strong function of temperature, approximately doubling every 7°C. Thus the maximum allowable line time becomes correspondingly shorter at high temperatures and longer at low temperatures. An important feature of the "C" device design is the low power dissipation which means that self-heating is negligible.

The switching noise is very dependent on clock rise and fall times and on circuit layout. With the drive circuits shown in Figures 7 and 8 and the amplifier circuit of Figure 10, its amplitude will be less than 5% of the saturation level. The switching noise is generally periodic except that it may have a 1,2 or 1,2,3,4 pattern due to the fact that alternate diodes are sampled on different clock phases. Because of its periodicity, this switching noise may be removed by filtering or by using a charge integration, sample and hold circuit such as the Reticon RC-100. The residual, non-periodic fixed pattern in the dark level will typically be less than 1% of the saturation level.

Thermodynamic noise is the random, non-repetitive fluctuations which are superimposed on the dark level. This is the ultimate limiting noise which can not be removed by signal processing. Its amplitude is typically 0.1% of the saturation level.

If the saturation level is compared to the amplitude of the dark signal non-uniformity, the dynamic range is typically better than 100:1.

If the saturation level is compared to the thermodynamic noise on each individual element a dynamic range of greater than 1000:1 can be achieved with these devices.
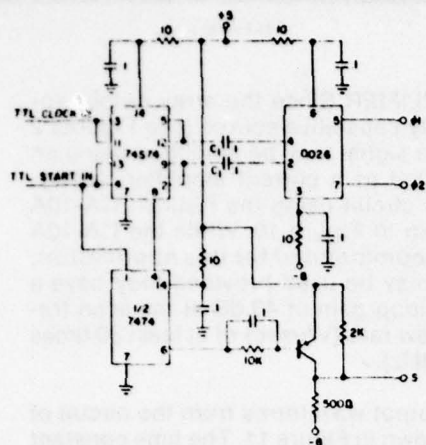
Figure 7. Two phase drive circuit and timing diagram for "EC" devices.
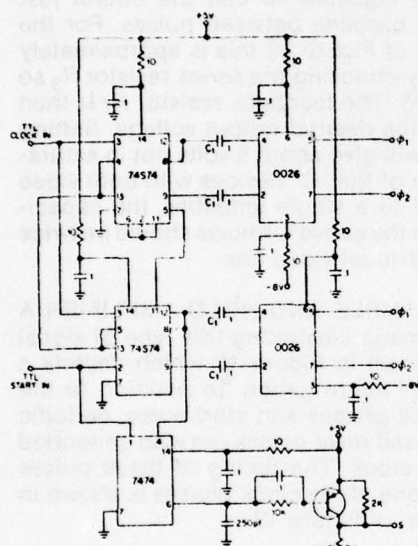

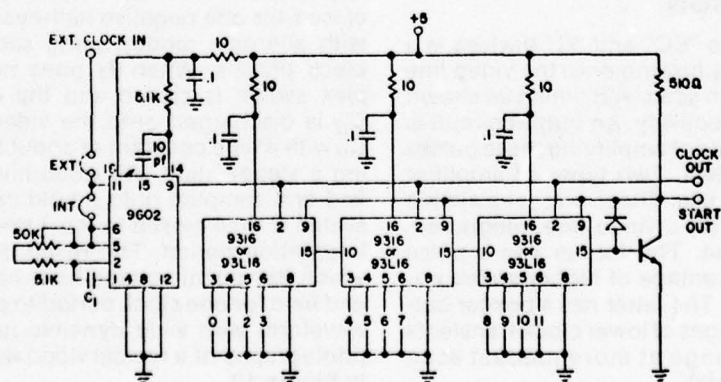Figure 8. Four phase drive circuit and timing diagram for "C" devices.

Figure 9. Clock and counter circuit for generating TTL clock and start pulses.

DRIVER REQUIREMENTS

Good clock drivers are essential in order to minimize switching noise in the video output and to obtain maximum performance at high scan rates. The clocks should have very fast rise and fall times with the rising edge of one phase matching the falling edge of the next phase. Recommended drive circuits along with their input and output waveforms are shown in Figures 7 and 8 for the "EC" and "C" series devices respectively.

In the specifications, all voltages are expressed with respect to array common. However, for compatibility with TTL clocks and ease of signal extraction, it is recommended that common be run at plus 5 volts. The clock phases should then swing between plus 5 and minus 6 to minus 8 volts. The start pulse should be coincident with $\emptyset_1$ going negative and should overlap one positive going transition of $\emptyset_1$ and $\emptyset_1'$.

The start pulse amplitude may be varied between 7.5 and 13 volts. If any non-uniformity is present on the first two elements, it can be eliminated by adjustment within this range. Four clock phases are required to drive the "C" devices while operation of the "EC" devices requires only two complementary clock phases.

The drive circuits of Figure 7 and 8 require TTL level clock and start inputs which may be provided from other parts of the system or generated using a circuit such as that shown in Figure 9. In this circuit the start pulse is obtained by counting clock pulses. By shorting the appropriate terminals of the 9316 integrated circuits, the count n may be set at any desired value greater than $N + 2$ for "EC" devices and $N + 4$ for "C" devices where N is the number of elements in the array. However, the total time between start pulses $t_L = n/f_S$ should not exceed approximately 40 msec (at room temperature) to prevent integrated dark current from making a significant contribution to the output charge.

SIGNAL EXTRACTION

The video output of the "EC" and "C" devices is a train of N charge pulses flowing onto the video line capacitance during each scan with timing as shown in Figures 7 and 8 respectively. An output circuit is required which is capable of amplifying these pulses to a useable voltage level. Two types of amplifier circuits are in common use. These are: (1) a simple current amplifier, and (2) a video line integration, sample and hold circuit. The former has a pulse output and has the advantage of higher speed operation (up to 10 MHz). The latter has a boxcar output and has the advantages of lower clock transients and wider dynamic range at more modest scan rates (up to about 2 MHz).

CURRENT AMPLIFIER Since the array output appears as a purely capacitive source (see Figures 2 and 3), the video signal may be amplified using an op amp connected as a current amplifier. A suggested amplifier circuit using the Reticon CA-10A op amp is shown in Figure 10. While the CA-10A is especially recommended for this application, other op amps may be used provided they have a minimum open loop gain of 40 dB at the scan frequency and a slew rate (V/μsec) of at least 30 times the scan rate (MHz).

Typical video output waveforms from the circuit of Figure 10 are shown in Figure 11. The time constant of the trailing edge of each video pulse is determined by the video line capacitance of the array C_V and the input resistance of the amplifier. To minimize clock noise without sacrificing MTF, this time constant should be adjusted so that the output just recovers to the baseline between pulses. For the amplifier circuit of Figure 10 this is approximately accomplished by choosing the series resistor R_S so that $R_S C_V f_S = .05$. The feedback resistor R_f is then chosen to give the desired output voltage. Setting $R_f = R_S C_V / 4pF$ will give about 5 volts out in saturation. In the case of the "C" devices with both video lines connected to a single amplifier, the capacitance C_V used in the above formulas should be twice that of each individual video line.

INTEGRATE, SAMPLE AND HOLD AMPLIFIER A simplified schematic illustrating this type of signal extraction is shown in Figure 12 which depicts a single cell under interrogation. In addition to the two or four clock phases and start pulse, periodic video sampling and reset pulses are also generated from the basic clock. The timing of these pulses with respect to one of the clock phases is shown in the lower portion of Figure 12.

After entering a start pulse, the diodes in the array are interrogated in sequence by connecting them through their internal MOS multiplex switches to the output video line. Each multiplex switch is closed for one negative half-cycle of a clock phase with alternate diodes being sampled by different clock phases. When $\emptyset_1$ goes negative, the multiplex switch is closed and the diode capacitance C_d is discharged onto the video line capacitance C_V with a time constant of about 5 nsec. After reaching a steady state, the video line voltage is amplified and sampled onto a hold capacitor. The reset switch is then closed to reset the diode for the next integration period. The result is a video output in which the signal voltage from each cell is sampled and held for one clock period to produce a "boxcar" waveform with wide dynamic range. Oscilloscope photographs of a typical video waveform are shown in Figure 13.
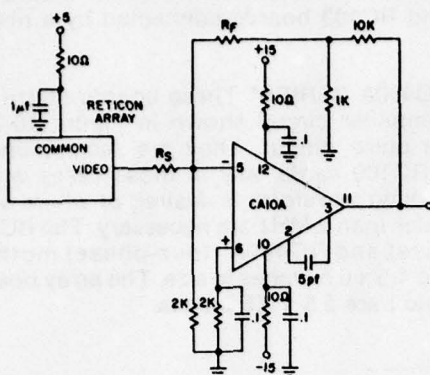
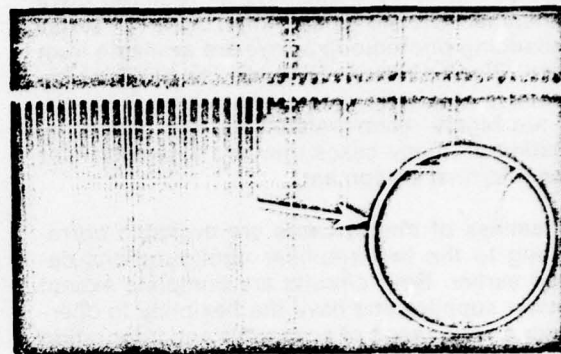Figure 10. Video output circuit using op amp connected as a current amplifier.

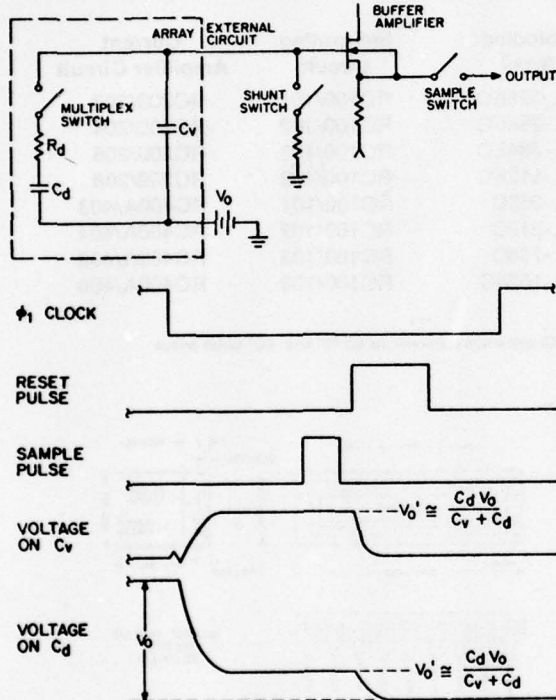Figure 11. Output video waveforms from circuit of Figure 10 (RC200 or RC400A).

Figure 12. Simple equivalent circuit and timing diagram of a photodiode being read out using video line integration, sample and hold technique.
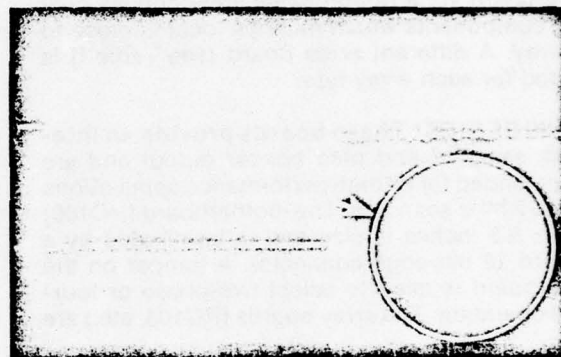

Figure 13. Output waveforms from circuit of Figure 12 (RC100).

Figure 14. Photograph of RC-100 board with RC-103 board connected by ribbon cable.

END OF SCAN

Output pulses are provided when the last elements are sampled by the shift register scanning circuit. These end-of-scan outputs are provided primarily for test purposes. When not in use they should be shorted externally to array common to avoid introduction of unwanted "glitches" into the video. In some applications, however, it may be desirable to use the end-of-scan outputs. In these cases, it is recommended that the voltage excursion on the end-of-scan terminals be minimized by using a circuit such as that shown in Figure 15.

Figure 15. End-of-scan output circuit.

A-7

CIRCUIT CARDS

Printed circuit cards containing all required drive and amplifier circuitry for operation of the "C" series self-scanning photodiode arrays are available from Reticon. Since component layout is of critical importance in obtaining good video output, these circuits are highly recommended for first time array evaluation. In many cases they are also useful for design into final equipment.

Two families of circuit cards are available corresponding to the two amplifier configurations described earlier. Both circuits are complete except for power supplies and have the flexibility to operate over a wide range of scan rates and integration times. Both are divided into two boards—a "motherboard" which contains most of the circuitry and a small "array board" which connects to the motherboard via a ribbon cable and contains only those components which must be located close to the array. A different array board (see Table I) is required for each array type.

RC-100 SERIES* These boards provide an integrated, sampled and held boxcar output and are recommended for all high performance applications at up to 2 MHz scan rate. The motherboard (RC100) is 4.5 x 6.5 inches in size and is terminated by a standard 22 pin edge connector. A jumper on the motherboard is used to select two-phase or four-phase operation. The array boards (RC103, etc.) are

3 inches square and have mounting holes in each corner on 2.6 inch centers. Figure 14 shows the RC100 and RC103 boards connected by a ribbon cable.

RC200/RC400A SERIES* These boards utilize the current amplifier circuit shown in Figure 10 and provide a pulse output. They are recommended over the RC100 cards only in those cases where a pulsed video waveform is desired or where scan rates greater than 2 MHz are necessary. The RC200 (two-phase) and RC400A (four-phase) motherboards are 4.5 x 6.5 inches in size. The array boards (RC203, etc.) are 2.5 x 3.5 inches.

---

*Separate data sheets are available for the RC100 series and for the RC200/400A circuits.

Photodiode Array	Integrating Circuit	Current Amplifier Circuit
RL-128EC	RC100/101	RC200/203
RL-256EC	RC100/102	RC200/204
RL-384EC	RC100/103	RC200/208
RL-512EC	RC100/103	RC200/208
RL-256C	RC100/101	RC400A/403
RL-512C	RC100/102	RC400A/404
RL-768C	RC100/103	RC400A/408
RL-1024C	RC100/103	RC400A/408

Table I. Circuit board requirements for "C" and "EC" series arrays

MECHANICAL SPECIFICATIONS

ELECTRICAL CHARACTERISTICS (25°C)

	Min	Typ	Max	Units
Video Line Bias[1]		-5	-8	Volts
Clock Amplitude[1]	-11	-12	-13	Volts
Start Pulse Amplitude[1]	-7.5	-10	-13	Volts
Clock Repitition Rate (f_S)			10	MHz
Interval Between Start Pulses (t_L)[2]			40	msec
Capacitance of Each Clock Line (C_C)				
RL1024C, 512EC		120		pF
RL768C, 384EC		90		pF
RL512C, 256EC		60		pF
RL256C, 128EC		30		pF
Capacitance of Each Video Line (C_V)				
RL1024C, 512EC		100		pF
RL768C, 384EC		75		pF
RL512C, 256EC		50		pF
RL256C, 128EC		25		pF
End of Scan Output Resistance		5		Kohm
DC Power Dissipation[3]				
"C" Devices		3		mwatt
"EC" Devices		1.5		mwatt

ELECTRO-OPTICAL CHARACTERISTICS (TYPICAL, 25°C)

	DEVICE TYPE				
	C	EC	C/17	EC/17	Units
Center-to-Center Spacing[4]	1	2	1	2	mils
Aperture Width[5]	1	1	17	17	mils
Sensitivity (S)[6]	0.7	1.1	12	19	$\frac{pA}{\mu watt/cm^2}$
Non-Uniformity of Sensitivity[7]					
RL256C, RL128EC	5	5	5	5	±%
RL512C, RL256EC	7	7	7	7	±%
RL768C, RL384EC	9	9	9	9	±%
RL1024C, RL512EC	11	11	11	11	±%
Saturation Exposure (E_{sat})	5.7	3.6	0.27	0.17	$\frac{\mu watt\ sec}{cm^2}$
Saturation Charge (Q_{sat})	4.0	4.0	3.2	3.2	pcoul

ABSOLUTE MAXIMUM RATINGS

	Min	Max	Units
Voltage Applied to any Terminal with Respect to Common	0	-20	Volts
Storage Temperature	-55	+125	°C
Temperature Under Bias	-55	+85	°C

NOTES:

[1] Measured with respect to common. Common is normally run at +5 volts for compatibility with TTL clock circuits.

[2] Devices can be run with longer integration time, but dark signal may increase to an objectionable level unless temperature is reduced. Dark signal changes by a factor of 2 every 7°C.

[3] The AC power is given by $mC_CV_C^2f_s/2$ where m is the number of clock phases, C_C is the capacitance of each clock line, V_C is the clock voltage, and f_s is the scan frequency.

[4] Sensor spacing is accurate to ±0.25 µ, ±1 µ cumulative.

[5] Aperture width is accurate to ±0.1 mil.

[6] Specified for 2870°K tungsten light source. Sensitivity and saturation exposure are sometimes expressed in units of pA/ft-cd and ft-cd sec respectively. The conversion factor between µwatt/cm² and ft-cd depends on the spectral distribution of the light source. At a color temperature of 2870°K, 50 µwatt/cm² corresponds to 1 ft-cd.

[7] Typical value specified for broadband 2870°K tungsten light neglecting first two and last elements. Uniformity is improved if only visible light is used. Maximum allowed non-uniformity is twice typical value.
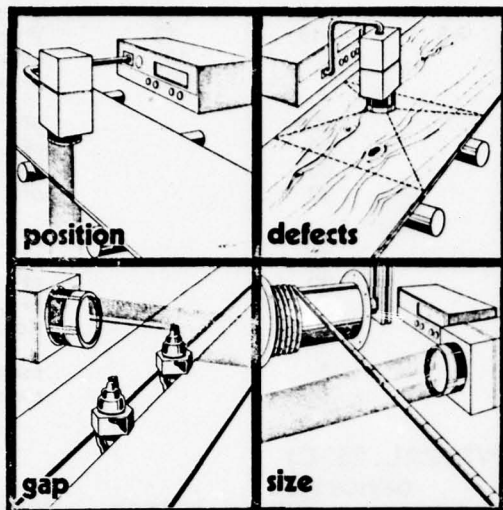
RETICON Solid-State Imaging Cameras are used for rapid, accurate, non-contact measurements of size, position, and shape, and for the detection of surface defects to facilitate the automatic control of manufacturing processes. They offer the precision, reliability, and drift-free characteristics of a totally solid state and digitally controlled electro-optical system. Typical applications include: inspection and edge control of webs such as textile, paper, hot or cold glass and steel strips; sorting of high-volume parts by dimensional analysis and pattern recognition; control of size of continuously formed or expanded materials. Solid-state imaging cameras are functionally similar to vidicon type TV cameras, but with the added advantages of greater geometric accuracy, extended spectral range, higher sensitivity and scan rates, digital output, small size, low voltage and power requirements, and the ruggedness and reliability of solid-state design.

Imaging cameras operate similarly to photographic cameras except that a RETICON Solid-State Image Sensor replaces the film plane. Both linear and two-dimensional (matrix) arrays of photo-sensitive elements are available in addition to a complete line of appropriate optics and camera accessories. Four basic camera models are offered in different physical configurations and output formats to enable users to select the optimum camera system for each application.

Fields of view range from a fraction of an inch to several feet, depending on the optics selected. The camera lens projects the field of view on the image sensor which is scanned electronically to produce a train of analog pulses. The pulse outputs are proportional in amplitude to the light intensity on the corresponding photosensitive element. These pulses are then thresholded and digitized within the camera for further processing by any standard RETICON RS600 Series Electronic Controller. These controllers can be programmed to display parameters such as edge position, object width, number of light-to-dark transitions per scan for code reading or surface condition, etc. Custom controllers, including microcomputer-based systems, have been designed by RETICON to meet a wide variety of special requirements.
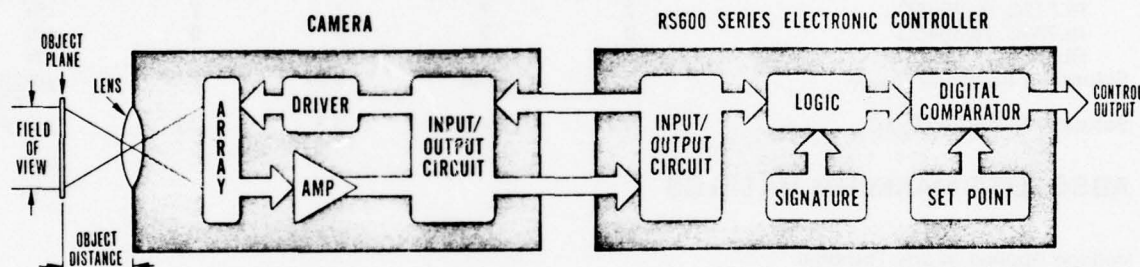
Figure 1. Typical camera-controller system diagram.

THE SOLID STATE IMAGE SENSOR

All RETICON cameras are based on a solid state image sensor also developed and manufactured by RETICON. A simplified schematic diagram of a typical such image sensor is shown in Fig. 2.
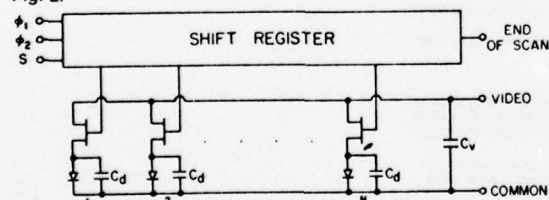
Figure 2. Simplified Schematic diagram of typical line scanner

The shift register is driven by a clock; each scan is initiated by a start pulse. The start pulse loads a bit which is clocked through the register, successively opening and closing the switches and thus connecting each photodiode, in turn, to the video line. As each photodiode is accessed, its capacitance is charged to the potential of the video line and is left open-circuited until the next scan. During the interval between scans, the capacitor is discharged by an amount equal to the instantaneous photocurrent in the diode, integrated over the line scan. Each time a diode is sampled, this integrated charge loss must be replaced through the video line. The resulting video signal is a train of charge pulses, each proportional in magnitude to the light intensity falling on the corresponding photodiode.

The total number of photodiodes in a single linear array ranges from 64 to 1024; two-dimensional matrix arrays are available in 32x32, 50x50, and 100x100 element configurations. The clock and start requirements for matrix arrays are similar to those for linear arrays; the output is on a single video line.

The sensitivity and spectral response of RETICON arrays are equivalent to high-quality discrete silicon photodiodes generally used between 400 and 1100 nanometers, and cover the entire visible and part of the IR spectrum.

THE LC-600 LINE SCAN CAMERA

The RETICON LC600 Solid State Line Scan Camera is available with standard arrays ranging from 64 to 1024 resolution elements with center-to-center spacing as small as 1 mil (25.4 microns). Seven standard lenses and three standard array aperture widths are available.

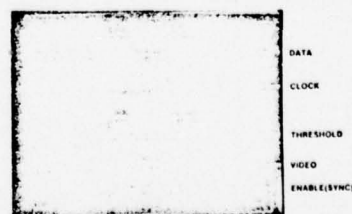The camera output is developed from a comparison of the

Figure 3. Outputs of line scan camera scanning across two light bars on a dark background.

RETICON CORPORATION • 910 BENICIA AVE. • SUNNYVALE, CALIFORNIA 94086

analog pulse train from the array with an electronically adjustable and preset threshold level as shown in Fig. 3. A digital output of logical ZERO results from light values below the threshold — dark — and a logical ONE level for light values above the threshold — light. Timing information is provided on separate differential output lines for use by the remote controller to correlate the output data with the position of each diode in the array, and includes a series of digital clock pulses synchronized to the diode sampling process and a data enable output. The data enable line becomes active when the first photodiode in the array is sampled, and remains active until the last diode is sampled; it notifies the controller that valid data is being transmitted. All data lines appear on differential line drivers at TTL level to facilitate long data lines and noise immunity.
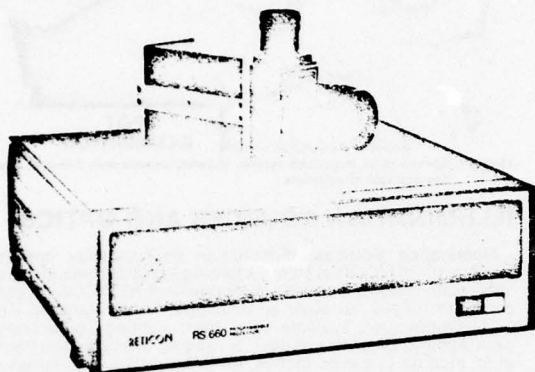
Figure 4. LC600V Camera (through-the-lens viewer) with T-mount lens, and RS660 Programmable Processor.

The user can easily set the element-to-element sampling rate or the total time between initiation of each line scan, based on the specific needs of each application. Instructions for the optimum setting are available from RETICON, as it depends on the available light level, the contrast between light and dark areas, the linear or rotational velocity of the viewed object, and similar factors. Scan rates are adjustable from 5 KHz to 1.05 MHz, representing from 128μsec to 40 msec required to complete a total line scan (depending on the array length).

The digital outputs can be processed by standard RETICON RS600 series control systems, or by user-supplied controllers or process computers. Control of the camera, for most applications, is entirely internal to the camera. However, the camera will respond to external clock and start pulses. The user may elect to supply either or both of these control inputs so that both the element-to-element sampling rate and the line scan times are externally controlled. The camera requires only a ±15 volt and +5 volt power supply at less than 4.2 watts of total power, also furnished by the RETICON RS600 series controllers. If a customer-supplied processor is used, supplemental power supplies should be planned which are also available from RETICON.
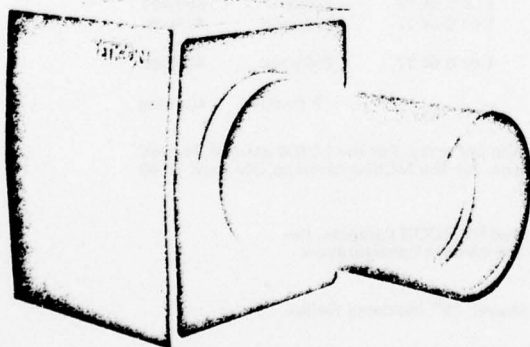

Figure 5. LC64P Camera with C-mount lens, lens hood, and lens protector

LC100 LINE SCAN CAMERA

The RETICON LC100 Line Scan Camera is physically identical to the LC600 camera and offers the same high degree of flexibility, but is designed for applications requiring higher scan

rates and further remote processing of the analog video. These cameras can be operated at scan rates from 2 KHz to 2 MHz, representing total line scan times from 64μsec to 40msec. The LC100 provides improved dynamic range and sampled-and-held boxcar analog output in addition to the corresponding thresholded digital output of the LC600 camera. Both analog and digital outputs are brought out on differential line drivers to provide stable and noise-free data transmission over longer cable lengths between the camera and the RS600 series controllers or other user-furnished equipment. The higher quality analog output allows multiple-bit digitizing of this signal for computer inputs. The LC100 is recommended primarily where either this type of A/D conversion or clock rates in excess of 1 MHz is required.

LC64P LINE SCAN CAMERA

The RETICON LC64P Line Scan Camera is a lower-cost, lower-resolution, and simplified version of the widely used LC-600 series camera. It is available in a single configuration using a 64-element photodiode array, with center-to-center spacing of 2 mils. The analog video output from the array is connected to a BNC connector on the rear panel, and is a "boxcar" type waveform at 0 to 1.5 volts in amplitude, with "dark noise" typically less than 10 mv.

The LC64P is built in a rugged, cast aluminum housing; it provides the same outputs as the LC600 camera and is compatible with all the lens and other accessories offered for that camera except the through-the-lens viewer. Power requirements are ±15 volts d.c. at less than 5 watts. The camera is compatible with all RETICON RS600 Series Controllers. The LC64P is recommended for applications where 64 elements of resolution are sufficient, and where the low cost of this camera is a major consideration.

MC500 SERIES MATRIX CAMERAS

RETICON MC500 Series Two-Dimensional Cameras are available with matrix arrays of either 100x100, 50x50, or 32x32 elements. The cameras can operate at clock rates up to 500 KHz, corresponding to 500 frames/sec for the 32x32, 200 frames/sec for the 50x50, and 50 frames/sec for the 100x100 element array. These cameras are available with various options providing an analog "boxcar" output, a digital thresholded output, or both. The analog output can be digitized by a remote A/D converter to furnish multiple grey level definition. The digital camera contains an internally adjustable threshold which can be set to generate TTL level digital data from the video similar to that provided by the LC600 series line cameras. Applications of the MC500 Series Camera include character recognition, code reading, checking of concentricity of rotating objects, and general dimensional analysis of at least momentarily stationary objects. The cameras are compatible with RETICON RS510 series power supplies.
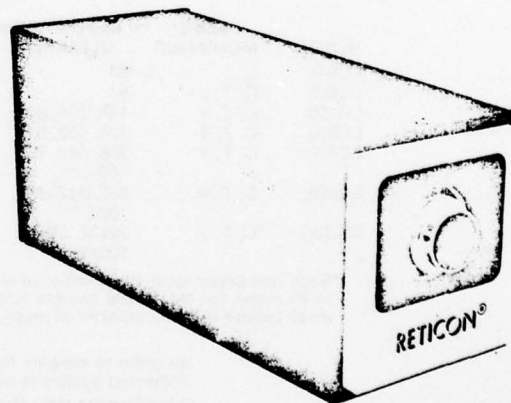

Figure 6. LCD-200 Camera with special lens mount to accept Leica-threaded lenses

SPECIAL-PURPOSE CAMERA

LCD-200 Dual array Camera. This special purpose camera uses two optically superimposed arrays to color scan at two specific wavelength bands. Infrared is used as the reference because it is insensitive to color; the visual spectrum is used to detect color changes. The outputs of the two arrays are compared on an element-by-element basis. When the ratio of signal levels between the two arrays exceeds preset limits, an error

ideal is provided. The LCD-200 is particularly effective in selection, sorting, and orientation of food products where blemishes and discoloration must be detected. The LCD-200 eliminates the need for background or reference color comparators used in conventional color scanners. The LCD-200 may be used with RETICON RS600 Series controllers; its output signals are compatible with computers and electro-mechanical sorting devices.

CAMERA CONTROL MODULES

The RS600 series controllers are designed to interface with RETICON line scan cameras to provide a complete non-contact measurement or inspection system. Through a connecting cable these modules supply power to the camera and accept the camera outputs for processing and display. Depending on the specific model chosen, the controllers give an indication that the light level is adequate, provide for selection of the pattern within the camera field of view which is to be measured and give both a digital display of the measurement and a corresponding BCD output for further processing.

Various standard options are available which provide for go-no go testing to preset limits or tolerances, automatic sorting into up to 10 categories, direct teletype printout of the measured data, display in engineering units (e.g., inches, millimeters, etc.), area measurements of irregular size objects, the retention of maximum and minimum dimensions, the addition of constants to allow the use of the camera as a vernier when small variations of a large dimension are of interest, self calibration, analog output for process control, and various package configurations (e.g., NEMA-12, 19" rack mount, etc.).

The RS600 provides power to RETICON Line Scan Cameras, and presents the camera outputs on a terminal strip.

The RS605 contains counting circuits as well as power supplies. It converts the camera output into a continuously updated count which represents a size or position measurement. The controllers can be set to measure a dark object against a light background or vice versa, or to count light-to-dark transitions, such as threads on machined parts or holes.

The RS610 can control two cameras—either separately or in conjunction—to measure two edges of a large object. A thumb-wheel-switch signature control enables any portion of a complex pattern to be measured.

The RS660 contains a microcomputer which can be used to perform further arithmetic manipulations on the raw data, and will in addition to the various features and options available with the RS605 and RS610 provides direct TTY interface.

The RS510 Power Supply Module is used with the MC500 matrix cameras. It provides power and presents the x, y, and z outputs of matrix cameras on BNC connectors for a CRT display.
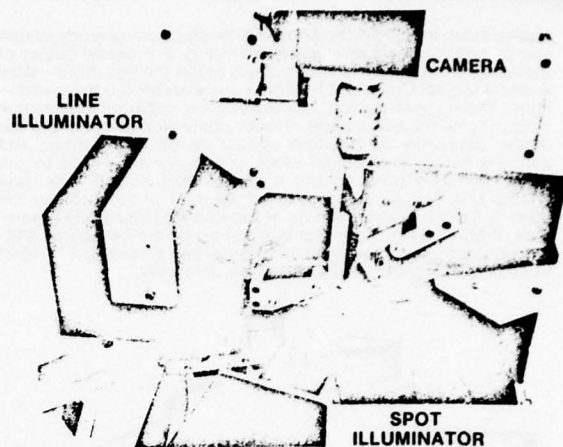

Figure 7. Special roller Inspection system, showing camera with C-mount lens and line and spot illuminators

ILLUMINATION SOURCES AND OPTICS

Illumination Sources. Illumination sources play important roles in all RETICON systems. Lighting systems compatible with solid-state image sensors are available from RETICON, or can be designed readily for most applications. Three standard RETICON illumination systems offer front lighting (reflection) or back-lighting (shadow) of objects ranging in size from a fraction of an inch up to eleven inches. All use quartz-iodide lamps and forced air cooling. In most applications the units can be operated at reduced voltages for thousands of hours of lamp life.

In many applications, the objects to be measured can be illuminated by available fluorescent light, incandescent light, or the object itself may have sufficient luminescence such as hot-rolled or extruded steel or molten glass.

Optics. RETICON also offers a complete line of standard C-mount, T-mount, and custom optics for use with all camera models. Accessories are provided such as lens protectors, lens extenders, threaded adapters, optically clear windows, etc. A through-the-lens viewer is also available to permit visual alignment of the object and the camera optics when no image display is available.

STANDARD CAMERA CONFIGURATIONS

MODEL	LENS MOUNTING	RESOLUTION ELEMENTS	ELEMENT SPACING (MILS)	APERTURE WIDTH (MILS)	LINE (FRAME) SCAN TIME* MIN	LINE (FRAME) SCAN TIME* MAX
LC64P	C	64	2	2	0.4msec	40msec
LC600	C, T, V	64	2 or 5	2 or 3	64µsec	40msec
LC100	C, T, V	128, 256, 512	2	1 or 6 or 17	64µsec	40msec
LC600	C, T, V	128, 256, 512	2	1 or 6 or 17	128µsec	40msec
LC100	C, T, V	256, 512 768, 1024	1	1 or 6 or 17	128µsec	40msec
LC600	C, T, V	256, 512 768, 1024	1	1 or 6 or 17	256 µsec	40msec
MC500	C, T, V	32x32, 50x50, 100x100	4	—	2 msec	40 msec

*Scan rate depends on the number of resolution elements per array. For the LC600 camera, N µsec to 40 msec, for the LC100 camera N/2 µsec to 40 msec, for the MC500 cameras, 2N µsec to 40 msec (where N is the number of resolution elements).

In order to simplify the identification of RETICON cameras, the following system is used to specify the camera configuration:

Line Camera (MC-Matrix Camera)
Style (64P, 100, 500)
Lens Mounting ("C" or "T" Mount, "V" indicates Reflex Viewer)

LC600 T 1024-1/17

Aperture Width (Mils)
Element Spacing (Mils)
Number of Elements (64 to 1024 and 32x32, 50x50, 100x100)

A-12

CUSTOM-DESIGNED SYSTEMS

Although most measurement applications can generally be handled by one or more standard cameras and controllers, there are still many instances where custom engineering is required. As an example, visual inspection applications in which the controller must recognize specific defects may require the design of a custom system.

Standard RETICON line scan cameras and light sources, in conjunction with a custom processor are used in the following applications.
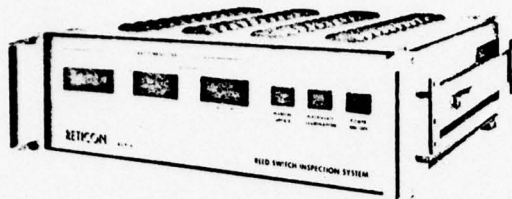
REED SWITCH LEAD CONCENTRICITY TESTER. In this system, two MC500 series matrix cameras are used to simultaneously measure the concentricity of the two axial leads of reed switches. The switches are rotated around the longitudinal axis, with the leads back illuminated and the shadows imaged on the matrix cameras. The custom controller — housed in a standard 19-inch rack cabinet with adapters — displays the length and concentricity of the leads. The computer-compatible output is designed to interface with the user's automatic manufacturing and inspection equipment.
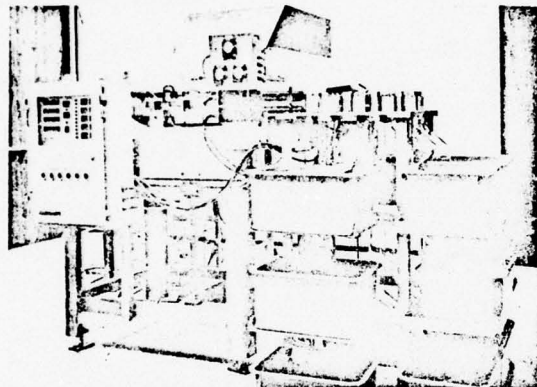
PLASTIC MOLDING INSPECTION SYSTEM. This integrated system consists of a rotating conveyer, a two-camera inspection station, an electronic processor, and a classification/sorter. The two RETICON cameras measure the volume of a plastic syringe barrel and sort them into eleven acceptable dimensional groups and two rejection categories, automatically and at a rate of 500 items/minute. A NEMA 12 housed controller displays the inspection results and permits classification criteria to be changed by thumbwheel operation. It also provides a continuous count of the accepted parts by categories which are set up to classify parts to an accuracy of 0.001 inch.
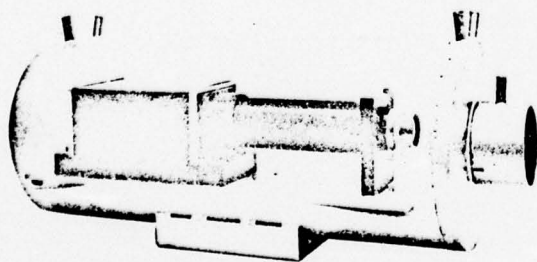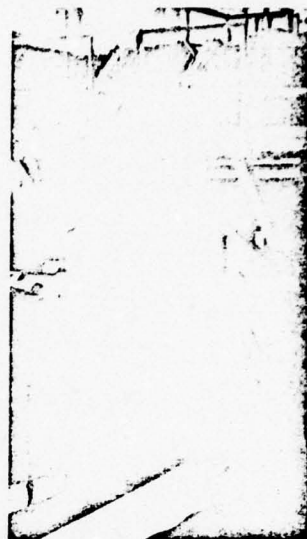
SPECIAL CAMERA HOUSING. This camera housing — shown in phantom view — is intended for use in extremely hot environments (steel and glass manufacture) and in corrosive atmospheres. The outer casing is made of stainless steel, the housing is water jacketed for cooling, and an air purged viewing window is provided.

HOT STRIP MEASUREMENT SYSTEMS (RS880 SERIES). These systems are designed for continuous and accurate monitoring of the width of hot-rolled steel and glass ribbons in float glass manufacturing plants. Two completely solid-state cameras are provided within rugged water-cooled stainless steel enclosures with air purged windows. These assemblies are mounted above the hot strips where the cameras make use of the available radiation of the hot strip or can be provided with back illumination for the measurement of colder objects.

The associated controllers are housed in a NEMA 12 enclosure, and provide continuous digital readout of the strip width, as well as computer interface for automated mills. Many standard display and control options are available to meet specific mill requirements. Monitoring stations with continuous display can be mounted along side the rolling line with the master processor located near other controls. System accuracy of better than $\frac{1}{16}$ inch provides increased manufacturing efficiency with payback typically less than a year.

OPTO-ELECTRONIC GAGING SYSTEM. This system is used to provide finer control of the distribution of air within the combustion chamber of jet aircraft engines. By accurate inspection of the holes around the outside flanges of the combustion cooling rings, Rolls Royce has been able to achieve a more even distribution of air and produce an engine which is cleaner, more reliable, and more efficient. The RETICON system is used to gage the size and position of these holes (as many as 4,000 — 0.020 inch in diameter) and, with the help of a micro-computer and printer, is able to provide information of hole area and distribution which is related directly to engine performance. Note the through-the-lens viewer for easy alignment of the camera to accommodate different flange diameters.

67230

A-13

APPENDIX B

SYSTEM THROUGHPUT ANALYSIS

Preamble

The throughput of an automatic line digitizing system is a function of (1) the processing algorithms, (2) the implementation of the algorithms, and (3) the system design. In this trichotomy the scanning operation, clearly an important determinant of the system throughput, is considered to be one of the processing algorithms.

This project is addressed to one of the key system design issues - whether to use a large linear array or a specially shaped geometric array. This system design consideration does not exist in isolation from the other system design features, but is closely related to them. Some of the other system design considerations are:

(1) Should the map be broken up into sections for processing? If so, how?

(2) Should there be an redundancy in the processing or error checking?

(3) Should a detection operation be done before encoding any map data or be done at the same time as the encoding operation?

(4) Given that large format manuscripts require a mechanical scan, should the map be scanned in a raster mode and the image data subsequently processed to convert it into lineal mode, or should the lines be followed directly during the scanning operation?

(5) What algorithms should be implemented in software and what algorithms should be in hardware?

(6) What operations should be done on-line and what operations should be done off-line?

(7) Should a flatbed or a drum scanner be used?

(8) What processing operations should be done in "parallel" and what ones in series?

The particular system design feature being addressed by this project is the type of sensor. For line digitizing a specially shaped geometric array would be used with a mechanical scan in which the sensor is mechanically moved about the map as it scans to directly sense line features. A large linear array would be used with a combination of electronic scanning and mechanical scanning. Because of these differences, the resulting throughput for a system using a specially shaped geometric array may be different from a system using a large linear array. An analysis has been made, using available information, of system throughput to determine if, in fact, there is a significant difference in throughput between these two system designs. It has been found, based on the assumptions made, and the model formulated, that there is not a significant difference in throughput between these two system design approaches.

Archetypical Map

An archetypical map was defined to be used as a standard comparison in the throughput analysis. The characteristics of this map are listed in Table B-1. As can be seen from the table, the map is 20" x 20" and contains 5,000 lineal inches of line. At a resolution of 1 mil, the image field of the map contains 400 million points. The line features cover 25 million image points or 6¼% of the total map area. This map is considered to be a representative topographic map. The throughput analysis is based on estimates of the time required to process this map.

The key factor affecting the throughput in the aspect of the system design being considered here is the efficiency with which the process finds the 6¼% of the image field which contains the line data and ignores the other 93-3/4% of the image field which contains no line data.

Approach

Quantitative results have been obtained by using the arche-typical map described above and by making some assumptions about processing times. The processing required for automatically encoding the line features on the map has been divided into four parts. They are:

(1) Scanning the map manuscript and transferring the data to the computer (data transfer).

(2) Locating the lines in the image field (detection processing).

(3) Line following - stepping along the line.

(4) Line processing - all the other processing required by the system including encoding, automatic editing, and data management.

Estimates were made for the amount of time required to perform each of these four steps for a system using a large linear array and for a system using a specially shaped geometric array. The amount of time required by some of the processing operations depends directly upon the amount of line data contained in the map; the processing time required by other operations is independent of the amount of line data but depends rather on the size of the map. Estimates were also made of the required processing times for different line densities.

It was necessary to make certain assumptions in order to esti-mate the time to process the map. These assumptions are based on our engineering judgment and on our experience in processing maps. They are given in the next section.

In this analysis it is assumed that the first step in processing the map is a detection operation which is functionally separate from any of the other processing. The detection process assumed is basic-

Table B-1   STANDARD TOPOGRAPHIC MAP

Dimensions of map	= 20" x 20"
Area of map	= 400 sq. in.
Resolution	= 1 mil (25.4 μm)
Dimensions of image field	= 20,000 points x 20,000 points
Area of image field	= 400 million points
Line width	= 5 mils = 5 resolution cells
Line length	= 5,000"
Line area	= 25 million points = 6¼% of total map area

B-4

ally that used by the Calspan DIGIMAP system. Both the linear array
and geometric array systems use the same line detection process
before doing any line following and line encoding.

In the linear array system line following is done in the computer
by computer software algorithms after the raster image has been trans-
ferred from the scanner to the computer. The geometric array system
does mechanical line following in which the sensing head on the scanner
is mechanically driven to follow the line being encoded on the map.

Assumptions

In the analysis presented here a number of assumptions have been
made in order to construct a model which yields quantitative results.
The conceptual assumptions are explained in the text as the model is
developed. Certain key quantitative assumptions regarding processing
times are also required. These have been made on the basis of
currently available information and engineering judgment. They are
as follows:

(1) Time to scan an image point (raster mode) and transfer its
intensity to the computer = 10 μs.

(2) Time to check an image point in the computer to see if it
is part of a line = 80 μs.

(3) Time to process a line detection = 8,000 μs = 8 ms. A
search line is 2 points wide; a data line is 5 points wide;
the intersection covers an area of (2) (5) = 10 points.
The required time is then (8,000 μs) $\div$ (10 points) =
800 μs/point.

(4) Time to follow one line increment in computer = 4,500 μs =
4.5 ms.

(5) Time to mechanically step scanning head
6 mils = 10,000 μs = 10 ms.

(6) Time to do line processing (encoding, automatic editing,
     data management) = 6,000 μs = 6 ms per line increment.

Equivalent Line Density

In order to estimate the number of line detections, a particular
pattern of lines has been assumed for the standard map. The pattern
is a set of horizontal, parallel lines, 5 mils wide, spaced to give
an average density of 12 lines/inch. Each line runs the full width
of the map and is therefore 20 inches long. A density of 12 lines/
inch implies the map has (20 inches) (12 lines/inch) = 240 horizontal
lines of data, or (20 inches) (240) = 4800 $\cong$ 5,000 inches of lineal
data.

Data Transfer

The time required to scan the map and transfer the image data
to the computer, an operation required in both systems for line
detection processing, is (400 M points) (10 μs/point) = 4,000 sec.

Line Detection

It is first necessary to find a line before processing and
encoding it. The assumed detection method is to scan the image field
with a grid of vertical and horizontal search lines, 2 points wide,
spaced 16 points apart horizontally and 500 points vertically. The
number of search lines is 1250 (horizontal) + 40 (vertical) =
1290[1]. The number of image points examined is 50[1] million or 12½%
of the total map area.

The time to complete this operation is the time to process the
points. Now the time required to process an image point in areas
where there is no line data is 80 μs. The time required when data is
present is considerably longer. When a line is detected additional

processing is required to confirm the detection. The search line is
2 points wide, the data line 5 points wide; thus each detection
covers (2) (5) = 10 image points. The time required to process a
line detection is 8,000 μs, or 8,000/10 = 800 μs/point. This time
is in addition to the 80 μs.

We next need to know how many of the 50 million points being
processed are data points. On the basis of the pattern of line data
previously described, each vertical search line will cross 240 data
lines and make 240 detections. There are 1250[1] vertical search
lines. Therefore, the number of data points in the detection process-
ing is (1250 lines)(240 detections/line)(10 points/detection)
= 3 million points. The time required to process the image points
in the detection operation is (50M)(80 μs) + (3M)(800 μs) = 4,000 +
2,400 = 6,400 sec. The total detection time consists of a term which
depends on the map area (4,000 sec.) and a term (2,400 sec.) which is
a function of the amount of line data contained on the map. The sec-
ond term is a linear function of the line density.

Line Following

In our system model the differences between the operation of
the linear array and the geometric array occur in the line following
operation. In the linear array system the line following is done by
the computer software; in the geometric array system it is done by
mechanically moving the scanning head and by the processing implicit
in the construction of the array.

Line following is done in increments of one or more scanner
resolution elements. An increment of 6 elements or 6 mils is assumed.
The time required to process an increment of line data in the computer

---

[1]Note: See end of Appendix B for these calculations, page B-12.

has been assumed to be 4,500 μs. The total time for processing the line data on the whole map is

$$\frac{(5,000 \text{ inches})(1,000 \text{ points/inch})(4,500 \text{ } \mu s/\text{increment})}{(6 \text{ points/increment})} = 3,750 \text{ sec.}$$
$$\approx 4,000 \text{ sec.}$$

This processing time is a linear function of the amount of line data.

In the geometric array system the line following is done by a combination of (1) mechanically stepping the scanning head in 6 mil increments and (2) processing done by the geometric array. It is assumed that a 6 mil step takes 10 ms and that the processing time required by the geometric array is negligible compare to this time. The total line following time for the geometric array is then

$$\frac{(5,000 \text{ inches})(1,000 \text{ points/inch})(10,000 \text{ } \mu s/\text{increment}}{(6 \text{ points/increment}} = 8,333 \text{ sec.}$$
$$\approx 8,000 \text{ sec.}$$

Line Processing

All of the other processing steps required after the line following operation are lumped together under line processing. The major functions are encoding, automatic editing, and data management. These operations are done in the computer in both the linear and geometric array systems. It has been assumed that the time required for the execution of these functions for a line increment is 6,000 μs. The time required for the whole map is

$$\frac{(5,000 \text{ inches})(1,000 \text{ points/inch})(6,000 \text{ } \mu s/\text{increment})}{(6 \text{ points/increment})} = 5,000 \text{ sec.}$$

Results

The map processing times resulting from this analysis of the
representative map are collected in the following tables. Tables
B-2A and B-2B give the times for the linear array system in seconds
and hours respectively, Tables B-3A and B-3B give the times for the
geometric array system. The columns, reading from left to right,
give the times for increasing line length (and constant area).

END
DATE
FILMED

7-78

DDC

Table B-2A PROCESSING TIMES (IN SECONDS) FOR
LINEAR ARRAY SYSTEM

Operation	Line Length				
	0	2,500	5,000	10,000	15,000
Data Transfer	4,000	4,000	4,000	4,000	4,000
Line Detection	4,000	5,200	6,400	8,800	11,200
Line Following	0	2,000	4,000	8,000	12,000
Line Processing	0	2,500	5,000	10,000	15,000
TOTALS	8,000	13,700	19,400	30,800	42,200

Table B-2B PROCESSING TIMES (IN HOURS) FOR
LINEAR ARRAY SYSTEM

Operation	Line Length in Inches				
	0	2,500	5,000	10,000	15,000
Data Transfer	1.1	1.1	1.1	1.1	1.1
Line Detection	1.1	1.4	1.8	2.4	3.1
Line Following	0	0.6	1.1	2.2	3.3
Line Processing	0	0.7	1.4	2.8	4.2
TOTALS	2.2	3.8	5.4	8.6	11.7

Table B-3A PROCESSING TIMES (IN SECONDS) FOR GEOMETRIC ARRAY SYSTEM

Operation	Line Length in Inches				
	0	2,500	5,000	10,000	15,000
Data Transfer	4,000	4,000	4,000	4,000	4,000
Line Detection	4,000	5,200	6,400	8,800	11,200
Line Following	0	4,000	8,000	16,000	24,000
Line Processing	0	2,500	5,000	10,000	15,000
TOTALS	8,000	15,700	23,400	38,800	54,200

Table B-3B PROCESSING TIMES (IN HOURS) FOR GEOMETRIC ARRAY SYSTEM

Operation	Line Length in Inches				
	0	2,500	5,000	10,000	15,000
Data Transfer	1.1	1.1	1.1	1.1	1.1
Line Detection	1.1	1.4	1.8	2.4	3.1
Line Following	0	1.1	2.2	4.4	6.7
Line Processing	0	0.7	1.4	2.8	4.2
TOTALS	2.2	4.4	6.5	10.8	15.1

The analysis shows that the linear system is faster by 17%. As all of the key times are estimated, the conclusion is that the system throughput is comparable, not that a linear array system is faster than a geometric array system.

CALCULATION OF DETECTION LINE AREA

(1) Area covered by vertical search lines:

$$\underbrace{\frac{(20 \text{ inches})(1{,}000 \text{ points/inch})}{(16 \text{ points})}}_{\text{number of lines} = 1250} \cdot \underbrace{(20 \text{ inches})(1{,}000 \text{ points/inch})}_{\text{line length}} \cdot \underbrace{(2 \text{ points})}_{\text{line width}}$$

$$= 50 \text{ million points}^2$$

(2) Area covered by horizontal search lines:

$$\underbrace{\frac{(20 \text{ inches})(1{,}000 \text{ points/inch})}{(500 \text{ points})}}_{\text{number of lines} = 40} \cdot \underbrace{(20 \text{ inches})(1{,}000 \text{ points/inch})}_{\text{line length}} \cdot \underbrace{(2 \text{ points})}_{\text{line width}}$$

$$= 1.6 \text{ million points}^2$$

(3) Total area = 50M + 1.6M = 51.6M ≅ 50M

MISSION
of
Rome Air Development Center

RADC plans and conducts research, exploratory and advanced development programs in command, control, and communications (C^3) activities, and in the C^3 areas of information sciences and intelligence. The principal technical mission areas are communications, electromagnetic guidance and control, surveillance of ground and aerospace objects, intelligence data collection and handling, information system technology, ionospheric propagation, solid state sciences, microwave physics and electronic reliability, maintainability and compatibility.